QUALITY OF SERVICE DESIGN ISSUES IN MULTIMEDIA COMMUNICATIONS OVER POWER LINE NETWORKS

By

SRINIVAS KATAR

A DISSERTATION PRESENTED TO THE GRADUATE SCHOOL
OF THE UNIVERSITY OF FLORIDA IN PARTIAL FULFILLMENT
OF THE REQUIREMENTS FOR THE DEGREE OF
DOCTOR OF PHILOSOPHY

UNIVERSITY OF FLORIDA

2006

I dedicate this work to my parents,
Katari Lakshmipathi Raju and Krishna Kumari

ACKNOWLEDGMENTS

I would like to thank my parents for their support and encouragement over all these years. None of this work would have possible without them. I would also like to express my heartfelt gratitude to my wife Keerti for her support and understanding throughout this endeavor.

I would especially like to thank Larry Yonge and Intellon Corporation for allowing me to work part time on my PhD. I would like to thank my colleagues, Brent Mashburn, Kaywan Afkhamie and Manjunath Krishnam for their valuable feedback. Working with them has always been a pleasure.

Finally, I would like to thank my advisors, Dr Haniph Latchman and Dr Richard Newman, for their valuable guidance throughout my studies. I would also thank Dr Oscar Crisalle and Dr Tan Wong for being part of my PhD supervisory committee.

TABLE OF CONTENTS

LIST OF TABLES

LIST OF FIGURES

Abstract of Dissertation Presented to the Graduate School
of the University of Florida in Partial Fulfillment of the
Requirements for the Degree of Doctor of Philosophy

QUALITY OF SERVICE DESIGN ISSUES IN MULTIMEDIA COMMUNICATIONS OVER POWER LINE NETWORKS

By

Srinivas Katar

May 2006

Chair: Haniph A. Latchman
Cochair: Richard E. Newman
Major Department: Electrical and Computer Engineering

Home Networking is one of the major hurdles in enabling ubiquitous data and multimedia distribution. Most houses are not equipped with specialized wiring for networking purposes and retrofitting them with new wiring is prohibitively expensive. Hence, the use of existing in-home power line infrastructure for networking purposes can go a long way towards solving the in-home connectivity problem.

In this dissertation we first investigate the viability of power line communications (PLC) by evaluating the performance of HomePlug 1.0. Detailed event based simulation models were used to show that HomePlug 1.0 can provide a maximum UDP and TCP data rates of 7.86Mbps and 5.90Mbps. Extensive field testing in 20 houses showed that HomePlug 1.0 provides an average of 2.3Mbps higher throughput compared to IEEE 802.11b.

While HomePlug 1.0 is good enough for data networking, it will not be able to support the newly emerging multimedia applications like audio and video streaming. We

study three issues that the new generation PLC systems need to overcome to enable multimedia communications: (a) AC line cycle variation in noise, (b) Impulse noise, and (c) Beacon Loss.

We use channel characterization measurements on 72 channels to investigate the performance enhancements that can be achieved by using a channel adaptation mechanism that is synchronized to the AC line cycle. The results show that a 30% improvement in physical layer (PHY) data rates can be obtained by continuously adapting to the AC line cycle. A time slot based adaptation that is more suitable for practical systems provided an average of 10% improvement in MAC data rates.

To effectively overcome impulse noise, we propose a novel 2-level MAC framing mechanism that enables efficient retransmissions. Our simulations and analysis show that this mechanism provides linear degradation in performance even under high FEC Block errors. Further investigation of the effect of transmission overheads on efficiency showed that low data rate, low latency QoS applications can incur significant loss in efficiency under high FEC block errors. Hence, PLC channel adaptation should take into account the application QoS requirements to optimize the overall system capacity.

Due to the unreliable nature of the power line channels, beacon reception cannot always be guaranteed. We investigate various persistent scheduling approaches to mitigate beacon loss. Our analysis shows that using persistent current and preview schedules, or persistent preview schedules, up to 10% beacon loss can be tolerated with minimal impact on MAC efficiency and QoS.

CHAPTER 1
INTRODUCTION

The explosive growth of the Internet is driving the need for ubiquitous data and multimedia communications in the twenty-first century. Major hurdles in realizing this objective are the "last mile (access)" and "last hundred feet (in-home)" connectivity problems. Approximately 50% of all network investments are spent on providing the "last mile" infrastructure. The high expense incurred in laying new wiring for broadband access to individual customers has forced service providers to use the existing cable and telephone lines. As much of the world still awaits broadband access, there is a need for alternative viable approaches to solving the last mile problem. In addition in-home distribution of multimedia content is still a challenge particularly for homes that are not equipped with proper wiring to support high-speed data and multimedia communications. Retrofitting the house with new wiring is prohibitively expensive and hence the need arises for new LAN technologies that enable affordable connectivity within the home. With more than a century of ongoing deployments throughout the world, electrical power lines represent by far the most pervasive network of wiring in the world. The use of power lines as a communications medium can come a long way toward solving the last mile and last hundred feet problems.

Several attempts were made starting from the early 1920's to develop a reliable power line communication (PLC) technology. However, the lack of sophisticated digital signal processing technologies hampered earlier PLC technologies from gaining widespread acceptance. For several decades, their applicability was limited to operation

and maintenance of the power supply grid. The explosive growth of the Internet in the recent decades has refueled the interest in developing high bandwidth (i.e., operating in 1-30 MHz frequency band) PLC technologies for in-home networking as well as for broadband access. However, the challenges to enabling high-speed communication over the power line are many.

Power lines were originally devised for transmission of power at 50–60 Hz and at most 400 Hz. At high frequencies the power line is very hostile for signal propagation [1, 2]. Power line networks operate on standard in-building electrical wiring and as such consist of a variety of conductor types and cross-sections joined almost at random. Therefore a wide variety of characteristic impedances will be encountered in the network. This impedance mismatch causes a multi-path effect resulting in deep notches at certain frequencies. While a typical channel may present an average attenuation of approximately 40 dB, it is not uncommon for portions of the bands to experience greater than 60 dB of attenuation. Power line networks are also affected by interference. Electric appliances with brush motors, switching power supplies and halogen lamps produce impulse noise that can reduce the reliability of communication signals. Due to high attenuation over the power line, the noise is also location dependent. Power line channels also show strong dependence on the underlying AC line cycle. All these factors make the design of PLC technologies extremely challenging.

In this dissertation we take a practical approach to understanding the issues in enabling high bandwidth communication over the power lines and how the PLC technologies based on HomePlug 1.0 and HomePlug AV standards overcome these challenges. A combination of analysis, simulations and field tests are used to determine

the effectiveness of the various approaches used by these standards. The organization of this dissertation is as follows.

Chapter 2 builds the background on power line communications. This chapter introduces the two major categories of PLC devices, low-bandwidth PLC and high-bandwidth PLC, and describes the various regulations constraints under which PLC devices should operate. Technology choices currently available for low and high bandwidth PLC systems are presented. This chapter also includes a detailed description of the power line channel characteristics at high frequencies (i.e., 1-30 MHz).

The first generation of high-bandwidth PLC technology, HomePlug 1.0, is investigated in Chapter 3. A detailed description of HomePlug 1.0 standard was followed by simulation based evaluation of its performance. Simulation results showed that HomePlug 1.0 provides a maximum throughput of 7.86 Mbps and 5.90 Mbps for UDP and TCP respectively. The MAC saturation throughput showed graceful degradation with increase in number of station in the network. Simulations with Voice over IP traffic showed that the priority contention mechanism in HomePlug 1.0 could guarantee low latencies for delivery delay sensitive traffic. Extensive field tests were also conducted to evaluate the performance of HomePlug 1.0 with competing home networking solutions, IEEE 802.11b and IEEE 802.11a. These results show that the first generation PLC technologies provide a ubiquitous and reliable home networking solution.

The HomePlug 1.0 standard was designed to transfer data with a maximum MAC throughput of 8 Mbps. While this is good enough for file sharing and Internet access, it will not be able to support newly emerging multimedia applications like audio and video streaming. Multimedia applications require not only significantly larger bandwidths, but

also require guarantees on QoS parameters like latency, jitter and packet loss probability. To address this new breed of applications, a new generation of HomePlug Standard, HomePlug AV, was released by the HomePlug Powerline Alliance. In Chapter 4 we provide a brief overview of the QoS requirements for various applications multimedia applications and the salient features of the HomePlug AV standard that enables it to support these applications.

To achieve data rates necessary to support multimedia applications, HomePlug AV uses a channel adaptation mechanism that is synchronized to the underlying AC line cycle. In chapter 5, we use channel characterization measurements and analysis to investigate the performance enhancements that can be received by using AC line cycle based channel adaptation. These results show that 30% improvement in the physical layer data rates can be obtained by continuously adapting to the underlying AC line cycle. Since continuous adaptation with respect to time is unduly complex for practical systems, we propose dividing the AC line cycle into multiple regions and adapting independently in each region. Results show that using a 1-2 milliseconds region size will provide optimal MAC performance on most paths tested.

Impulse noise sources (like dimmers, halogen lamps, etc.,) are very common in power line networks. Impulse noise will produce temporal effects in channel capacity. Between two impulse noise events, the channel capacity can be very high, while during the impulse noise the capacity is very low. To obtain low FEC block error rates, the channel has to be adapted close to the lower end of its capacity (i.e., capacity near impulse noise event) and hence is undesirable. Physical layer adapting to the higher end of the channel capacity hinges on the ability to efficiently retransmit corrupted portions

of the data at the MAC layer. Chapter 6 presents a novel 2-level MAC framing mechanism that enables efficient re-transmission of corrupt data. Both analytical and simulation results are used to compare the performance of the 2-level MAC framing with other viable approaches. These results show that 2-level MAC framing provides linear degradation in performance even under high error conditions and it outperforms other approaches.

Apart from the MAC framing overheads, each transmission will also incur overheads due to physical layer headers, acknowledgments and interframe spacings. The impact of these transmission overheads on the TDMA allocation requirements and efficiency of multimedia streams is investigated in Chapter 7. Results show that the allocation has to be increased by one or more transmission overhead to support low latency applications. Further the increase the increase in allocation requirements is not highly dependent on the application data rate. Hence, low data rate applications can incur significant loss in efficiency. These results show that channel adaptation should take into consideration the application data rate to improve the overall capacity of the system.

HomePlug AV uses a beacon based Time Division Multiple Access (TDMA) technique for providing guaranteed bandwidth to multimedia streams. Beacons in HomePlug AV carry TDMA allocation (or scheduling) information for various active multimedia streams. Since a station that missed a beacon will not know the schedule for that beacon period, it will not be able to transmit. Due to the large attenuation and impulse noise, beacon detection cannot always be guaranteed. To overcome occasional beacon loss, HomePlug AV uses persistent beacon schedules. Persistent schedules are valid for multiple beacon periods, thus enabling a station to transmit even if it misses one

or more beacons. In Chapter 8, we use a Markov chain based analysis to investigate the impact of beacon loss on systems with and without persistent beacon schedule. Results show that by using persistent current and preview schedule or persistent preview schedules, HomePlug AV systems can tolerate up to 10% beacon loss with minimum impact of MAC efficiency and QoS guarantees.

A brief summary of the major contributions of this dissertation and the scope for future work are presented in Chapter 9.

CHAPTER 2
BACKGROUND

Power line communications stands for the use of power supply grid for communication purpose. Power line network has very extensive infrastructure in nearly each building. Because of that fact the use of this network for transmission of data in addition to power supply has gained a lot of attention. Since power lines are devised for transmission of power at 50-60 Hz and at most 400 Hz, the use this medium for data transmission, at high frequencies, presents some technically challenging problems. Besides large attenuation, power line is one of the most electrically contaminated environments, which makes communication extremely difficult. Furthermore, the restrictions imposed on the use of various frequency bands in the power line spectrum limit the achievable data rates.

Power lines connect the power generation station to a variety of customers dispersed over a wide region. Power transmission is done using varying voltage levels and power line cables. Power line cable characteristics and the number of crossovers play an important role in determining the kind of communication technology that needs to be used. Based on the voltage levels that are used, power lines can be categorized as follows:

1. High-tension lines: These connect electricity generation stations to distribution stations. The voltage levels on these lines are typically in the order of hundreds of kilovolts and they run over distances of the order of tens of kilometers.
2. Medium-tension lines: These connect the distribution stations to pole mounted transformers. The voltage levels are of the order of a few kilo volts and they run over distances of the order of a few kilometers.

3. Low-tension lines: These connect pole-mounted transformers to individual households. The voltage levels on these lines are of the order of a few hundred volts and these run over distances of the order of a few hundred meters.

High-tension lines represent excellent carriers for RF energy as we only find open wire equipment with very few crossovers. A transmission power of about 10 watts is often sufficient to overcome distances of more than 500 kilometers. Around the year 1922 the first carrier frequency system (CFS) began to operate on high-tension lines in the frequency range of 15-1500 KHz [3, 4, 5]. During the past and even nowadays the main purpose of CFS was to maintain the operability of the power supply. While in former times speech transmission was dominant, today we have more and more digital data communications due to the rapid progress of overall automation. Through the application of modern digital modulation and coding schemes, a significant enhancement of bandwidth efficiency could be achieved for CFS.

Medium- and low-tension lines are characterized by a large number of cross connections and different conductor types (e.g., open wire and cable). Long distance RF signal propagation is extremely bad in this environment because of high attenuation and impedance matching problems. Around the year 1930 ripple carrier signaling (RCS) began to operate on these lines. These used a frequency range below 3 KHz down to 125 Hz with amplitude shift keying (ASK) modulation technique. The data rate achieved by RCS is in the order of a few bits per second. Load management and automatic reconfiguration of power distribution networks were among the most important tasks performed by RCS.

We see that historically the use of power line communications was mainly for use by the utility corporations (UCs) in maintaining the seamless power supply. The UCs generally regarded the power distribution wiring as a “natural” medium for their

communication needs, as all important stations are connected. The lack of sophisticated signal processing techniques at affordable cost points limited the applicability of PLC technologies in the past.

2.1 Low Bandwidth PLC

In the mid 90's, data communications over low-tension lines regained a lot of attention for enabling "smart houses." A "smart house" can be defined as a building equipped with numerous sensors and actuators, where for example heating, air-conditioning and illumination can be automatically and remotely controlled and supervised. Furthermore safety systems such as burglar or fire alarms may be included [4, 6, 7]. New generations of low bandwidth PLC systems were designed for addressing this market.

2.1.1 Regulatory constraints

Frequency bands used by these devices are restricted by the limitations imposed by the regulatory agencies [8]. These regulations are developed to ensure harmonious coexistence of various electromagnetic devices in the same environment. The frequency restrictions imposed in two of the main markets, North America and Europe, are shown in Figure 1-1. The Federal Communications Commission (FCC) and the European Committee for Electro technical Standardization (CENELEC) govern regulator rules in North America and Europe respectively.

In North America frequency band from 0 to 500 KHz can be used for power line communications. However the regulatory rules in Europe are more stringent. The spectrum is divided into five bands based on the regulations. They are

4. Frequency Band from 3 – 9 KHz: The use of this frequency band is limited to energy provides; however, with their approval it may also be used by other parties inside consumer's premises.

5. Frequency Band from 9 – 95 KHz: The use of this frequency band is limited to the energy providers and their concession-holders. This frequency band is often referred as the “A-Band”

6. Frequency Band from 95 – 125 KHz: The use of this frequency band is limited to the energy provider’s costumers; no access protocol is defined for this frequency band. This frequency band is often referred as the “B-Band”

7. Frequency Band from 125 – 140 KHz: The use of this frequency band is limited to the energy providers customers; in order to make simultaneous operation of several systems within this frequency band possible, a carrier sense multiple access protocol using center frequency of 132.5 KHz was defined. This frequency band is often referred to as the “C-Band”

8. Frequency Band from 140 – 148.5 KHz: The use of this frequency band is limited to the energy provider’s customers; no access-protocol is defined for this frequency band. This frequency band is often referred to as the “D-Band.”

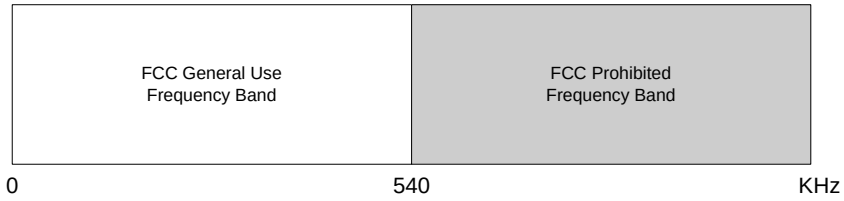

(a) FCC Frequency Band Allocation for North America

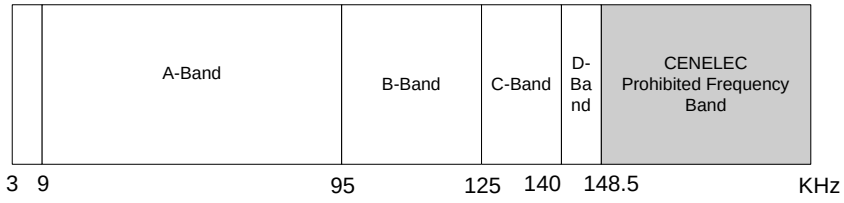

(b) CENELEC Frequency Band Allocation for Europe

Figure 1-1: FCC and CENELEC frequency band allocation

Thus in Europe power line communications are restricted to operating in the frequency range from 95 – 148.5 KHz. Apart from band allocation, regulatory bodies also impose limits on the radiations that are emitted by these devices. These reflect as restrictions on the transmitted power in each of these frequency bands.

2.1.2 Technologies

Various protocols have been developed for use by low bandwidth digital devices for communication on power line. Each of these protocols different in the modulation technique, channel access mechanism and the frequency band they use. Various products based on these protocols are available in the market and are mainly used for home automation purposes. A brief overview of these protocols is presented here.

2.1.2.1 X-10

The X-10 technology is one of the oldest power line communication protocol. It uses a form of amplitude shift keying (ASK) technique for transmission of information. Although it was originally unidirectional (from controller to controlled modules) recently some bi-directional products are being implemented. X-10 controllers send their signals over the power line to simple receivers that are used mainly to control lightning and other appliances. Some controllers available today implement gateways between the power line and other medium such as RF and infrared.

A 120 KHz amplitude modulated carrier, 0.5 watt signal, is superimposed into AC power line at zero crossings to minimize the noise interference. Information is coded by way of bursts of high frequency signals. To increase the reliability each bit of information is transmitted separately, which limits the transmission rate to 60 bits per second. This represents poor bandwidth utilization while the reliability of transmission is severely compromised in a noisy environment. These are the main reasons why this technology has limited applications.

2.1.2.2 CEBus

The CEBus protocol uses peer-to-peer communication model. To avoid collisions a carrier sensed multiple access with collision resolution and collision detection

(CSMA/CRCD) is used. The power line physical layer of the CEBus communication protocol is based on spread spectrum technology patented by Intellon Corporation. Unlike traditional spread spectrum techniques (that used in frequency hopping or time hopping or direct sequence), the CEBus power line carrier sweeps through a range of frequencies as it is transmitted. A single sweep covers the frequency band from 100-400 KHz. This frequency sweep is called a chirp. Chirps are used for synchronization, collision resolution and data transmission. Using this chirp technology data rate of about 10 KHz can be obtained. The frequency used by this technology restricts its use in only North American market.

2.1.2.3 LonWorks

LonWorks is a technology developed by Echelon Corporation and provides a peer-to-peer communication protocol, implemented using Carrier Sensed Multiple Access (CSMA) technique. Unlike CEBus, LonWorks is a narrowband spread spectrum modulation technique using the frequency band from 125 KHz to140 KHz. It uses multi-bit correlator intended to preserve data in the presence of noise with a patented impulse noise cancellation. An advantage of the narrowband signaling is that it can be used in both North American and European markets.

2.2 High Bandwidth PLC

High-speed communication over low-tension power lines has recently gained lot of attention. This is fueled by the unparalleled growth of the Internet, which has created accelerating demand for digital telecommunications. High bandwidth PLC devices are designed to exploit this market. More specifically, these devices use the existing power line infrastructure within the apartment, office or school building for providing a local area network (LAN) to interconnect various digital devices. Some of the applications

include high-speed Internet access, multimedia, smart appliances/remote control, home automation and security; data back up, telecommunications, entertainment and IP-telephony.

2.2.1 Regulatory constraints

High bandwidth PLC devices for communication on power line use the frequency band between 1 MHz and 30 MHz. In contrast to low bandwidth digital devices, the regulatory standards for this region of the spectrum are still being developed. Currently, United State is the only country where the regulations for High Bandwidth PLC systems are well defined. In United States, PLC systems operate under FCC Part 15 rules using the frequency band between 1.8-30 MHz. Several sub-bands within this range have to be notched to prevent interference with licensed services.

2.2.2 Channel characteristics

Power lines were originally devised for transmission of power at 50-60 Hz and at most 400 Hz. At high frequencies power line is very hostile for signal propagation [1, 2]. In the section that follows gives a brief overview of power line channel characteristics in the frequency band between 1 MHz and 30 MHz.

2.2.2.1 Attenuation characteristics

High frequency signals can be injected on to the power line by using an appropriately designed high pass filter. Received signal power will be maximum when the impedance of the transmitter, power line and the receiver are matched. Dedicated communication channels like Ethernet have known impedance, thus impedance matching is not a problem. However, power line networks are usually made of a variety of conductor types and cross sections joined almost at random. Therefore a wide variety of characteristic impedances will be encountered in the network. Further, the network

terminal impedance will tend to vary both at communication signal frequencies and with time as the consumer premises load pattern varies. The multipath effect resulting from impedance mismatch and the attenuation caused by the electric wiring makes power line channels highly frequency selective [9]. While a typical channel may present an average attenuation of approximately 40 dB, it is not uncommon for portions of the bands to experience greater than 60 dB of attenuation. Similarly, while most power line channels have a significant delay spread of 1 to 2 μs, it is not uncommon for some channels to exhibit a delay spread larger than 5 μs. Figure 2-1 and Figure 2-2 show a sample power line channel impulse and frequency response.

One of the unique characteristics of power line channels is the dependence of channel characteristics on the AC line cycle. Electric appliances may turn on and off, and/or draw electric power as a function of the AC line cycle. While this may change both the channel's frequency response and noise profile, it is more common to see changes in only the noise profile.

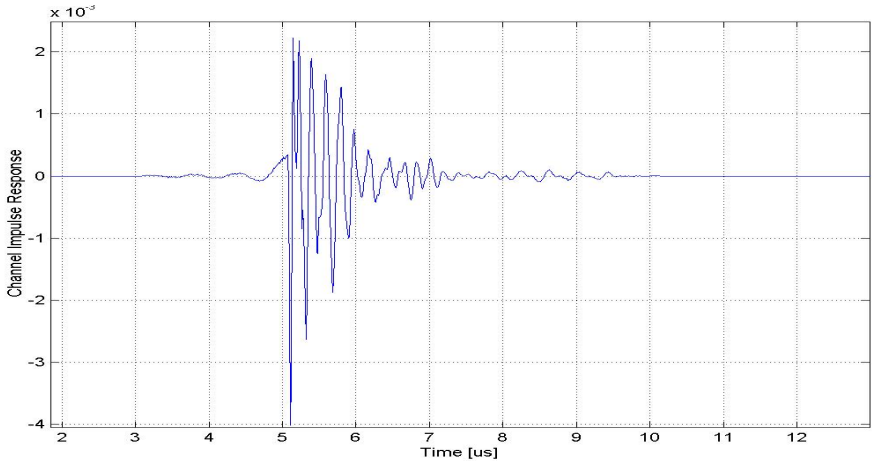

Figure 2-1: Power line channel impulse response

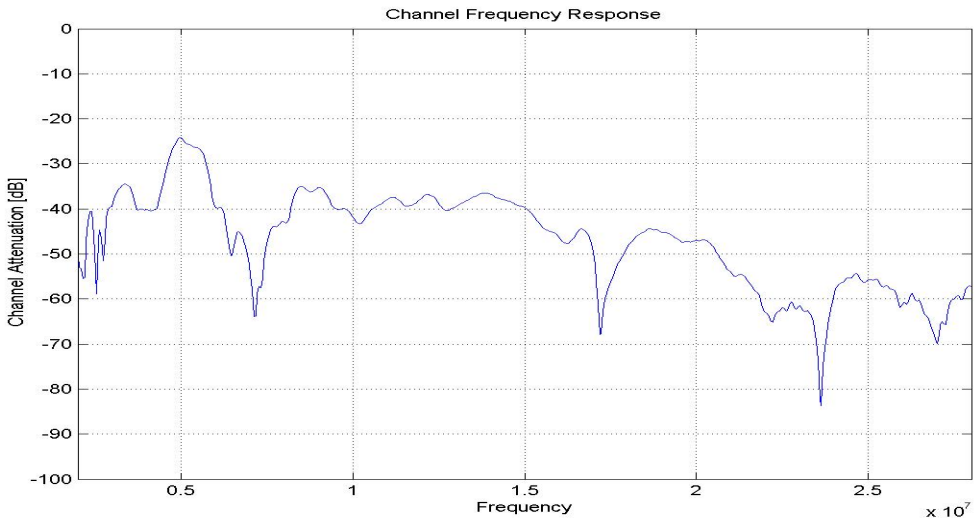

Figure 2-2: Channel frequency response

2.2.2.2 Noise characteristics

The major sources of noise on the power line are from electrical appliances, which generate noise components that extend well into the high frequency spectrum. Worse, there are often impulse noise sources. Impulse noise can be categorized as periodic or continuous based on when it occurs relative to the underlying AC line cycle. Figure 2-3, 2-4 and 2-5 respectively show periodic impulse noise from light dimmer, yard light and halogen lamp in addition to the data signal (rectangular shape). Devices that contain brush motors (Figure 2-6) also produce impulse noise. Induced radio frequency signals from broadcast, commercial, military, citizen band and amateur stations also impair certain frequency bands. Because much of the noise experienced by each node may be highly localized due to attenuation, the noise profile seen by each PLC device may be significantly different. Therefore, power line channels are not typically symmetric.

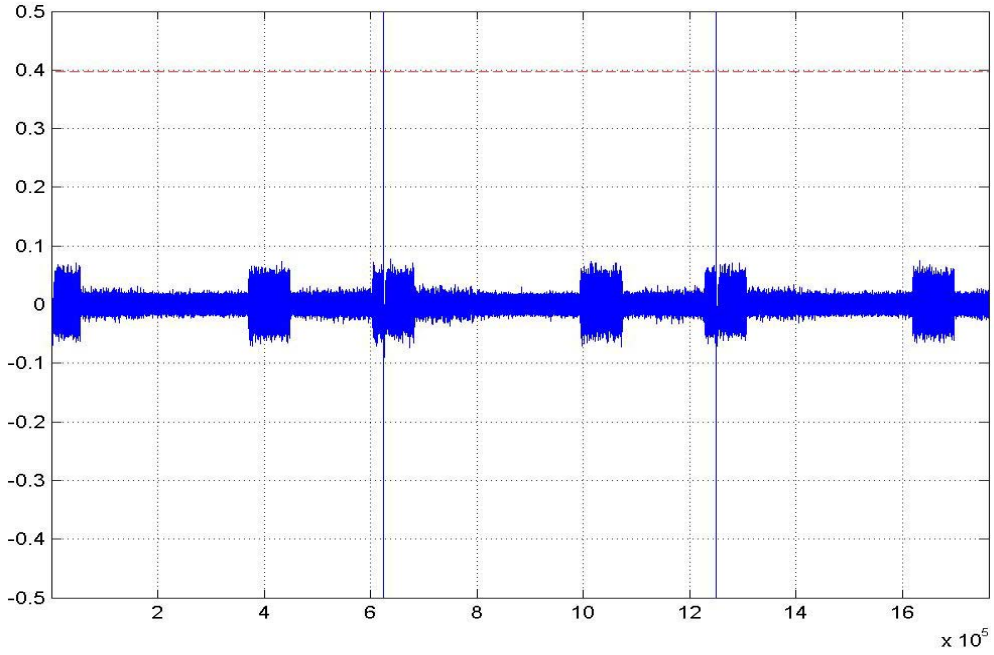

Figure 2-3: Noise generated by light dimmer

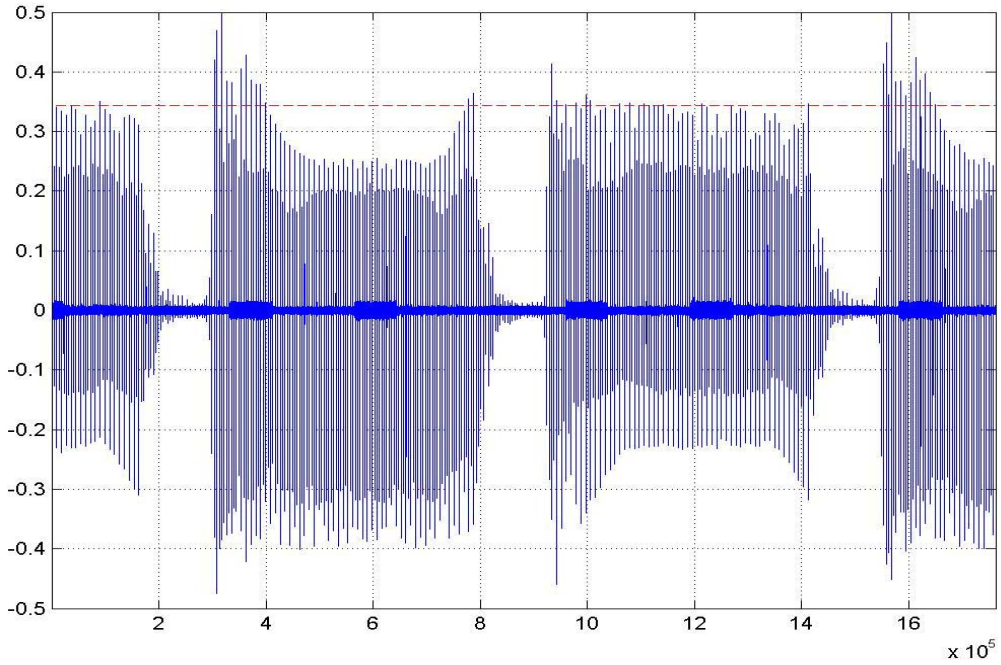

Figure 2-4: Noise generated by yard light

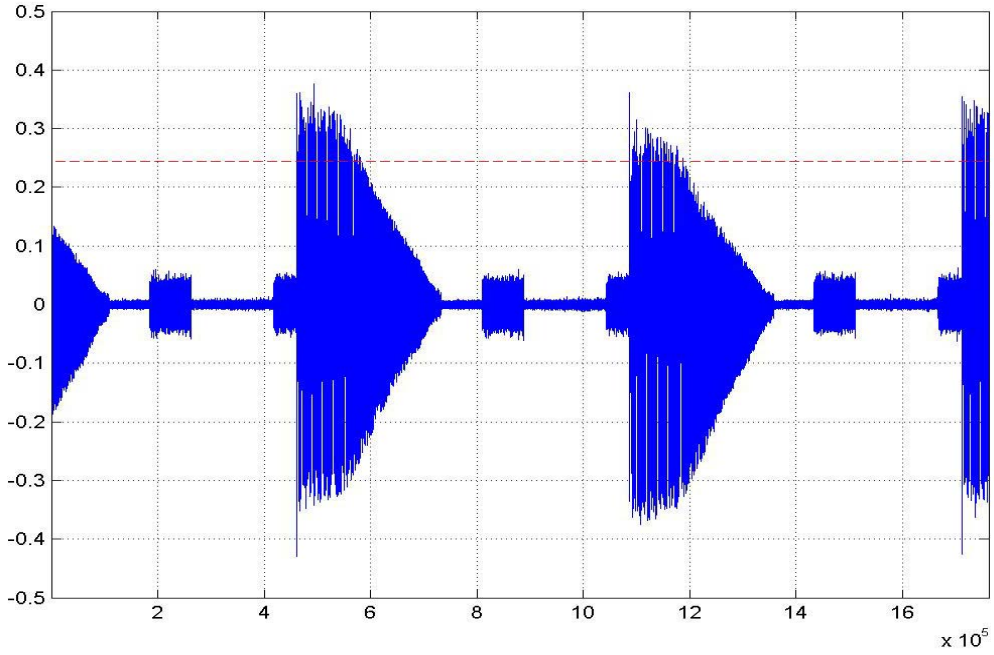

Figure 2-5: Noise generated by halogen lamp

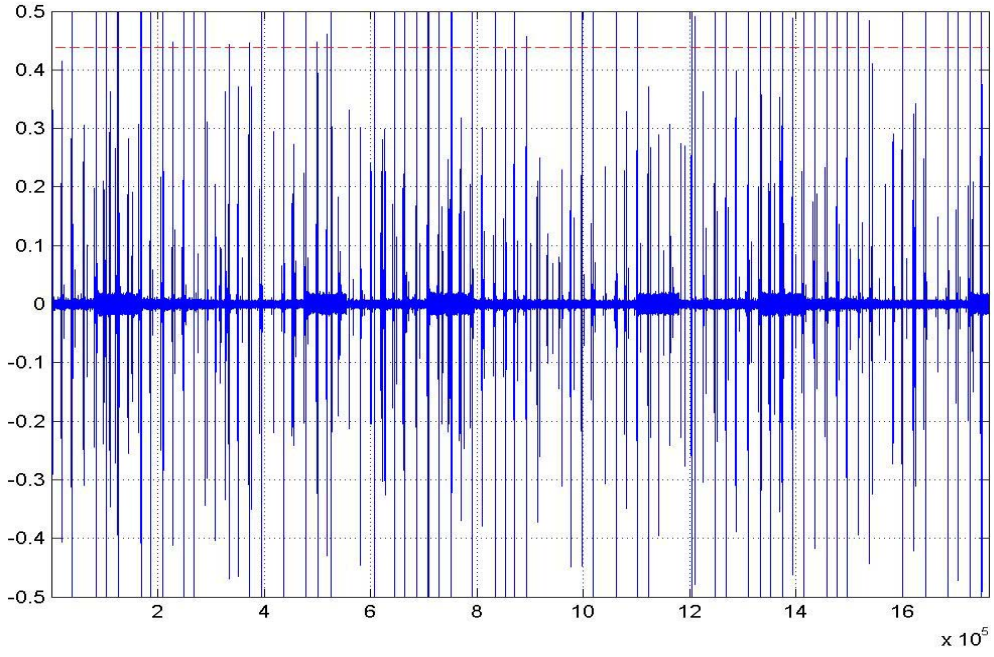

Figure 2-6: Noise generated by hair dryer

2.2.3 Technologies

The first generation of high bandwidth PLC systems were developed to enable high-speed data communications in a Small Office Home Office (SOHO) environments. These technologies represented a gain leap in exploiting the power lines as a true communication medium. The most widely deployed first generation PLC systems are based on HomePlug 1.0 Standard. HomePlug 1.0 was developed by HomePlug Powerline Alliance; a non-profit industry association that was formed in March of 2000 by a group of industry leading companies to enable standards based power line networking products. In the next chapter, we take a detailed look at the technology behind HomePlug 1.0 and how it enabled it to overcome the harsh power line environment. The performance of this technology against other popular SOHO networking options was also presented.

As home networks become more and more common, there is increasing demand for enabling multimedia communications within the home. Multimedia applications not only require high bandwidth but also need guarantees on various QoS elements like delay, jitter and packet loss probability. A second generation of HomePlug Standards, HomePlug AV was developed to address this need. In Chapters 5, 6, 7 and 8, we investigate some of the design choices made in HomePlug AV and evaluate their performance.

CHAPTER 3
HOMEPLUG 1.0 – TECHNOLOGY DESCRIPTION AND PERFORMANCE EVALUATION

Affordable broadband Internet communication to residential customers is now available via Cable Modems and various flavors of Digital Subscriber Lines (DSL). In turn there is a growing need for in-home networks to share this single full-time Internet access link, along with network connectivity for various computers and printers in the home. A good home networking solution should be easy to setup, zero maintenance, cost effective and should also be able to provide reliable performance throughout the house With multiple outlets in every room, residential power lines are already the most pervasive networks in the home. Using this existing infrastructure to provide high speed networking capabilities provides several benefits. First of all, there is no need for expensive rewiring of the house. Secondly, almost all devices that need to be networked are already connected to the AC wiring. Thus, home networking becomes as simple as plugging the device in the AC outlet.

HomePlug 1.0 Standard was developed to enable ubiquitous, easy to use and affordable home networking. In this chapter we present detailed description of HomePlug 1.0 technology and evaluate its performance based on simulations and field tests. A more thorough treatment of the material can be found in the following papers we published [10, 11, 12]. The organization of this section is as follows. In Section 3.1 we provide a brief overview of various options for home networking and their pros and cons. Details of HomePlug 1.0 technology and simulation based evaluation of its performance is

presented in Section 3.2 and Section 3.3, respectively. Field test based performance comparison of HomePlug 1.0 and IEEE 802.11b/a are presented in Section 3.3.

3.1 Home Networking Solutions

A variety of technological alternatives are available to home networking. These technologies can be grouped into three different categories based on the medium they use for transfer of data. They are:

1. New Wire
2. Wireless
3. No New Wires

3.1.1 New wire solution

New Wired solutions use specialized cable to connect various devices. There are the most matured technologies and have found wide spread acceptance in enterprise, campus and industrial networks. Some examples include Ethernet, Token Bus and Token ring.

Ethernet is one of the most widely used networking solution inside the home these days. The major drawback is that it would require retrofitting the house with these specialized cables. This is quite an expensive proposition as it could involve drilling holes in the walls. Further, most of the electricians have little or no knowledge on how to install these cables. For example, a simple mistake of improper termination of Ethernet wire will make the network useless. Another drawback of Ethernet is the lack of proper QoS provisions that are very critical for any networking technology to be successful in the home networking market. The recently developed IEEE 1394b [13] specification also targets the home networking market. This is an extension of the popular IEEE 1394 [14] (also known as FireWire or i.Link) that supports cord lengths up to 100 meters. Using Cat 5 UTP cords, it can support data rate of 100 Mbps over 100 meters distance. Using 50µm

fiber, data rates of up to 3200 Mbps can be supported for cord lengths of up to 100 meters.

3.1.2 Wireless solution

Wireless technologies use high frequency radio waves to transfer data. The most predominant technologies include,

1. IEEE 802.11b/a/g,
2. BlueTooth,
3. HomeRF, and
4. Ultrawide band.

The main benefit of using wireless networks is the freedom to move around the house while maintaining network connection. IEEE 802.11x [15, 16, 17, 18] are the most popular wireless home networking technology. IEEE 802.11b uses Direct Sequence Spread Spectrum (DSSS) in the 2.4GHz Industrial, Scientific and Medical (ISM) band and provides PHY rates of up to 11 Mbps. The extensions of this technology include IEEE 802.11g and IEEE 802.11a. IEEE 802.11g uses the same frequency bands as IEEE 802.11b, but with OFDM modulation and provides PHY rate of up to 54 Mbps. IEEE 802.11a uses the 5 GHz Unlicensed National Information Infrastructure (U-NII) bands along with OFDM modulation to provide up to 54 Mbps data rates. The main draw back of this technology has been coverage and quality of service.

BlueTooth technology [19, 20] uses the 2.4GHz ISM band with frequency hopped spread spectrum technology. This technology should be treated more like a Personal Area Networking solution rather than a Home Networking solution due to lower transmit power required by the kind of applications they serve.

HomeRF also uses the 2.4GHz ISM band with frequency hopped spread spectrum technology. This technology had limited acceptance in the market. The only advantage of this when compared to IEEE 802.11b is a better support for VoIP traffic.

The use of Ultrawide Band (UWB) technology [21, 22] was recently approved by the FCC in February 2002. UWB is defined as any radio technology having a spectrum that occupies a bandwidth greater than 20 percent of the center frequency, or a bandwidth of at least 500 MHz. There are two competing UWB standards.

1. Multi-Band OFDM (MBOA) UWB standard developed by WiMedia Alliance, and
2. Direct Sequence Code Division Multiple Access (DS-CDMA) UWB standard developed UWB Forum

UWB technologies can enable data rates of up to 480Mbps. As with Bluetooth, Ultrawide band signals have limited range and are more suitable for Personal Area Networks.

3.1.3 No new wire solutions

No New wire solutions use existing wiring inside the house to provide high-speed communication capabilities. These technologies include

5. HomePlug 1.0, HomePlug AV
6. HomePNA, and
7. MoCA

HomePlug 1.0 and HomePlug AV technologies uses the existing power line wiring inside the house and provide maximum PHY data rates of 14Mbps and 150Mbps, respectively. The ubiquity of power outlets is the greatest advantage when compared to other wired technologies.

HomePNA uses existing phone line as an infrastructure to provide home networking. The HomePNA 3.0 standard [23] released in 2003 enables data rates up to

128 Mbps with optional extensions to 240 Mbps. It also has deterministic QoS, but suffers from a limited number of available outlets in the house.

Multimedia over Coax (MoCA) [24] uses existing coax wiring to provide home networking. To avoid interference with video channels, MoCA uses 850MHz to 1500MHz frequency band. Similar to using existing telephone wiring, cable outlets are typically limited to 3 or 4 in the average home and are certainly not present in all rooms. Use of splitters may also limit bi-directional transmission.

As we have seen in this section, there are several technologies that have targeted the home networking technologies. Most of the technologies have gained limited acceptance due to coverage or ubiquity problems. HomePlug and IEEE 802.11x are the most important contenders at present due to their ubiquity.

3.2 HomePlug 1.0 Technology

HomePlug 1.0 technology [11, 12, 25, 26] overcome the harsh channel conditions on the power lines by using an adaptive approach that uses robust transmission technique combined with sophisticated forward error correction (FEC) [27, 28], error detection, data interleaving, and automatic repeat request (ARQ) [29].

3.2.1 HomePlug Physical layer

Orthogonal Frequency Division Multiplexing (OFDM) is the basic transmission technique used by the HomePlug. OFDM is well known in the literature and in industry [30]. It is currently used in DSL technology [31], terrestrial wireless distribution of television signals, and has also been adapted for IEEE's high rate wireless LAN Standards (802.11a and 802.11g). The basic idea of OFDM is to divide the available spectrum into several narrowband, low data rate sub-carriers. To obtain high spectral efficiency the frequency response of the sub-carriers are overlapping and orthogonal,

hence the name OFDM. Each narrowband sub-carrier can be modulated using various modulation formats. By choosing the sub-carrier spacing to be small the channel transfer function reduces to a simple constant within the bandwidth of each sub-carrier. In this way, a frequency selective channel is divided into many flat-fading sub-channels, which eliminates the need for sophisticated equalizers.

The OFDM used by HomePlug is specially tailored for power line environments. It uses 84 equally spaced sub-carriers in the frequency band between 4.5MHz and 21MHz. Cyclic prefix and differential modulation techniques are used to completely eliminate the need for any equalization. Impulsive noise events are overcome by means of forward error correction and data interleaving. HomePlug payload uses a concatenation of Viterbi and Reed-Solomon FEC. Sensitive frame control data is encoded using turbo product codes.

The power line channel between any two links has a different amplitude and phase response. Furthermore, noise on the power line is local to the receiver. HomePlug technology optimizes the data rate on each link by using channel adaptation. Channel adaptation is HomePlug 1.0 involves Tone Allocation, modulation selection and FEC selection. Tone allocation is the process by which certain heavily impaired carriers are turned off. This significantly reduces the bit error rates and helps in targeting the power of FEC and Modulation choices on the good carriers. HomePlug allows for choosing from differential binary phase shift keying (DBPSK), differential quadrature phase shift keying (DQPSK) on all the carriers, with either ½ or ¾ FEC code rates. The end result of this adaptation is a highly optimized link throughput.

Certain types of information, such as broadcast packets, cannot make use of channel adaptation techniques. HomePlug uses an innovative modulation called ROBO, so that information is reliably transmitted. ROBO modulation uses a DBPSK with heavy error correction with bit repetition in time and frequency to enable highly reliable communication. ROBO frames are also used for channel adaptation.

3.2.2 HomePlug 1.0 MAC

The choice of Medium Access Control (MAC) protocol provides a different set of challenges. Home networks should be able to support a diverse set of applications ranging from simple file transfer to QoS demanding applications such as Voice-over-IP (VoIP) and low data rate streaming media. The HomePlug MAC is built to seamlessly integrate with the physical layer and addresses these needs.

HomePlug MAC is modeled to work with IEEE 802.3 frame formats. This choice simplifies the integration with the widely deployed Ethernet. HomePlug MAC appends the Ethernet frames with encryption and other management before transmitting it over the power line. A segmentation and reassembly mechanism is used to in cases where the complete packet cannot be fit in a single frame.

3.2.2.1 Frame formats

HomePlug technology uses two basic frame formats (refer Figure 5-1). A Long Frame consists of a Start of Frame (SOF) delimiter, Payload and End of Frame delimiter (EOF). A Short Frame consists of a Response Delimiter and is used as part of the Stop-and Wait automatic repeat request (ARQ) process. ARQ mechanism causes retransmission of corrupt packets, thus reducing the packet error rate.

All the delimiters share a common structure. A delimiter consists of a Preamble and Frame Control information field. The Preamble is a form of spread spectrum signal that is

used to determine the start of a delimiter. This is followed by Frame Control information, which is encoded using a robust Turbo Product Code and can be detected reliably even at several dB below the noise floor. Among other things, delimiters convey timing information that is used by MAC to determine the availability of the medium. The robust design of the delimiter helps the nodes to obtain a very high level of synchronization, thus reducing unintended collisions. The details of the various field contained in the Frame Control are given in Table 3-1. The Payload of the Long Frame delimiter is encoded based on the channel adaptation. The first 17 bytes of the payload contain the Frame Header. This field contains the source address, destination address and segmentation information.

HomePlug technology limits the maximum length of the payload field in the Long Frame to 160 OFDM Symbols (~1.3 msec). This manifests as better guarantees of QoS as the delay incurred by higher priority traffic due to on going lower priority transmission is reduced. If the packet cannot be fitted into a Long Frame, a segmentation and reassembly mechanism is used to send it in multiple Long Frames. The frame header contains information that is used by the receiver to properly reconstruct the segmented packet. The Payload is protected by a Frame Check Sequence (FCS) to detect uncorrected errors.

3.2.2.2 Channel access mechanism

The channel access mechanism used by the HomePlug MAC is a variant of the well-known CSMA/CA protocol. A typical CSMA/CA protocol would require nodes to sense the medium (this is the carrier sensing part) for other traffic. If the medium is busy, nodes will defer from transmitting until the medium becomes idle. When the medium becomes idle, nodes will wait for a randomly chosen duration (this is the collision avoidance part). A node will transmit only if it detects no other traffic on the medium

during this randomly chosen duration. HomePlug channel access scheme builds upon this mechanism by providing prioritized access along with high network utilization. The overall protocol includes a carrier sensing mechanism, a priority resolution mechanism and a backoff algorithm.

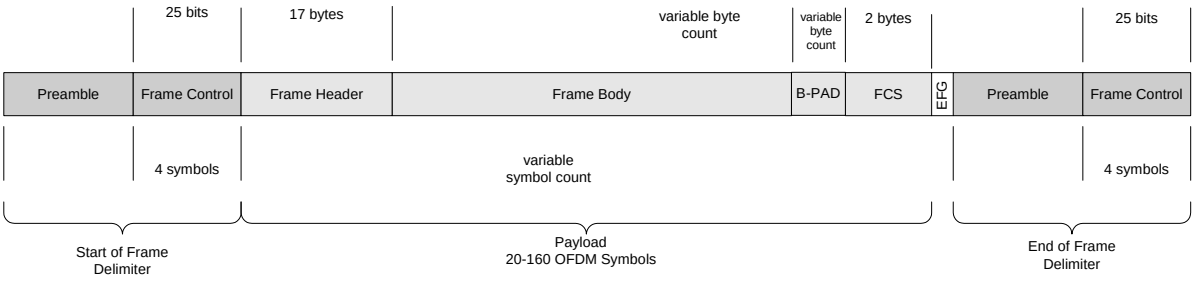

Figure 3-1: Long Frame format

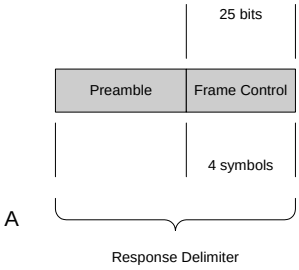

Figure 3-2: Short Frame format

The carrier sense mechanism helps HomePlug nodes to synchronize with each other. At the heart of this mechanism are the delimiters. HomePlug technology uses a combination of Physical Carrier Sense (PCS) and Virtual Carrier Sense (VCS) to determine the state of the medium (i.e., if the medium is idle or busy and for how long).

PCS is provided by the HomePlug PHY and basically indicates whether a preamble signal is detected on the medium. VCS is maintained by the HomePlug MAC layer and is updated based on the information contained in the delimiter (refer Table 1). Delimiters contain information not only on the duration of current transmission but also on which priority traffic can contend for the medium after this transmission. PCS and VCS information is maintained by the MAC to determine the exact state of the medium.

Table 3-1: Frame Control information fields

Delimiter Type	Fields	Meaning
Start of Frame (SOF)	Type	This can be SOF with response expected or an SOF with no response expected depending on whether a Short Frame delimiter is expected at the end of this Long Frame
	Contention Control	When set to 1, this prevents all HomePlug nodes with packets of priority level equal to or less than the current Long Frame's priority from accessing the channel. However, higher priority nodes can still interrupt this transmission
	Frame Length	This indicates the length of the payload in multiples of OFDM symbol blocks
	Tone Map Index	This is an index to the channel adaptation information stored at the receiver. Note that the variable length Payload is encoded using the maximum transfer rates that can be achieved by the link.
End of Frame (EOF)	Type	This can be EOF with response expected or an EOF with no response expected depending on whether a Short Frame delimiter is expected at the end of this Long Frame.
	Contention Control	The information conveyed is same as that conveyed by this field in SOF delimiter. This redundancy helps in better synchronization.
	Channel Access Priority (CAP)	This field indicates the priority of the current Long Frame.
Response (Resp)	Type	This can be ACK (positive acknowledgment), NACK, (negative acknowledgment indicating faulty reception) , or FAIL (negative acknowledgment indicating lack of resources)
	Channel Access Priority (CAP)	This field indicates the priority of the preceding Long Frame

The Priority resolution mechanism provides prioritized access of the medium in a highly distributed manner. Due to the distributed nature of this mechanism, there is no need for a central node to coordinate access over the medium as in the case of some networking technologies. HomePlug allow up to four different priority levels. At the heart of this priority resolution mechanism are the priority resolution slots (PRS) and the priority resolution signals. Priority resolution signals use a form of spread spectrum signal that has a high tolerance to delay spread and is also very robust. High tolerance to delay spread prevents destructive interference when multiple nodes assert in the same priority resolution slot. After the end of every transmission, two slots are allocated for priority resolution. Figure 3-3 shows the occurrence of priority resolution signals with respect to the end of previous transmission and the subsequent contention period. After priority resolution slots, contention will be only between nodes that have the highest available priority in the network. For example, when all four priorities are present in the network, Priority 3 and Priority 2 nodes will transmit priority resolution signal in PRS0. Priority 1 and Priority 0 nodes will detect this signal, causing them to defer to the higher priority traffic. Priority 3 nodes will transmit a priority resolution signal in PRS1, which will be detected by the Priority 2 nodes, causing them to defer. Thus only Priority 3 nodes will contend in the Contention Period.

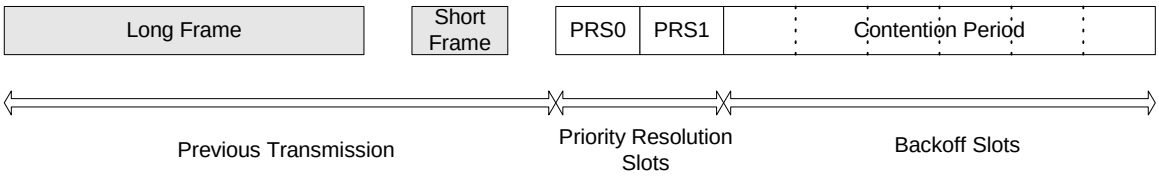

Figure 3-3: Priority resolution and backoff scheme

The backoff algorithm used by HomePlug MAC is designed to provide high network utilization (which manifests itself as high network throughput) even under

heavily loaded conditions. It is also tailored to seamlessly integrate with the priority level construction and the applications that each of these priorities is expected to support. Note that only nodes that have the highest priority available in the network will contend during the Contention Period and all other nodes will defer. From a HomePlug view of the power line network, all traffic with priority a less than the maximum available traffic priority in the network is pretty much ignored. Lower priority traffic will have to wait till all the higher priority traffic is transmitted.

As with other CSMA/CA algorithms, the backoff slot is chosen to be a random integer between 0 and the Contention Window Size. The growth of the contention window under HomePlug is controlled by the estimation of traffic on the network as well as on the priority of the traffic. This helps HomePlug nodes achieve higher network utilization and also control the latency for higher priority traffic.

3.2.2.3 Segmentation and reassembly mechanism

HomePlug uses an adaptive approach to maximize the throughput on each link. Furthermore, the maximum size of the long frame is limited to 160 OFDM symbols for the payload. For cases in which the complete Ethernet packet cannot be fitted in a single long frame, segmentation and reassembly mechanism is used. The necessary information for proper reassembly at the receiver is included in the segment control field of the frame header. Multiple segments can be transmitted in a single burst to obtain high throughputs. However, each segment is required to go through priority resolution mechanism. This ensures that a segment burst can be interrupted by higher priority traffic, thus reducing the latency for higher priority traffic. HomePlug allows extension of this segment bursting across multiple Ethernet packets to provide contention free access.

3.3 HomePlug 1.0 Performance based on Simulations

In this section we report the measurements observed using an event-based C program to simulate a HomePlug 1.0 power line network. All scenarios assume QPSK and a 3/4 coding rate on various links. In this simulation, we use UDP, TCP, and VOIP traffic. Both TCP and UDP traffic sources are configured to generate 1460 byte packet at priority 0. TCP and UDP traffic is generated with exponential inter-arrival time with 100 microsecond average. This will ensure that the network will remain saturated. VOIP traffic is modeled as isochronous with a 20 msec interarrival time. The packet size of VOIP is 160 bytes and is assigned the highest priority, 3.

In Table 3-2, we provide the of simulation results of a power line network. The UDP traffic simulation scenario 1 shows the best throughput in our simulations since there is no contention at all. Table 3-2 also shows channel contention with 2 and 3 UDP nodes causes a modest reduction in channel throughput. In the TCP traffic simulation, though scenario 1 has only one traffic source, the bandwidth must be shared with data and response frames (e.g., TCP ACK packets) thus it provides lower performance than the UDP traffic simulation. The MAC throughput represents the total number of transmitted bytes of Ethernet payload transmitted by the MAC divided by the simulation time. The UDP throughput represents the total number of transmitted bytes of UDP payload divided by the simulation time. Similarly, TCP throughout represents the total number of transmitted bytes of TCP payload divided by the simulation time.

The third metric we provide in Table 3-2 is the PLC simulation results of one VOIP and multiple UDP connections. The high priority VOIP always wins the contention and the UDP nodes can send packets only when there is no VOIP traffic. In this simulation, the VoIP Delay indicates the average network delay (i.e., queuing delay and channel

access delay) incurred by the VoIP packets. These results show that the priority contention mechanism in HomePlug 1.0 can guarantee very low latency for delay sensitive traffic. The Table 3-2 also shows the simulation results of one VOIP and multiple TCP connections. The throughput of VOIP is small; the total throughput is dominated by the TCP component. The slight increase in VoIP delay is due to the increase in channel access time due to higher number of contending source (i.e., contention between TCP Data and TCP ACK).

Table 3-2: HomePlug 1.0 simulation results

Simulation Results			
Throughput of multiple UDP Traffic Streams			
	Scenario 1 (1 UDP)	Scenario 2 (2 UDP)	Scenario 3 (3 UDP)
MAC Throughput	8.08 Mbps	7.46 Mbps	7.46 Mbps
UDP Throughput	7.86 Mbps	7.26 Mbps	7.26 Mbps
Throughput of multiple TCP Traffic Streams			
	Scenario 1 (1 TCP)	Scenario 2 (2 TCP)	Scenario 3 (3 TCP)
MAC Throughput	6.16 Mbps	6.15 Mbps	6.12 Mbps
TCP Throughput	5.90 Mbps	5.89 Mbps	5.87 Mbps
Throughput of one VoIP and multiple UDP traffic streams			
	Scenario 1 1 VoIP, 1 UDP	Scenario 2 1 VoIP, 2 UDP	Scenario 3 1 VoIP, 3 UDP
MAC Throughput	7.89 Mbps	7.33 Mbps	7.29 Mbps
UDP Throughput	7.53 Mbps	6.99 Mbps	6.96 Mbps
VoIP Delay	2.75 msec	3.00 msec	3.00 msec
Throughput of one VoIP and multiple TCP traffic streams			
	Scenario 1 1 VoIP, 1 TCP	Scenario 2 1 VoIP, 2 TCP	Scenario 3 1 VoIP, 3 TCP
MAC Throughput	6.04 Mbps	5.85 Mbps	5.77 Mbps
TCP Throughput	5.65 Mbps	5.47 Mbps	5.39 Mbps
VoIP Delay	3.25 msec	3.25 msec	3.25 msec

3.4 HomePlug 1.0 Field Test Results and Comparison with IEEE 802.11b/a

To understand the real-world performance of HomePlug 1.0 and to compare it with a popular home networking alternative, IEEE 802.11a/b, we conducted field tests in 20 houses located in the Gainesville, Ocala, Orlando, and Belleview areas of Florida. The

choices of the houses used in the tests were in the medium to large range (1500–5000 ft^2), since larger houses provide a better range on the performance parameters of interest.

The equipment used in this test included the following.

- AP server: A Sony notebook with a 700 MHz Pentium III processor and 128 Mbytes RAM running Windows2000
- Mobile Station: An HP notebook with a 500MHz Pentium III processor and 128 Mbytes RAM running Windows2000
- Linksys HomePlug 1.0-based Powerline-to-Ethernet bridges
- Netgear IEEE 802.11b Access Point and PCMCIA Card
- D-Link DWL-5000AP IEEE 802.11a Access Point and D-Link DWL-A650 PCMCIA card

For PLC testing the two laptops were connected through the power line via Powerline-to-Ethernet bridges. For wireless testing, a modified infrastructure mode (MIM) was used. The AP server was connected to an access point using an Ethernet crossover cable to the built-in Ethernet socket. A PCMCIA slot in the mobile station was used to connect the wireless card. Note that typical wireless networks use an infrastructure mode (IM). In this mode, all wireless nodes communicate with each other through the access point, and must share the bandwidth over two hops. Furthermore, since these tests had the AP server connected to the access point via Ethernet, there was no other contention possible, so the test results should represent the best case scenarios in this regard.

3.4.1 Experiment method

The TCP throughput and distances were measured for various locations of AP and mobile stations inside the house. The AP server was located close to a phone or cable outlet, the most probable locations for the home network to be connected to the

broadband access network. The mobile station was located at various places where it would be likely to find other networked devices in the home. The AP Server antenna and Mobile Station antenna were placed randomly to minimize the effect of directional antenna gain. We argue that this is the typical antenna placement since ordinary users probably don't know how to set antenna directions to maximize throughput. Besides, not all locations are susceptible to antenna direction adjustment due to the surrounding environment.

WSTTCP, a popular TTCP implementation ported to Windows sockets, was used. The TCP buffer size was chosen to be 11,680 bytes (1460 × 8). The number of TCP buffers transmitted was chosen such that each test ran for approximately 60 seconds. A single run of WSTTCP involved starting the WSTTCP in receive mode at the receiver on a selected port. WSTTCP was then started at the transmitter with a specific TCP buffer size, number of TCP buffers to be transferred, receiver IP address, and receiver port number. At the end of transmission, WSTTCP (at both the transmitter and receiver) provided the throughput observed on the link. For several of these tests, real-time packet capture was also obtained to observe TCP stability. All the procedures were automated and required minimal human operation.

3.4.2 Results

The amount of data collected is too large to be presented, so only a summary of the most interesting findings is presented.

3.4.2.1 IEEE 802.11a indoor performance

The performance and coverage results of IEEE 802.11a are depicted in Fig. 3-4. Figure 3-4a shows the connectivity (i.e., percentage of good links) as a function of house area. As expected, the connectivity decreased as the house area increased. Results show

that connectivity is poor even in moderate size (2500 ft^2) houses. For larger houses (>4000 ft^2) the connectivity decreased to 20 percent. Figure 3-4b shows a scatter plot of throughput as a function of distance. It is interesting to note that IEEE 802.11a connectivity is almost zero when the distance is larger than 50 ft. Figure 3-4c shows the percentage of links that exceed the throughput values indicated on the x-axis. Note that the maximum IEEE 802.11a throughput obtained from the product being tested was larger than those expected from theory. This could be because of manufacturer-specific proprietary enhancements like the use of higher-level modulations. In summary, the statistics show that:

- IEEE 802.11a failed on at least one link in 19 of the 20 houses tested.
- 802.11a failed to connect in 45 percent of the links that were tested.
- 802.11a showed close to zero connectivity at distances larger than 50 ft.
- For shorter distances, 802.11a provided excellent throughput in most cases.

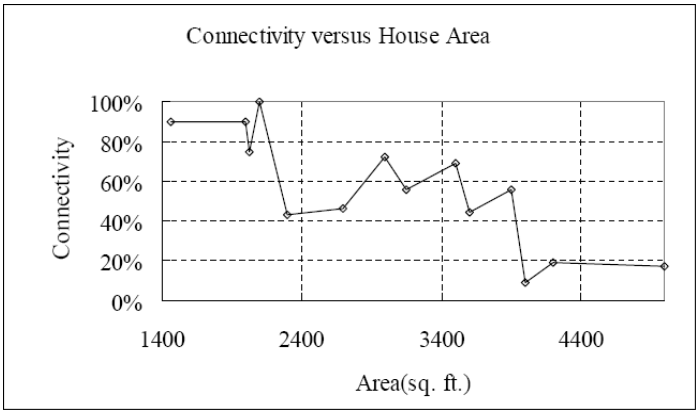

(A)

Figure 3-4: IEEE 802.11a indoor performance A) Connectivity versus house area B) Throughput versus distance C) Percentage of links versus throughput

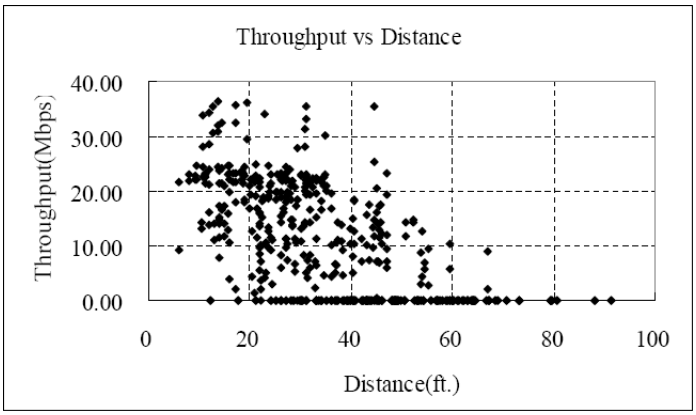

(B)

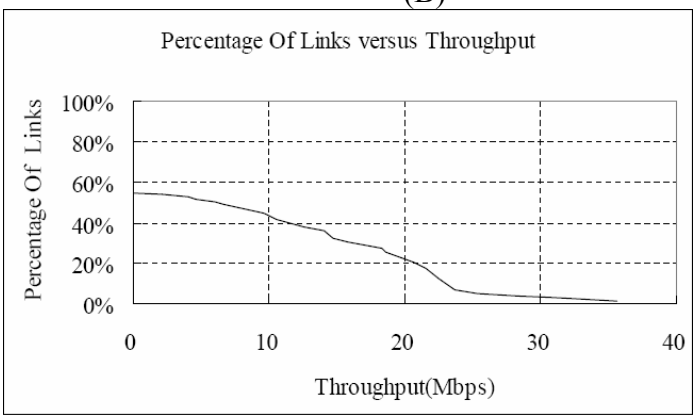

(C)

Figure 3-4: Continued

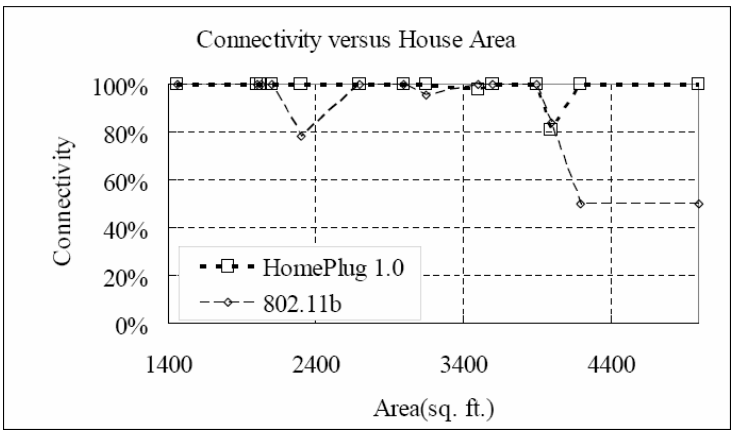

(A)

Figure 3-5: HomePlug 1.0 and IEEE 802.11b indoor performance A) Connectivity versus house area B) Throughput versus distance C) Percentage of links versus throughput (MIM) D) Percentage of links versus throughput (MIM)

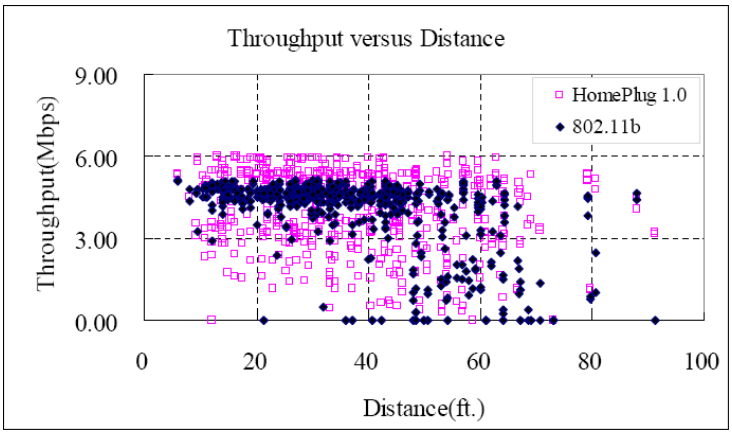

(B)

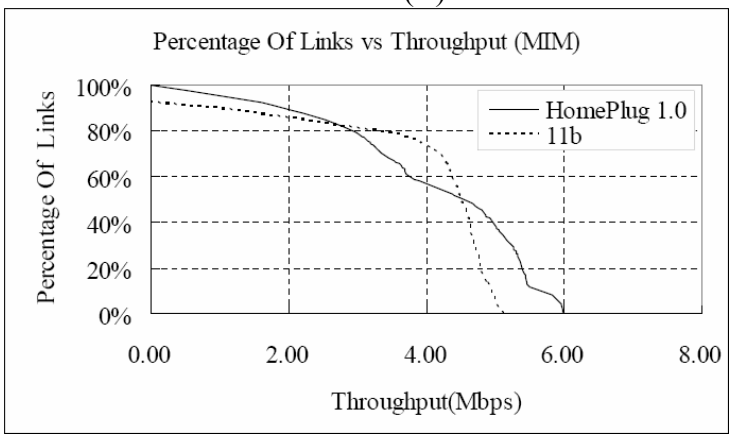

(C)

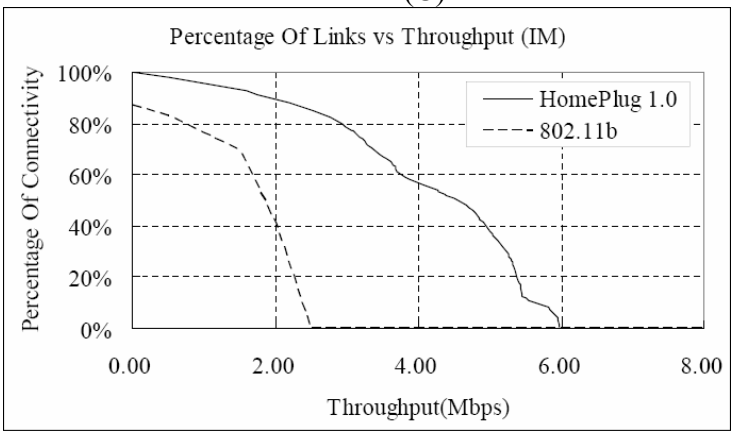

(D)

Figure 3-5: Continued

3.4.2.2 IEEE 802.11b and HomePlug 1.0

To facilitate comparison, the performance and coverage results of IEEE 802.11b and HomePlug 1.0 are shown together in Fig. 3-5. Figure 3-5a shows connectivity as a

function of house area. Both technologies show high connectivity for houses of less than 4000 ft^2. For houses larger than 4000 ft^2, the connectivity for IEEE 802.11b dropped dramatically to 50 percent in both of the houses tested, while HomePlug 1.0 continued to show high connectivity. Figure 3-5b shows a scatter plot of throughput as a function of distance. IEEE 802.11b typically provides close to maximum throughput at distances of less than 50 ft; for distance larger than 50 ft, the performance exhibited large variations. On the other hand, the HomePlug 1.0 system performance is not correlated with the line of sight distances measured in this experiment. This is because HomePlug 1.0 signals have to pass through the convoluted power line cable runs to reach the mobile station. Figure 3-5c shows the percentage of links that exceed the throughput value depicted on the x-axis.

Our experiments showed that the overall coverage of 802.11b was 92 percent. The maximum throughput observed in field-testing was 5.13 Mb/s. Figure 3-5c shows that around 70 percent of the connections operated at more than 4 Mb/s and 10 percent above 5 Mb/s. For HomePlug 1.0, the overall coverage is 98 percent. The maximum throughput observed in testing was 5.98 Mb/s. For HomePlug 1.0, 58 percent of the connections operated above 4 Mb/s and 38 percent had throughput above 5 Mb/s. The interesting crossover phenomena displayed in the graph reflect three aspects of the systems. First, the paucity of data rates supported by 802.11b hurts its performance when channel conditions are sub optimal. Second, HomePlug 1.0's ability to adapt to the channel conditions with a nearly continuous selection of data rates allows it to perform better under mediocre channel conditions. Finally, the higher maximum data rate of HomePlug 1.0 allows it to outperform 802.11b when channel conditions are favorable.

Note that, as mentioned earlier, in this experiment, throughput was measured between the access point and the mobile station in a MIM. However, this may not always be the way IEEE 802.11b stations communicate with each other. IEEE 802.11b networks can be configured in either ad hoc mode or IM. In ad hoc mode, wireless stations communicate with each other directly. However, typical home networks use an IM in which each wireless station communicates with the access point, which in turn forwards the data to the designated receiver. Some of the reasons for using IM include ease of setup, better coverage, and security. Furthermore, most wireless equipment is configured in IM out of the box, and must be reconfigured to ad hoc mode by the customer. Thus, in a typical IEEE 802.11b home network, all station-to-station transmissions, other than those designated to the access point itself (i.e., the access point is the final destination of the transmission) or those that originate from the access point, will be retransmitted by the access point. This reduces the effective throughput experienced between such stations.

We use a simple method to extrapolate the IM throughput from the MIM link throughput data collected in the field tests. A random sample was chosen from the set of collected data and used as the throughput (R1) from a TCP source to the access point. Another random sample was chosen from the sample and was used as the throughput (R2) from the access point to the TCP destination. The aggregate IM throughput then can be obtained by assuming that a fixed packet size of x bits is transmitting through two links with speeds R1 and R2. The total time to transmit this packet will require $x/R1 + x/R2$ s. Thus, throughput can be calculated by $R1 \times R2/(R1 + R2)$. Multiple iterations were used to obtain the distribution of the IM throughput. Although this method is not

fully accurate, it is reasonable to expect the actual performance in IM to be close to the values obtained.

Figure 3-5d shows the percentage of links that exceed the calculated IM throughput value depicted on the x-axis. These results show that HomePlug 1.0 stations provide superior coverage and throughput to IEEE 802.11b stations in IM. From the statistics, we make the following key observations:

- HomePlug 1.0 had a larger maximum throughput than 802.11b (about 1 Mb/s larger).
- On 60 percent of the links HomePlug 1.0 performed better than 802.11b links in MIM.
- On an average basis, HomePlug 1.0 gave approximately 0.2 Mb/s higher TCP throughput than 802.11b in MIM.
- In six of the 20 houses tested, IEEE 802.11b failed on at least one link.
- In two of the 20 houses tested, HomePlug 1.0 failed on at least one link.
- On an average basis, HomePlug 1.0 gave approximately 2.3 Mb/s higher TCP throughput than 802.11b would be expected to give in IM.

In summary, HomePlug 1.0 was found to provide better coverage and slightly better average TCP throughput than IEEE 802.11b in MIM, which would be typical for Internet access. In IM, HomePlug 1.0 was estimated to have throughput about 2.3 Mb/s greater than 802.11b. For shorter line-of-sight distances, 802.11x performed better than HomePlug 1.0, but for longer distances, the nearly continuous adaptation capability of HomePlug 1.0 allowed it to make better use of mediocre channels.

CHAPTER 4
POWER LINE MULTIMEDIA NETWORKING

Current generation PLC-based home networking technologies are mainly data centric. While these are good enough for applications like web browsing and file transfer, they cannot support multimedia applications such as audio/video streaming and multi-player gaming as these applications require much higher bandwidths and QoS than those provided by current technologies [32]. Table 4-1 shows the bandwidth and QoS requirements for typical multimedia applications. For example, High Definition MPEG2 streams (HDTV streams) will require quasi-error free performance at up to 24 Mbps of application throughput, and about 300 msec of delay with less than a few microseconds of jitter. Furthermore, typical home network usage scenarios include simultaneous transfer of multiple multimedia streams. Hence, home networks should be capable of providing 50-60 Mbps application level throughput within the network.

Table 4-1: Bandwidth and QoS requirements for multimedia applications

Application	Bandwidth (Mbps)	Latency (msec)	Jitter	Packet Loss Probability
High Definition (HD) Video Streaming	11 – 24	100 – 300	0.5 µs to several msec	Quasi Error Free
Standard Definition (SD) Video Streaming	2 – 6	100 – 300	0.5 µs to several msec	Quasi Error Free
DVD quality Video	6 – 8	100 – 300	0.5 µs to several msec	Quasi Error Free
Internet Video Conferencing	0.1 – 2	75 – 100	several msec	10^{-3}
Home Theater Audio (Multiple streams of audio)	4 – 6	100 – 300	0.5 µs to several msec	Quasi Error Free
Voice over IP (VoIP)	< 0.064	10 – 30	10 – 30 msec	10^{-2}
Network Gaming	< 0.1	10 – 30	10 – 30 msec	Quasi Error Free

1) msec => milliseconds
2) Quasi Error Free => Less than 1 packet dropped in 2 hours

To support the data rates and QoS required by the new generation of multimedia applications HomePlug Powerline alliance has released a new generation of HomePlug Standards, HomePlug AV. The HomePlug AV physical layer is designed to operate as close as possible to the channel capacity of the Power line. Due to the regulatory constraints, a spectrally efficient PHY is essential to ensure that multiple multimedia streams can be supported simultaneously and delivered to the whole house. HomePlug AV PHY incorporates the following salient features.

1. Bit-loading and higher order modulations (including 8, 16, 64, 256, and 1024-QAM) to allow each carrier to take full advantage of the SNR it experiences.
2. Coherent modulation, for increased the SNR given a fixed transmit power.
3. Long symbol time to minimize guard interval overhead.
4. Forward error correction based on parallel concatenated convolutional codes, to decrease the probability of path “no-connects” and ensure high throughput.
5. Transmission synchronized with respect to the AC line cycle, for stable and improved throughput.
6. MAC-PHY cross-layer design for handling impulse noise.

These enhancements enable HomePlug AV to achieve a maximum physical layer data rate of 150 Mbps. The exact details and rationale for the choice of various PHY parameters is beyond the scope of this work. Further details of HomePlug AV physical layer can be found in [33, 34].

The HomePlug AV Medium Access Control (MAC) layer is based on a hybrid of Time Division Multiple Access (TDMA) and Carrier Sense Multiple Access (CSMA). Each network has a designated device, the Central Coordinator (CCo), that coordinates the access to medium. The CCo periodically generates a beacon with information on

TDMA and CSMA allocation. TDMA is used by applications requiring QoS, while CSMA is used for transport of regular data. Some of the salient features of the HomePlug AV MAC are,

1. Beacon Period Synchronized to the AC line cycle to enable AC line cycle based channel adaptation by the PHY,
2. 2-Level MAC framing to effectively deal with impulse noise,
3. Beacon Schedule Persistence to mitigate beacon loss,
4. Dynamic TDMA allocations to deal with changing channel conditions,
5. Jitter Control based on the use of Arrival Time Stamps and Clock tracking,
6. Proxy Coordination function to deal with hidden stations,
7. Neighbor network mode of operation to deal with overlapping networks,
8. Coexistence with HomePlug 1.0 devices,

For further details of HomePlug AV MAC, refer to [33, 34]. In this dissertation, we investigate the first three features of the HomePlug AV MAC and evaluate their performance.

CHAPTER 5
CHANNEL ADAPTATION BASED ON CYCLO-STATIONARY NOISE CHARACTERISTICS

As power line communication (PLC) systems become more pervasive, there is increasing demand for new generations of PLC systems that enable bandwidth intensive applications like audio/video streaming and broadband access. To achieve the data rates necessary to support such applications within the current regulatory constraints, PLC systems should exploit the inherent characteristics of the power line channel that enable a more aggressive and optimized channel adaptation. One such characteristic is the cyclic variation of the noise power with the phase of the underlying AC line cycle.

In this section, we use extensive channel characterization measurements and analysis to investigate the performance enhancements that can be achieved by using a channel adaptation mechanism that exploits the cyclic variation in power line noise characteristics. The results show that a 30% improvement in physical layer (PHY) data rates can be obtained by continuously adapting to, and synchronizing communications with, the AC line cycle. Since continuous adaptation with respect to time is unduly complex for practical systems, we propose dividing the AC line cycle into multiple regions and adapting independently in each region. Results show that using a region size of 1-2 milliseconds provides optimal MAC throughput on most paths tested. A subset of the results presented in this chapter is also published in [35].

5.1 Introduction

The future evolution of PLC systems is driven primarily by an increasing demand for higher throughput. In LAN scenarios, the requirement to support multimedia applications like audio and video streaming is driving the need for higher throughput. In broadband access, the need to provide higher access speeds to a larger customer base (sharing the same medium) is causing the demand for higher throughputs. The design of PLC systems that enable this new generation of high data rate applications should exploit the unique channel characteristics observed on the power line channels to provide higher throughput within the current regulatory constraints.

A typical power line network consists of a variety of conductor types joined almost at random and terminating into a variety of electrical appliances. The conductors were primarily designed for transmission of power at 50-60 Hz and at most 400 Hz. At higher frequencies they provide characteristic impedances that not only vary based on the conductor type but also as a function of frequency. Impedance mismatches in power line networks result in a multipath effect that often cause deep nulls in certain frequency bands. Electrical appliances connected to the power line also significantly impact the PLC channel characteristics. Several common electric appliances turn on/off via switching power supplies and/or draw a varying amount of electric power as function of the underlying AC line cycle voltage. During these processes noise is generated that extends well into the higher frequency bands where PLC systems operate. One of the unique characteristics of this man-made noise is its cyclic dependency on the phase of the underlying AC line cycle.

The cyclic nature of noise in power line networks has been well known for several years. One of the first PLC based home automation technology, X10, exploited the low

noise characteristics at the zero crossing of the AC line cycle to increase the system robustness. O. Ohno and M. Katayama [36, 37] were among the first to characterize the noise in (0-500Kz) frequency band as 'cyclo-stationary'. In [38] Y. Hirayama et al., have investigated and confirmed the cyclo-stationary noise characteristics in the band from DC to 25MHz. Apart from noise, the channel response (or attenuation characteristics) can also change with the AC line cycle. F.J. Canete, J.A. Cortes, et al., [39, 40] has recently proposed a Linear Periodically Time Varying (LPTV) model for the PLC channel response. While in general both channel response and noise characteristics can vary as a function of the AC line cycle, it is more common to see significant variations in noise profile compared to that of the channel impulse response. In this section, we study the effect of the cyclic variation of power line noise on the performance of PLC systems.

The organization of the remaining sections is as follows. Section 5.2 describes the test setup used to measure channel attenuation and noise characteristics. Mechanisms for channel adaptation over cyclic channels and the various tradeoffs involved are presented in Section 5.3. Processing of the field test data to compute channel capacities is presented in Section 5.4. The results obtained are discussed in Section 5.5 and conclusions are presented in Section 5.6.

5.2 Channel Measurements

A total of 72 channels in two locations were characterized for use in this study. The characterization of each path involved computation of channel impulse responses and time domain noise captures spanning a single 60 Hz AC line cycle. The paths characterized were chosen at random within each location.

The setup for measuring the channel impulse response is shown in Figure 5-1. An arbitrary waveform generator, functioning as a transmitter with a digital-to-analog

converter (DAC), was loaded with a sounding waveform sampled at 75MS/s. The signal out of the DAC was amplified and coupled on to the power line. At the receiver side, the signal is coupled off of the power line medium, passed through a 2 to 30 MHz band pass filter, digitized at 75 MS/s using an analog-to-digital converter (ADC) card, and passed to Matlab for subsequent processing. Similarly, noise captures were performed by turning off the transmitter and simply digitizing a long portion of the ambient noise on the power line.

The transmit waveform consisted of a repeating OFDM symbol, specifically a frequency sweeping "chirp" occupying approximately 2 to 30 MHz. After digitizing the waveform at the receiver, ten consecutive chirps were time domain averaged to reduce noise. Frequency domain division of the received signal by the transmitted signal (along with calibration factors to remove the gain and/or frequency response of the amplifiers, couplers, etc.) was used to estimate the channel frequency response.

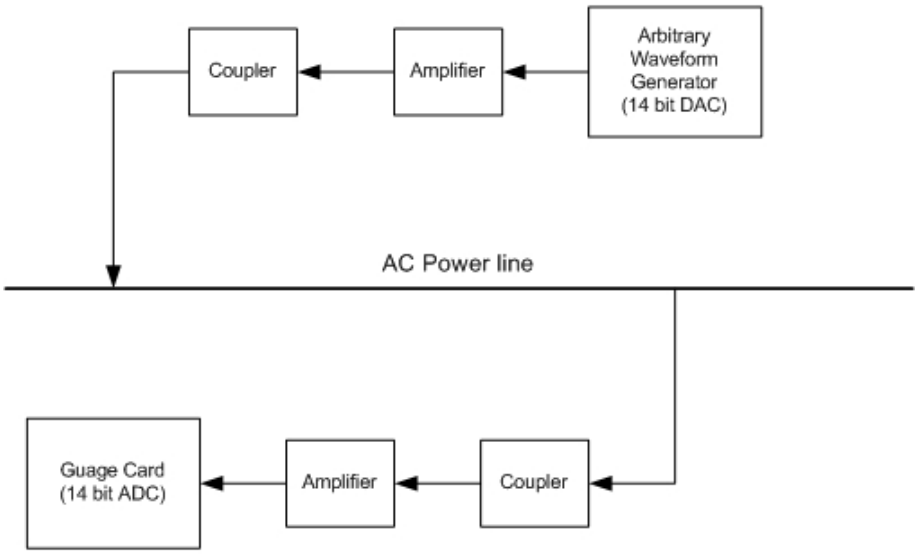

Figure 5-1: Channel measurement setup

5.3 Channel Adaptation

Channel adaptation in communication systems enables fine-tuning of the underlying PHY parameters to optimize the system performance. For periodically time-varying PLC channels, channel adaptation should also determine the dependency of the PHY parameters on the underlying phase of the AC line cycle. One simple means of accomplishing this is by dividing the AC line cycle into multiple regions and determining the PHY parameters independently for each such region.

Note that there is an important trade-off involved in the choice of number of regions and the system performance/complexity. By increasing the number of regions, a finer adaptation to temporal periodic channel characteristics can be obtained. However, this also increases the complexity of the system. A larger number of regions requires the transmitter and receiver to determine and maintain a larger set of PHY parameters and to apply them with higher accuracy within the AC line cycle. The bandwidth and memory requirements for generation, storing and exchanging the PHY parameters can be prohibitively expensive. Apart from this, inefficiencies are also incurred at the MAC Layer due to the need to limit the transmission of each physical layer protocol unit (PPDU) to a single region. Since most practical implementations will apply a single set of PHY parameters on a single PPDU, any transmission that spans across two or more regions will have to be divided into multiple transmissions (or PPDUs) with each PPDU occupying a single region. The extra overhead incurred in each PPDU transmission, due to frame synchronization and control overheads at the beginning every PPDU, will adversely affect the overall efficiency. For the analysis in this section, we use 130ms of incurred overhead per PPDU, based on the HomePlug AV standard [33, 34].

By decreasing the number of regions, the complexity of the channel adaptation mechanism can be reduced but the performance of the system suffers. This is due to the need to choose "worst case" PHY parameters within each region so that reliable communications can be guaranteed throughout the region. In the following section we investigate the effect of region size on the PHY and MAC layer data rates.

5.4 Computation of Channel Capacity

To investigate the effect of cyclic variation of noise on the performance of a PLC system, we first divide the 60Hz AC line cycle into 160 microslots. Each microslot (@104μs) forms the basic atomic for estimating the variation of signal-to-noise ratio (SNR) and Shannon Capacity [41] with respect to the AC line cycle. When computing SNR and Capacity, the bandwidth from DC to Nyquist (37.5 MHz) was divided into 192 subbands. This value was chosen as it provides an intermediate level of frequency domain resolution while at the same time enabling accurate noise power estimation as twenty consecutive 384-FFT outputs (5.12μs per FFT) may be averaged in each microslot. This entire process is described in the following steps.

First, a fixed subband transmit power, S_{TX}, was used for all subbands. This fixed power was picked to be comparable to the peak power spectral density allowed by HomePlug standards and hence compliant with FCC regulations. (Since this is merely a measurement of channel response, and not a data transmission, adherence to FCC regulations is not strictly required, but resulting SNR measurements are realistic for a practical system).

Next, the received carrier signal power, S_{RX} is measured across the frequency band of interest, and used to derive the channel attenuation, α. Preliminary observations show

that the channel attenuation coefficients typically exhibit little variation throughout the AC line cycle compared to the variation of the channel noise. Therefore only one set of coefficients is used in our analysis

$$\alpha[c] = \frac{S_{TX}}{S_{RX}[c]} \quad for \;\; c = 10, 11, 12, ..., 153$$

Noise power in the j[th] microslot, N_{RX}, was then computed by averaging over twenty consecutive 384-FFTs, F, of the noise waveform as shown below,

$$F[i, j] = fft\left(NoiseWfm\left[j \times 7812.5 + (i \times 384 : i \times 384 + 383)\right]\right)$$
$$where \; i = 0,1,2,...,19$$

$$N_{RX}[i, j] = \tfrac{1}{20} \sum_{i=0}^{19} | F[i, j] |$$

Finally, the Shannon capacity was used to estimate throughput in the j[th] microslot, D[j],

$$D[j] = \tfrac{37.5}{192} (153 - 10 + 1) \sum_{c=10}^{153} \log_2 (1 + \tfrac{S_{RX}[c]}{N_{RX}[c, j]})$$

For a PLC system that can adapt independently in each microslot, the average channel capacity can be obtained by averaging the microslot capacities over a full AC line cycle. In practice, supporting 160 channel adaptation regions is unduly complex. We study the effect of a smaller number of regions on performance by grouping a varying number of microslots to form a macroslot. For example, by grouping 20 microslots into a macroslot, only 8 (160/20) independent regions need to be supported. The average capacity of a macroslot that contains N microslots is obtained as follows,

$$D_{macroslot} = \max\left\{\left(D[i] \frac{N - i}{N} \right), \; for \;\; i = 0 \ldots N - 1\right\}$$

Where, {D[0], D[1], …, D[N-1]} are the capacities of the constituent microslots arranged in ascending order. This choice can be justified as follows. In each macroslot, the PHY parameters could be chosen such that reliable trans-mission is guaranteed in all its microslots. In this case, the minimum of the capacity for all constituent microslots (i.e., D[0]) will be the capacity of a macroslot. However, for PLC system that can tolerate errors at the physical layer (for example, by using MAC layer re-transmissions), it is possible to achieve a larger aggregate throughput (in certain channel conditions) by choosing more aggressive PHY parameters. In general, PHY parameters based on, D[i] (where i>0), can be chosen. However, in such cases, transmission in "i" microslots will not be successful as transmission rate will exceed capacity. Hence the average capacity will be $\left(D[i]\frac{N-i}{N} \right)$. In our analysis we chose the PHY parameters that provide the optimal PHY data rate. However, it has to be noted that maximization of the PHY data rates may not be the best choice under all conditions. For example, in PLC systems that support Quality of Service (QoS) sensitive multimedia streams, the probability of physical layer errors should also be bounded. Performance analysis for such cases is beyond the scope of this study.

5.5 Discussion of Results

For each of the measured paths, we computed the average PHY capacity for various choices of macroslot sizes. Since we are interested in the performance gain obtained by AC line cycle based adaptation, we measured the gain in data rate in comparison with the case when the macroslot spans a complete AC line cycle (i.e., no AC line cycle based adaptation). Figure 5-2 shows the inverse cumulative distribution (i.e., 1-cdf) of the percentage gain in PHY data rates ob-served over the measured paths for various choices

of macroslot size. The average gain in PHY data rates over all measured paths as a function of macroslot size is shown in Figure 5-4 (solid line). These results allow the following observations:

- Using a 1 millisecond long macroslot, more that 35% improvement in PHY data rates can be obtained on 30 % of the paths,
- Using a 1 millisecond long macroslot, more that 55% improvement in PHY data rates can be obtained on at least 15 % of the paths,
- Using continuous adaptation to cyclic noise (i.e., microslot based adaptation), a 30% increase in PHY data rates can be obtained (MAC overhead renders this adaptation method impractical how-ever, as seen in Figure 5- 4),

MAC layer data rates can be computed from the PHY data rates by taking into account the additional overheads incurred for transmissions that span multiple regions (or macroslots). We compute the MAC level throughput as follows,

$$MAC\,Throughput = PHY\,Throughput\,\frac{MacroSlot\,Size\,in\,\mu s - 130\mu s}{MacroSlot\,Size\,in\,\mu s}$$

Note that a 130μs incurred overhead per PPDU was used for this analysis, based on the HomePlug AV standard as mentioned earlier. Figure 5-3 shows the inverse CDF of the percentage gain in MAC layer data rates observed over the measured paths for various choices of macroslot size. The average gain in MAC layer data rates over all measured paths as a function of macroslot size is shown in Figure 5-4. It is notable that MAC performance suffers when the macroslot size is chosen to be either too large or too small. In the former case, the drop in PHY data rates is due to lack of proper AC line cycle based adaptation. In the latter case, excessive PPDU overhead incurred due to the large number of regions negatively impacts the MAC performance. For the paths tested, these results can be summarized as follows,

- Using 1 millisecond long macroslots, more than 30% improvement in MAC layer data rates can be obtained on 20% of the paths,
- Using a macroslot that spans 1-2 milliseconds pro-vides the highest MAC performance,
- AC line cycle based adaptation can provide an average of 10% improvement in MAC data rates,
- In 40% of the paths, less than 5% improvement in MAC performance was observed. This suggests that AC line cycle based adaptation does not al-ways improve performance. The choice of using AC line cycle based adaptation should be made selectively based on the observed channel characteristics.

5.6 Conclusions

In this section, we investigated the performance enhancements that can be achieved by using a channel adaptation mechanism that is synchronized to the AC line cycle. Analysis of channel characteristics on 72 channels has shown that an average of 10% improvement in MAC data rate can be achieved by using AC line based cycle adaptation. Furthermore, on 20% of the paths, we have seen more than 30% improvement in MAC layer data rate. The analysis also showed that using 1-2msec regions provides the largest gain in MAC performance for most of the channels. Apart from an increase in throughput, AC line cycle based channel adaptation also enhances the stability of channel adaptation and allows for better control of physical layer errors. Both of these features are invaluable for supporting QoS applications over power lines.

The results presented in this section can be considered preliminary as they are based on 72 paths from two buildings in North America. Further research incorporating a larger number of channels, as well as taking into account both the frequency response and noise power variation with the AC line cycle, would help to fully understand the potential performance gains offered by the use of line cycle based adaptation in PLC systems.

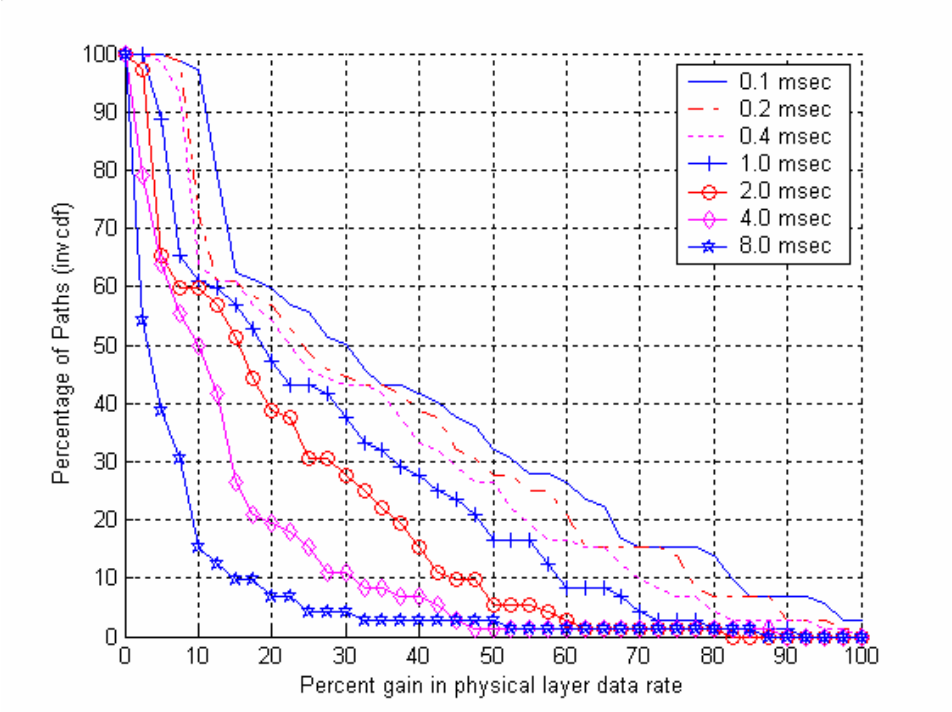

Figure 5-2: Performance gain in PHY data rates as a function of macroslot size

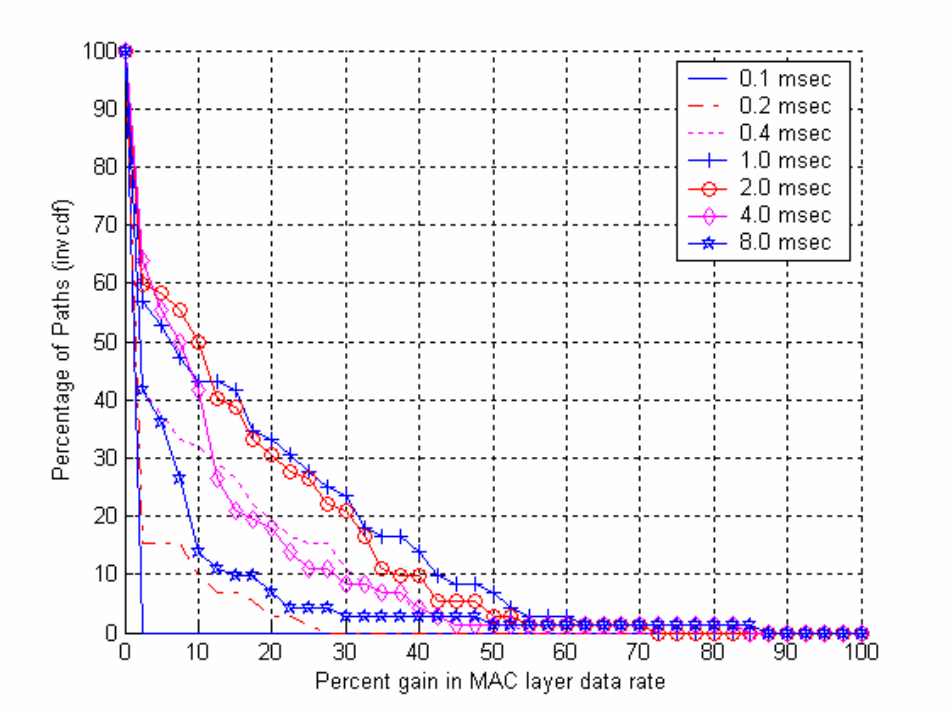

Figure 5-3: Performance gain in MAC data rates as a function of macroslot size

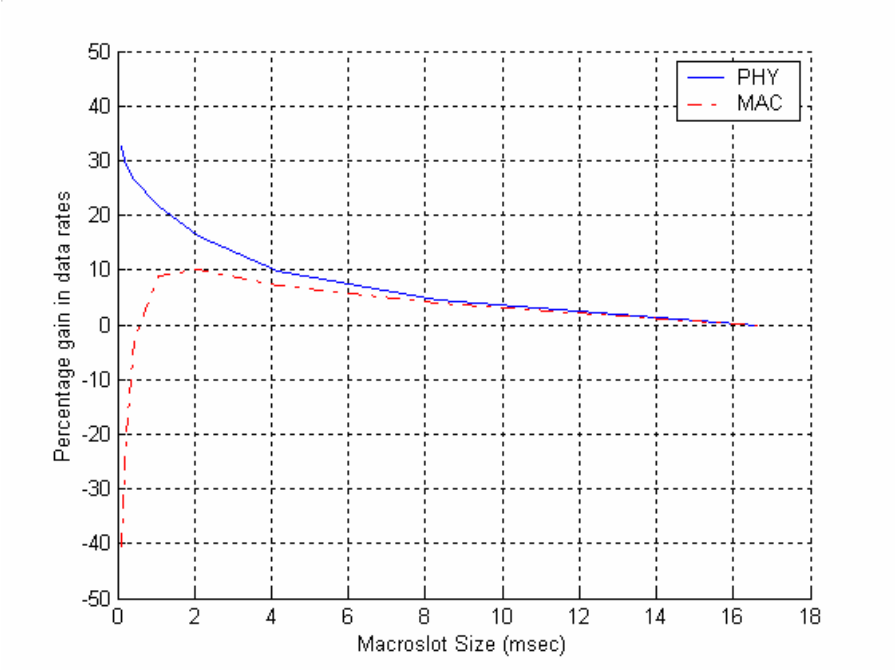

Figure 5-4: Average gain in MAC and PHY data rates

CHAPTER 6
MAC FRAMING

In power line communications (PLC) more so than in many other media, there is a strong interaction between the Medium Access Control (MAC) layer and the Physical (PHY) layer. This chapter investigates one of the manifestations of this interaction, that of MAC framing and error recovery with PHY transmission characteristics. MAC framing for high-speed PLC systems should be capable of concatenating multiple MAC Service Data Units (MSDUs, e.g., Ethernet or IP packets) in order to amortize the high and fixed overheads associated with each MAC Protocol Data Unit (MPDU). By itself, this is easy. However, transmission errors may damage portions of an MPDU, which can further rob a system of efficiency. This chapter presents a 2-level MAC framing mechanism that enables efficient re-transmission of corrupted data. Both analytical and simulation results are used to compare the performance of the proposed MAC framing scheme with other existing viable approaches. The results show that the proposed scheme is significantly superior to existing approaches. A subset of the results presented in this chapter is also published in [42].

The organization of the remaining sections is as follows. Section 6.1 gives an overview of MAC framing and provides an intuitive definition of Framing Efficiency. In Section 6.2, various approaches for MAC framing are presented. Simulation and analytical results on the performance of each of these approaches are presented in Section 6.3. Performance comparison between various MAC framing approaches and conclusions are presented in Section 6.4 and Section 6.5 respectively.

6.1 MAC Framing and Framing Efficiency

MAC framing deals with the process of converting Service Data Units received by the MAC from higher layer (i.e., MAC Service Data Unit, MSDU) into a Protocol Data Unit that the MAC handovers to the physical layer (i.e., MAC Protocol Data Unit, MPDU). MAC framing process not only depends on the PHY, but also on MAC features like channel access mechanism, network architecture, Layer-2 encryption etc. For example if one of the MAC features is to provide privacy, the MAC framing process will include fields for passing encryption relevant information. For a token passing MAC, the MAC framing process will contain fields to indicate busy token etc.

When the underlying PHY is unreliable, MAC framing will also have to add fields for error detection and retransmissions. Thus the MAC framing process depends heavily on system details and the approach used at the MAC layer to address them. Once the MAC framing process generates an MPDU, it is handed over to the physical layer. The physical layer adds the PHY headers and transmits it to the destination (refer Figure 6-1).

Apart from the physical layer overheads, MAC protocols also incur overheads due to interframe spacing, transmission of control information, collisions etc. All these overheads along with the MAC framing overheads will determine the MAC Efficiency. In this chapter, we are interested in studying the performance of the MAC framing process with respect to recovery of errors. To decouple analysis from other system level details, we assume that the only overheads incurred are those required for error recovery at the MAC layer. We define the MAC framing Efficiency to be the average number of MSDU bits delivered per MPDU divided by the total bits per MPDU. MAC framing Efficiency depends on PHY errors, MAC framing approach, MSDU size, and MPDU size.

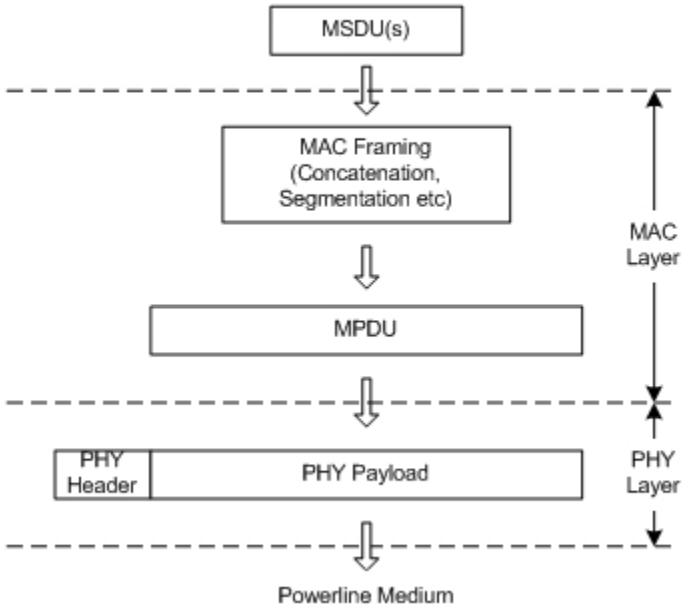

Figure 6-1: MAC framing Process

6.2 MAC Framing Strategies

Concatenation is essential for high-speed PLC systems due to the large and fixed overheads per MPDU. These occur due to PHY overheads and interframe spacings. In Home-Plug 1.0 [11], each MPDU transmission will incur a minimum overhead of 351.02 microseconds. If a system is ported to 100 Mbps without any concatenation, the maximum efficiency (assuming 1518 byte Ethernet packet as the MSDU) that can be obtained per transmission is ~25%, even in the absence of errors. Thus, concatenation is essential.

Three different packet concatenation mechanisms are investigated here. All three assume that some of the contents of an MPDU may be deliverable even if the MPDU is partially damaged. Without this stipulation, the efficiencies are so low in the presence of errors that these approaches are not considered further. In each case, we assume that the MPDU body is sent in one or more fixed size FEC blocks of a PPDU.

Given that multiple MSDUs may be concatenated to form an MPDU, we consider several basic stages. First, the MPDU may be acknowledged as a whole - either all of the constituent MSDUs are received correctly or none are, thereby requiring retransmission of the entire MPDU contents. This approach has a very low overhead, but is too inefficient when there are errors. The second main stage is to allow each MSDU to occupy its own, individually acknowledged, MAC frame. In this case, only the MAC frames that could not be recovered from a damaged MPDU must be retransmitted. We consider two variations of this approach; Simple Concatenation and Explicit Demarcation based Concatenation. Finally we consider two-level concatenation. Here, the individual FEC blocks hold their own header information, which allows retransmission of uncorrectable FEC blocks as well as resynchronization of MAC frames.

6.2.1 Simple concatenation

This is a very straightforward extension of the case without concatenation. Each MSDU is prepended with a Sequence Number (SN) and a Length Field (Len). A CRC based error detection field in attached at the end of the MSDU. Sequence numbers are needed to ensure in-order delivery and the Length field enables demarcation of each packet at the receiver. Thus, multiple MSDUs can be concatenated at the transmitter and de-concatenated at the receiver. Figure 6-2 shows the MAC Frame format for simple concatenation. This approach has two main disadvantages. Firstly, each MPDU has to be padded to fit into the PPDU. Secondly, a single FEC Block error will result in loss of information contained in all subsequent FEC Blocks.

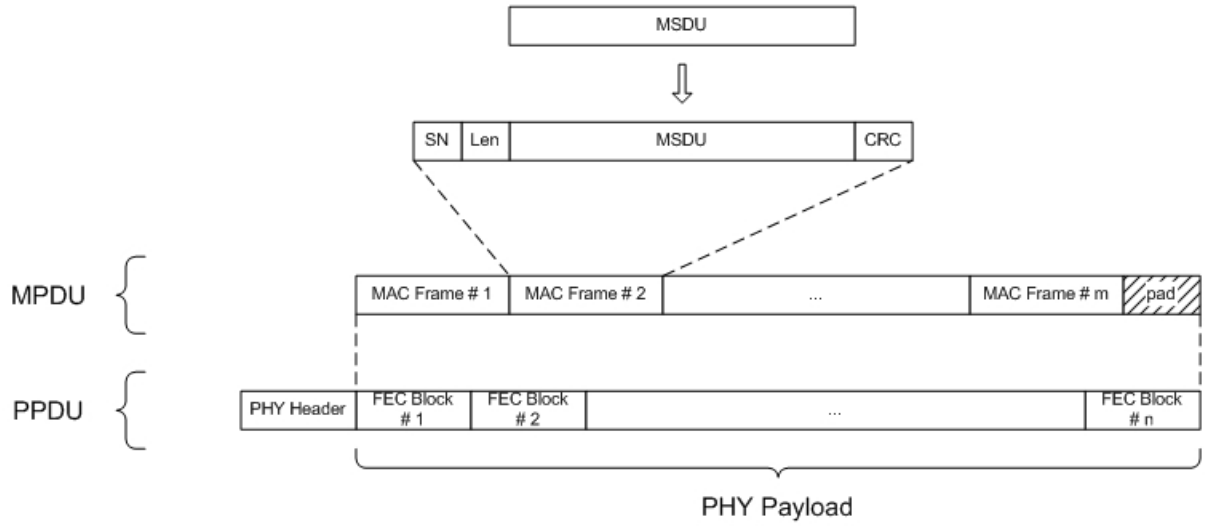

Figure 6-2: Simple concatenation

6.2.2 Concatenation with explicit demarcation

One of the main disadvantages of simple concatenation is that all information following the location of the first FEC block error is lost. This loss is mainly due to the loss of MAC Frame demarcation. So, it is quite likely that several MAC Frames might have been received without errors at the receiver but the receiver has to discard them due to loss in demarcation information. One simple approach is to add a Header Check Sequence (HCS) for detecting errors on the header fields in the MAC Frame. Thus, whenever the receiver detects a MAC Frame with errors, it can scan through the received bits to check for the next header. Once a proper header is confirmed by means of the HCS, it has the necessary demarcation information for receiving the remaining MAC Frames within the MPDU. MAC Frame header should also include an Identifier (ID) field. ID can be set to zero for the first MAC Frame in an MPDU and incremented for each subsequent MAC Frame. This enables the receiver to use a simple bit map for indicating the reception status of each MAC Frame within a MPDU. Figure 6-3 shows the MAC Frame format for Concatenation with Explicit demarcation.

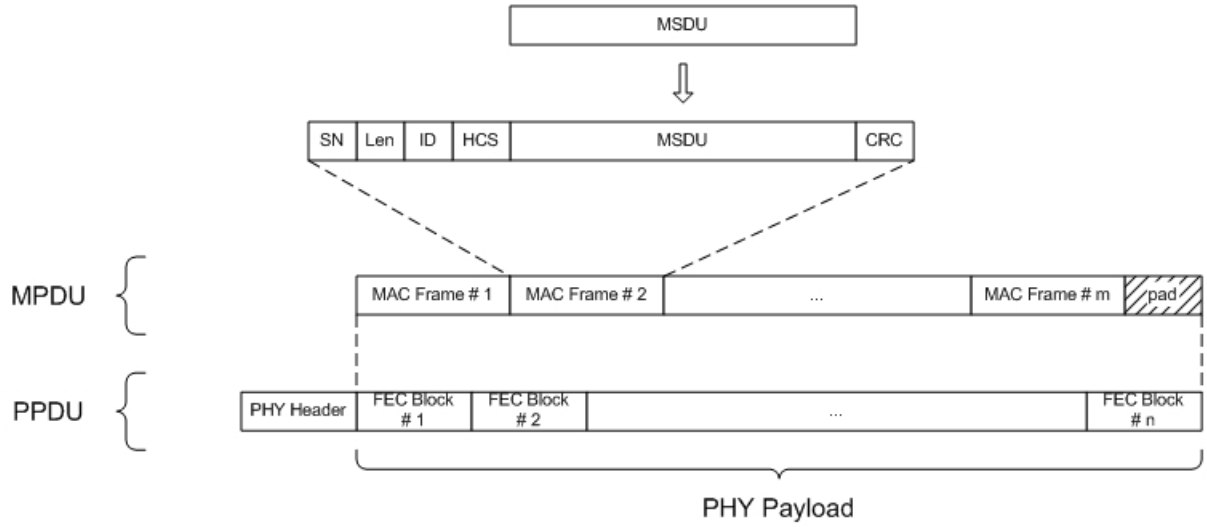

Figure 6-3: Concatenation with explicit demarcation

6.2.3 2-Level framing

PHY errors occur on an FEC block basis. Hence, an optimal framing strategy is one in which only the corrupted FEC blocks need retransmission. 2-Level framing is based on this principle. Here, framing is done in two steps.

In the first step each MSDU is prepended with a Length (Len) field. This entity is referred as a MAC Frame. Multiple MAC Frames that are awaiting delivery are concatenated together to form a MAC Frame Stream. MAC Frame Stream thus generated is treated as a stream of bytes and is then divided into segments of fixed size that match the FEC Block size. Each segment is prepended with a Sequence Number (SN) and a MAC Frame Boundary Offset (MFBO) field. The SN provides the relative location of the Segment within the stream while the MFBO field indicates the location of the first MAC Frame boundary (if any) within the Segment. A CRC based error detection field in attached at the end. The resulting entity is referred to as a PHY Block. Each PHY Block is mapped on to FEC Block at the PHY layer (refer Figure 6-4). It might be necessary to

add a pad to the MAC frame stream when there are not enough bytes to transmit a Segment. Note that a pad is not necessary if there are enough pending MAC Frames. All the results presented in this section assume that the padding overhead for 2-Level Concatenation is negligible.

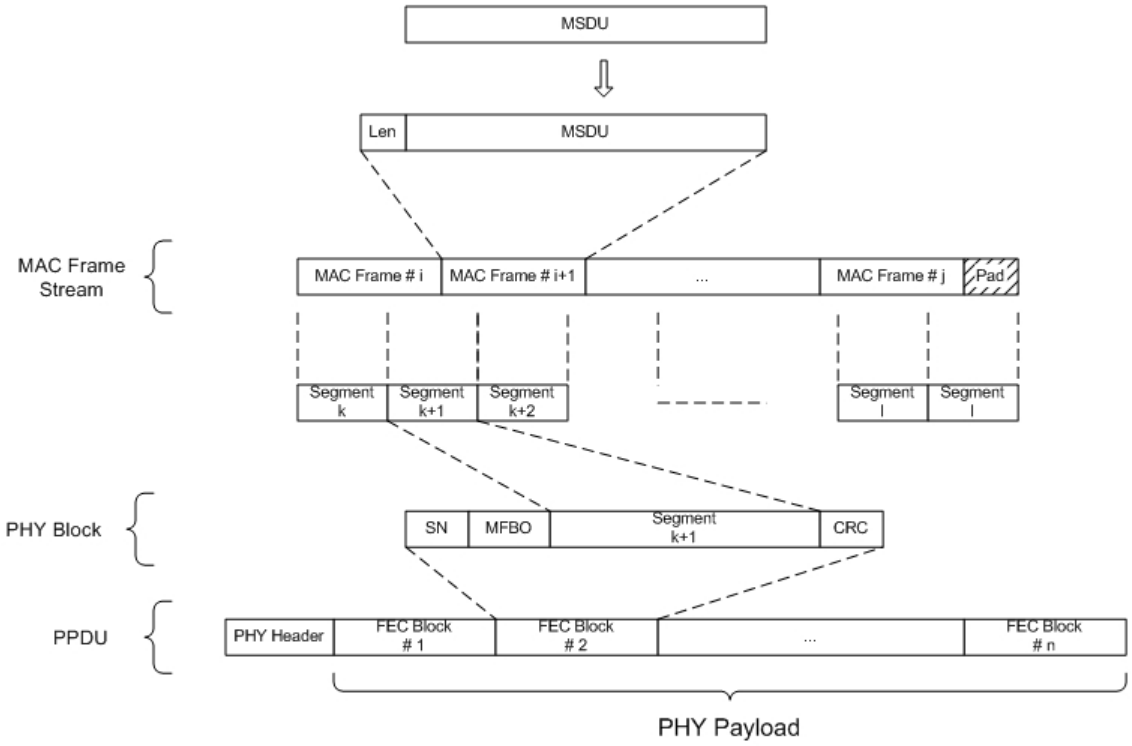

Figure 6-4: 2-Level MAC framing

Table 6-1: MAC framing overheads

	SN	Len	HCS	ID	CRC	MFBO
Simple Concatenation	2	2	-	-	4	-
Explicit Demarcation	2	2	2	1	4	-
2-Level Concatenation	2	2	-	-	4	2

6.3 Efficiency Analysis

We have derived equations for the efficiency of the Simple Concatenation and the 2-Level Framing schemes. For Explicit Demarcation based concatenation, simulation results were used to obtain the efficiency. For the results presented in this section, the overheads shown in Table 6-1 are used. We also assume that all MSDUs are of the same size. Results are presented for the case of 520-byte FEC Blocks [33, 34]. The FEC block errors in an MPDU are assumed to be independent of each other.

6.3.1 Simple concatenation

In the following analysis of Simple Concatenation, we assumed that a single FEC block error would result in loss of all MAC Frames that are contained (either partially or fully) within it. Due to the loss in demarcation information of MAC Frames, all information subsequent to the first FEC Block error is also lost. Thus, if k^{th} FEC block is the first FEC block that was corrupted the number of MAC Frames that will be successfully delivered is given by $\left\lfloor \frac{k L_{fec}}{L_{mf}} \right\rfloor$, where L_{fec} is the length of the FEC Block and L_{mf} is the length of the MAC Frame. L_{mf} is the sum of the size of the MSDU, L_{msdu}, and the overhead added per MSDU, i.e., $L_{OH,SC}$. If p is the probability of an unrecoverable FEC Block error and N is the number of FEC Blocks, the efficiency for Simple Concatenations η_{SC} is given by,

$$\eta_{SC} = \left[\left\{ \sum_{k=1}^{N-1} (1-p)^k \, p \left\lfloor \frac{k L_{fec}}{L_{mf}} \right\rfloor \right\} + (1-p)^k \left\lfloor \frac{k L_{fec}}{L_{mf}} \right\rfloor \right] \frac{L_{msdu}}{N L_{fec}}$$

Figure 6-5 shows the efficiency of Simple Concatenation as a function of FEC Block error rate for $N = 25$ and various MSDU sizes. Figure 6-6 shows the efficiency as a function of N for $p = 0.1$ and various MSDU sizes.

6.3.2 Concatenation with explicit demarcation

For Explicit Demarcation based concatenation, we assume that a single FEC block error will result in loss of all MAC Frames that are contained (either partially or fully) within it. The number of MAC Frames successfully delivered will not only depend on the number of FEC Block errors, but also on how and where they occur. For example, when two side-by-side FEC blocks have errors, then they tend to produce fewer MAC Frame errors than if they are far apart. Hence, it is not possible to derive a simple analytical result for this case. Simulation results were used to study the performance of this MAC framing Scheme.

Figure 6-7 shows the efficiency of Concatenation with Explicit Demarcation as a function of FEC Block error rate for $N = 25$ and various MSDU sizes. Figure 6-8 shows the efficiency as a function of N for $p = 0.1$ and various MSDU sizes.

6.3.3 2-level framing

With 2-Level Framing, only FEC Blocks that were corrupted need to be retransmitted. If p is the probability of FEC Block error, then the average number of FEC Blocks delivered per MPDU is (1-p) times the number of FEC Blocks, . The efficiency with 2-level concatenation, η_{2L} , is given by

$$\eta_{2L} = (1-p)\left(\frac{L_{fec} - L_{OH,sb,2L}}{L_{fec}}\right)\left(\frac{L_{msdu}}{L_{sb}}\right)$$

where $L_{OH, sb, 2L}$ is the overhead per FEC block.

Figure 6-9 shows the efficiency of 2-Level Concatenation and Segmentation as a function of FEC Block error rate for $N = 25$ and various MSDU sizes. Figure 6-10 shows the efficiency as a function of N for $p = 0.1$ and various MSDU sizes.

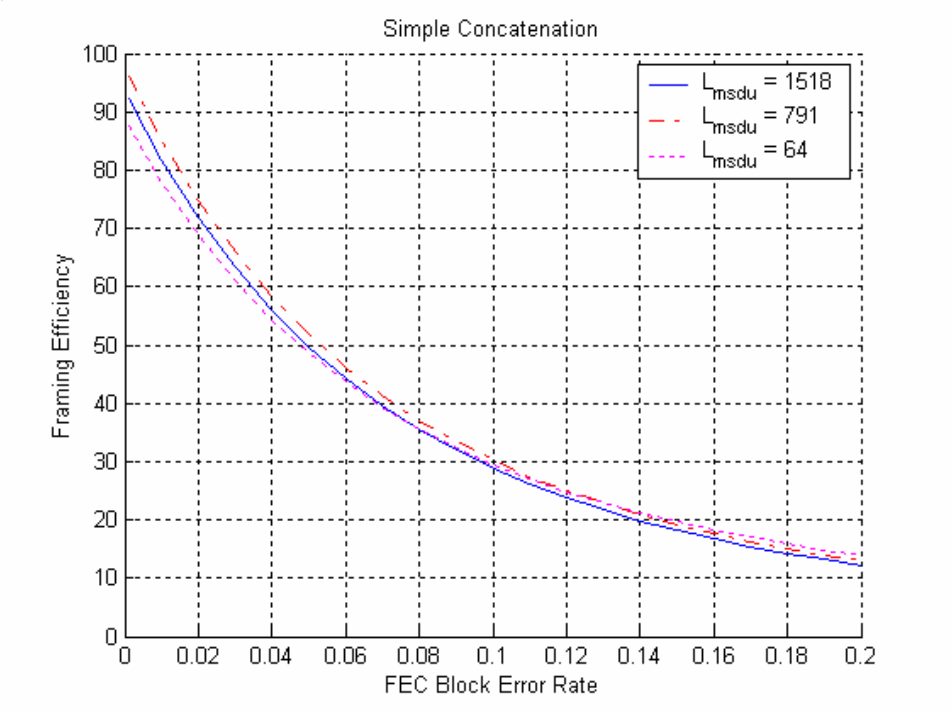

Figure 6-5: Simple concatenation- efficiency with varying FEC block rrror rate and N = 25

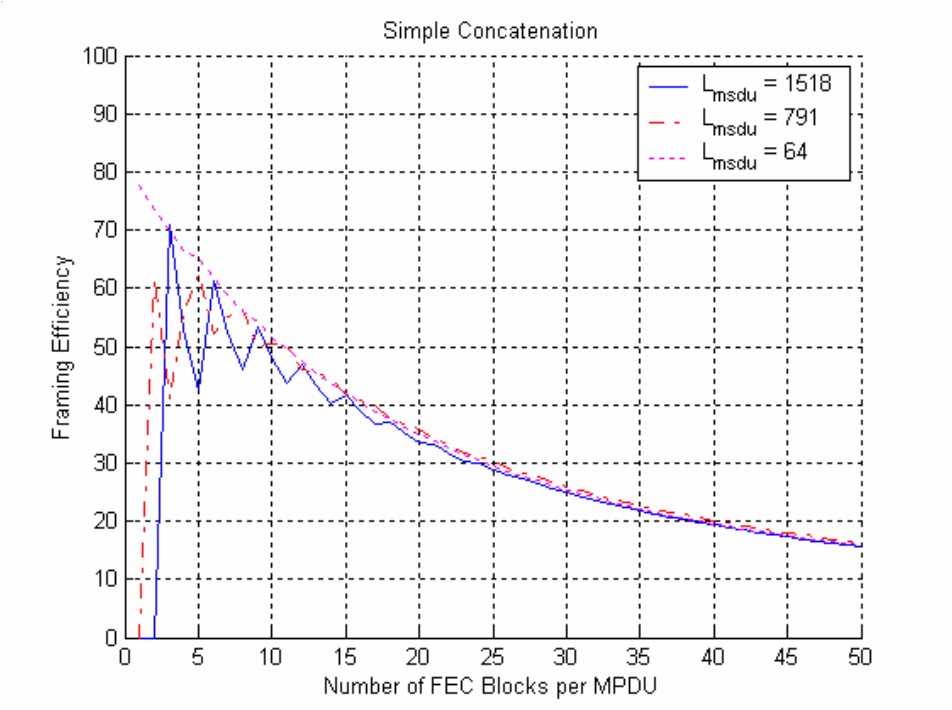

Figure 6-6: Simple concatenation efficiency with varying number of FEC blocks and p = 0.1

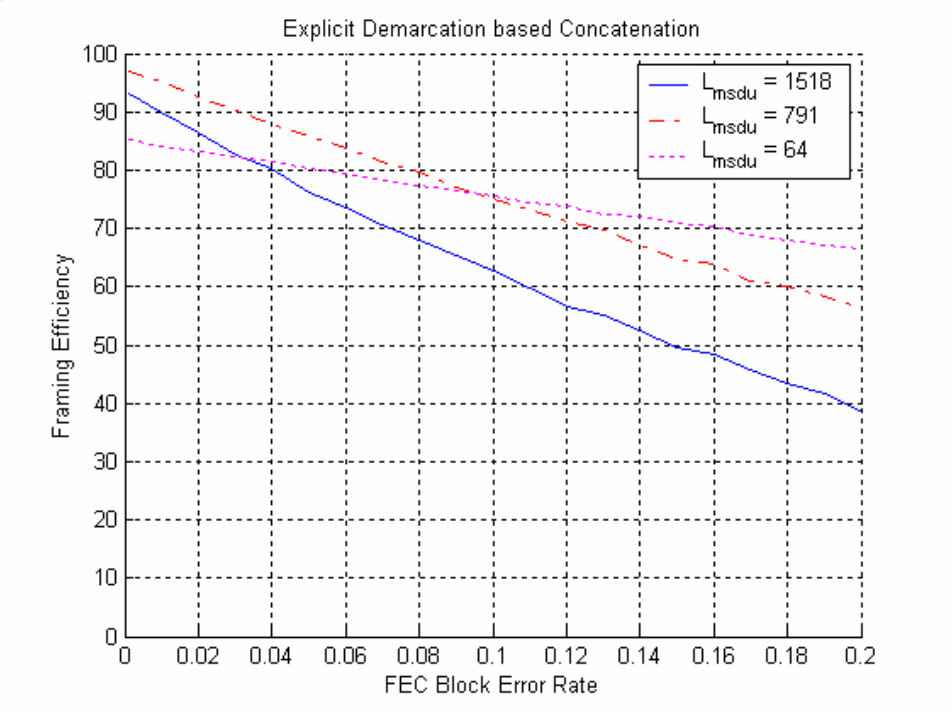

Figure 6-7: Explicit demarcation based concatenation - efficiency with varying FEC block error rate and $N = 25$

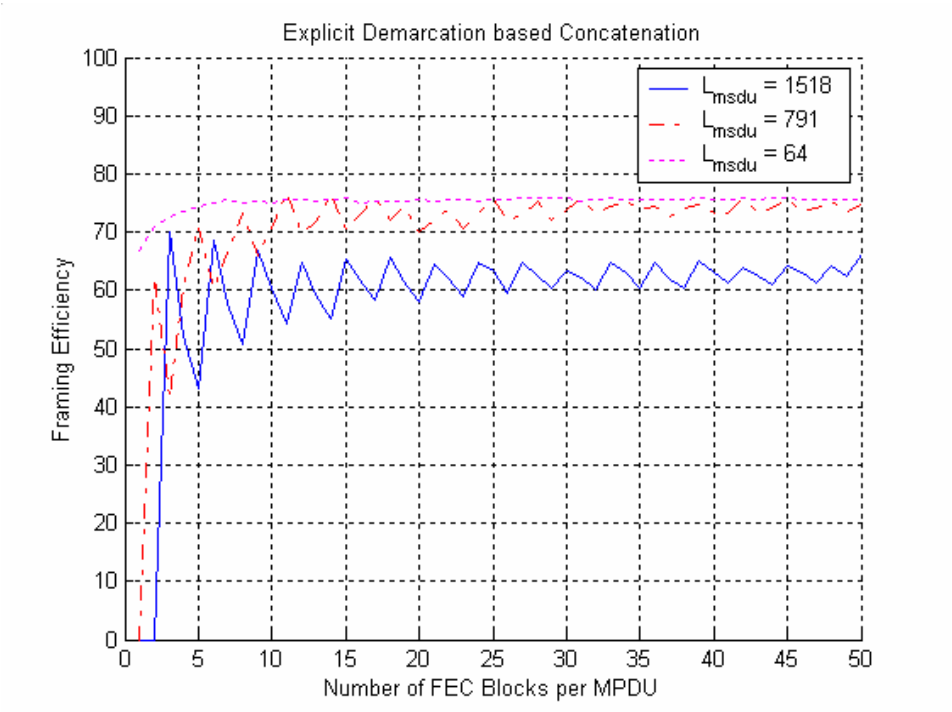

Figure 6-8: Explicit demarcation based concatenation - efficiency with varying number of FEC blocks and $p = 0.1$

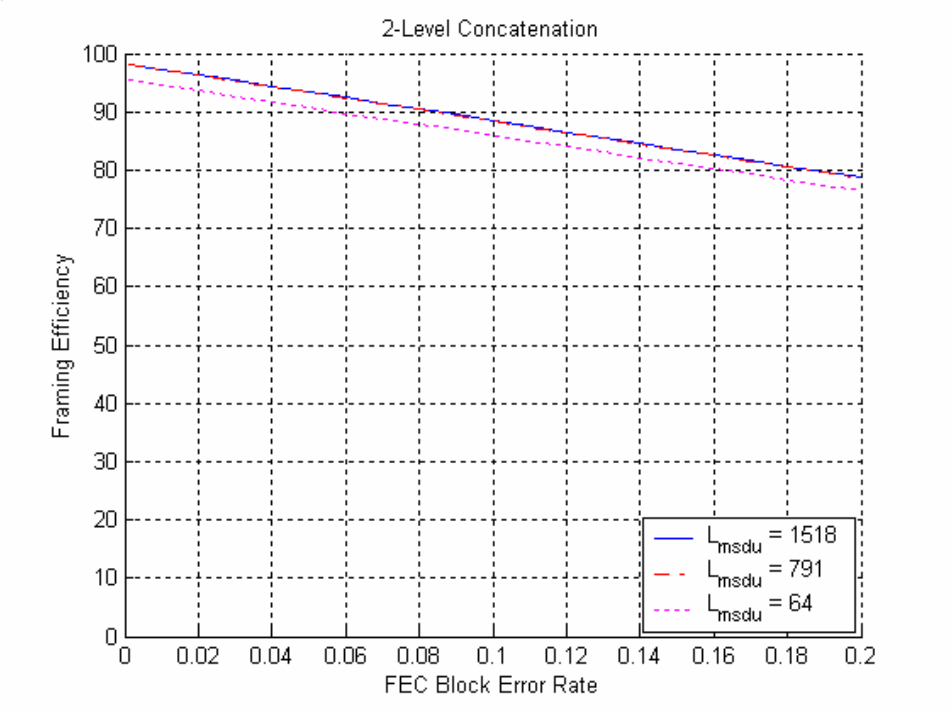

Figure 6-9: 2-Level framing - efficiency with varying FEC block error rate and $N = 25$

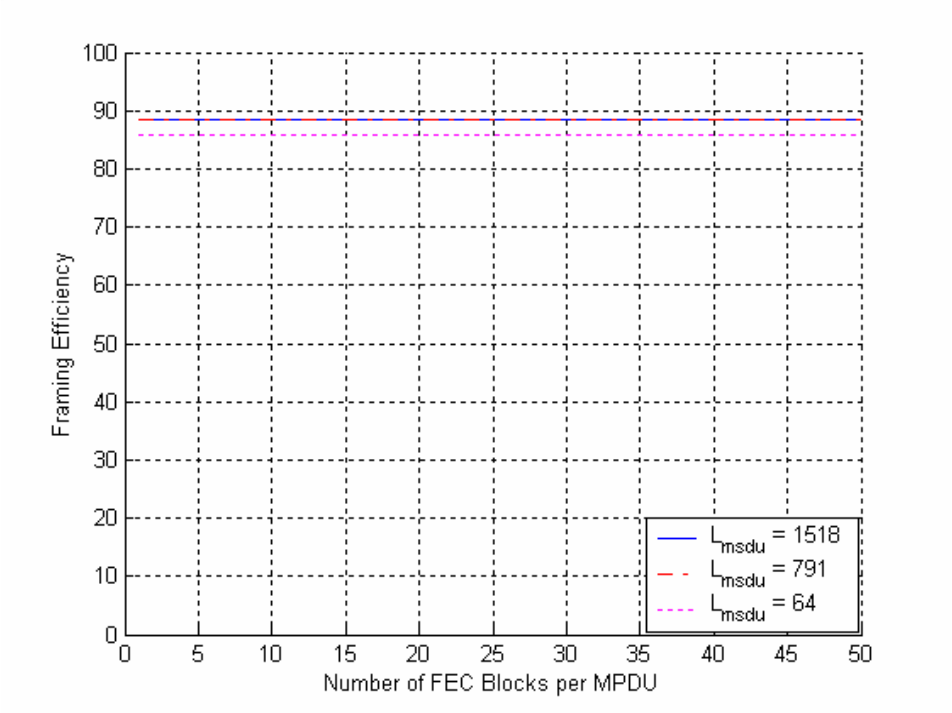

Figure 6-10: 2-Level framing - efficiency with varying number of FEC blocks and $p = 0.1$

6.4 Comparison of Performance between various Framing Schemes

Using Simple Concatenation, a single FEC block error results in loss of all MAC Frames that it intersects and all subsequent MAC Frames in the MPDU. This approach is very sensitive to FEC block error rate, p, and number of FEC blocks per MPDU, N. For example at 10% FEC block error rate, the efficiency drops to 30%. The effect of MSDU size on efficiency is small compared to that of the FEC block loss probability. Larger MSDUs will also incur higher overheads due to padding (since a number of whole MSDUs are required to fit in each MPDU), thus resulting in lower performance.

Using Explicit Demarcation based Concatenation, a single FEC block error results in loss of all MAC frames that it intersects. Simulation results show that the efficiency loss is linear with p and is strongly dependent on the MSDU size. At low p, smaller MSDU sizes show poor performance due to framing overhead. However, as p increases, larger MSDUs sizes suffer higher loss in efficiency since each single FEC block error results in larger number of MAC frame bits lost.

With 2-Level Concatenation, only FEC blocks that were corrupted need to be retransmitted. Results show that the efficiency is linear with respect to p, and independent of N. Figure 6-11 shows the relative performance of the three framing approaches for 1518 byte MSDU size with varying FEC block error rate. The results show that the performance of 2-level concatenations is superior to that of other approaches.

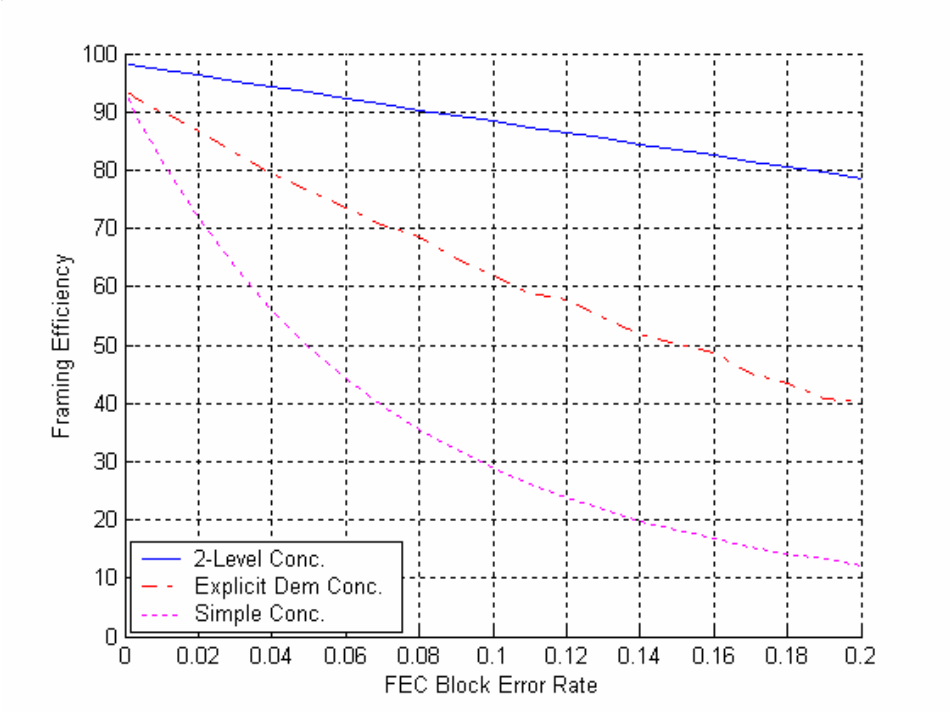

Figure 6-11: Performance comparison of various MAC framing strategies with varying FEC block error rate, N= 25, L_{msdu} = 1518

6.5 Conclusions

This chapter has highlighted the necessity of concatenation when framing at the MAC level in high-speed PLC communication systems. Five approaches were considered, with three analyzed and simulated in some detail. Approaches varied according to their ability to retransmit at the MAC frame or the FEC block level, and in their ability to resynchronize at the MAC frame level. The results show that 2-Level Framing was far superior to the others in its efficiency. It was also seen to be independent of the number of FEC blocks per MPDU, unlike the other two approaches.

CHAPTER 7
ALLOCATION REQUIREMENTS FOR SUPPORTING LATENCY BOUND TRAFFIC

Impulse noise sources such as dimmers, halogen lamps etc., are quite common in power line networks. Hence, high-speed power line communications systems should be designed to deal effectively with them. HomePlug AV uses aggressive channel adaptation at the physical layer and efficient retransmissions at the MAC layer to deal with impulse noise. This approach can lead to very high probability (up to 20%) of Forward Error Correction (FEC) block errors under some channel conditions. HomePlug AV also has large transmission overhead to ensure reliable communication over the power line. Transmission overhead can negatively impact the MAC efficiency on channels with high FEC Block Error Rate due the need for a large number of retransmissions to successfully deliver packets.

This section studies the complex interaction between FEC block errors, transmission overhead, Quality of Service (QoS) requirements of a multimedia stream and its TDMA allocation requirements. Our results show that, to support low latency applications at high BLERs, the average allocation size has to be increased by one or more transmission overheads. Further, the increase in average allocation is not a strong function of application data rate. Hence, low data rate applications can suffer significant loss in efficiency at high FEC Block errors. Our results also show that using a fixed size TDMA allocation can lead to poor utilization when the latency requirements of the application are less than four beacon periods. These results indicate that channel

adaptation in HPAV should take into consideration the application QoS requirements to optimize the overall system capacity.

7.1 Introduction

The HomePlug AV (HPAV) Medium Access Control (MAC) layer is based on a hybrid of Time Division Multiple Access (TDMA) and Carrier Sense Multiple Access (CSMA). Each HPAV network has a designated device, the Central Coordinator (CCo), which coordinates access to the medium. The CCo periodically (with a period of either 33.33msec or 40msec [33, 34]) generates a beacon with information about the temporal locations of TDMA and CSMA allocations. Multimedia applications use TDMA allocations to provide guarantees on QoS while CSMA allocations are used by regular data traffic. Since power line channels can change with time, each station continuously provides information on the physical layer (PHY) data rates and the size of its queue (i.e., backlog) to the CCo. The CCo uses this information to dynamically adjust the size of TDMA allocations.

HPAV stations use channel adaptation to choose the best set of physical layer parameters (carrier modulation, FEC code rate etc.,) for communication with other stations. Channel adaptation in HPAV is also tailored to effectively deal with impulse noise [43, 44]. In most communication systems, the channel adaptation mechanism is used to reduce the PHY layer errors to a range where they can be effectively corrected by the MAC layer. For example, the channel adaptation can be chosen such that the FEC block errors are less than 1/100 and the MAC retransmissions can be used to recover the uncorrectable errors. Such a technique is not viable under power line channel environments due to the presence of impulse noise. Impulse noise channels will display temporal effects in channel capacity. In between two impulse noise events, the channel

capacity can be very high, while at the impulse noise the capacity is very low. To obtain less than 1/100 FEC block error rate, the channel has to be adapted close to the lower end of its capacity (i.e., capacity near impulse noise events) and hence is undesirable when high throughput is required. A better approach is to adapt aggressively and use a MAC ARQ mechanism to correct errors. In some environments, to achieve optimal performance an HPAV station may need to operate at FEC block error rate as high as 20%.

To effectively recover from large number of FEC Block errors, HPAV uses a novel 2-level MAC framing mechanism and selective acknowledgments (SACK). The 2-level MAC framing essentially concatenates and then segments higher layer packets (or MAC Service Data Units) into fixed size block (referred to as Segments) that fit into a single 520-octet FEC block. Since errors at the physical layer occur on an FEC block basis, only Segments that get corrupted needs to be retransmitted. Further details on 2-level MAC framing can be found in Chapter 6 [42].

Apart from the MAC framing overheads, each transmission will also incur overheads due to physical layer headers, selective acknowledgments and interframe spacings. Figure 7-1 illustrates the overheads incurred in HPAV during TDMA allocations. Segments are transmitted in Long Physical Layer Protocol Data Units (PPDUs). Each long PPDU consists of a Start of Frame (SOF) delimiter followed by one or more FEC blocks that carry Segments. A Delimiter in HPAV consists of a preamble sequence followed by 128-bit frame control information. Preambles are used to demarcate the start of each PPDU. A SOF frame control contains broadcast information that is necessary for proper demodulation of the PPDU payload. The frame control of a

SACK delimiter contains the reception status of the FEC Blocks in the Long PPDU. Since proper reception of the delimiter is critical for reliable exchange of data, delimiters in HPAV are designed to be highly robust and hence are quite long (110.48μsec). Typically, a Response Interframe Spacing (RIFS_AV) of 100μsec is used between the transmission of long PPDU and the corresponding SACK. A SACK and the subsequent Long PPDU are typically separated by 100μsec (note that HPAV allows variable interframe spacing to enable flexibility for a variety of implementations). Thus we see that each PPDU transmission will incur an overhead of around 420μsec.

Due to the fixed transmission overhead in HPAV, the retransmission strategies can greatly influence the MAC efficiency. For example, Figure 8-1 also shows a scenario where Segment contained in FEC Block#2 gets corrupted during the initial transmission and is retransmitted immediately. Since a 420μsec overhead is incurred for retransmitting a single Segment, this reduces efficiency. In this section, we refer to this retransmission strategy as ‘Immediate Retransmission’ strategy. A strategy that can overcome the inefficiencies of immediate retransmissions is shown in Figure 8-2. In this approach, the transmitter waits until sufficient numbers of new Segments are available before retransmitting the corrupt Segment(s). We refer to this retransmission strategy as ‘Delayed Retransmission’ strategy. In essence, the delayed retransmission strategy reduces the average overhead incurred for transmission of each segment, thus improving the efficiency. The drawback of this strategy is that, additional delays are incurred while the transmitter aggregates new Segments. While such additional delays are not an issue for data traffic, they may not be acceptable for QoS sensitive multimedia streams.

Multimedia streams require guarantees on both latency and packet loss probability. Since multimedia streams are provided with one TDMA allocation per beacon period, each Segment will have a fixed number, L, of TDMA allocations within which it need to be delivered. In contrast, to achieve a given packet loss probability, Segments belonging to the applications will need to be guaranteed a certain number of transmission opportunities, TXOPS. In situations where L ≥ TXOPS, delayed retransmissions can be used. Otherwise, a hybrid of immediate and delayed retransmission strategies has to be used to meet the packet loss requirement. Inefficiencies will be incurred in the later case, due to additional transmission overheads.

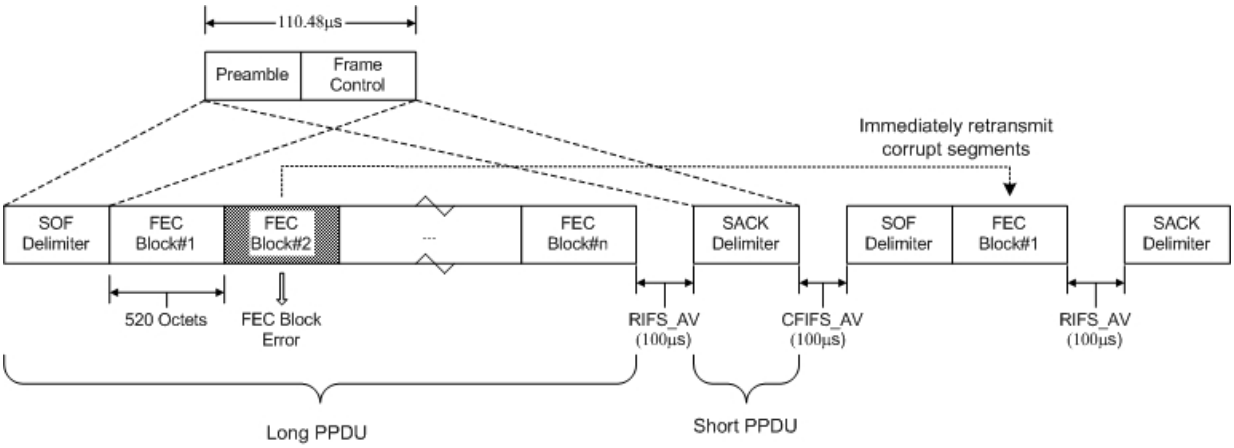

Figure 7-1: Transmission overheads in HomePlug AV

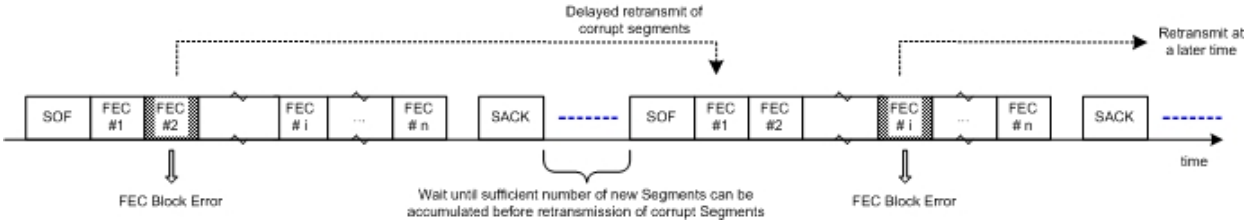

Figure 7-2: Illustration of delayed retransmission strategy

In this section we analyze the effect of FEC block errors and transmission overheads on the allocation requirements for the multimedia streams. The characteristics

of the streams that are of interest are its data rate, latency and packet loss tolerance. We are interested in two different types of allocation requirements,

1. Fixed Allocation – This is the duration of the fixed size TDMA allocation that is required to satisfy the QoS requirements of the multimedia stream. It is important to note that due to the statistical nature of the FEC errors, it is possible that the Fixed Allocation may not always be fully utilized.

2. Average Allocation – This is the average duration of a variable size TDMA allocation that will be required to satisfy the QoS requirements of the multimedia stream.

To simplify our analysis and presentation of the results we make the following assumptions,

- We assume that the application generates constant bit rate traffic. Application data rate is measured in terms of the number of Segments (N), that it generates per beacon period,

- We measure the application latency L in multiples of beacon period. Each Segment will have transmission opportunities in L number of TDMA allocations before it is considered stale.

- We measured packet loss probability in terms of the packet loss event probability (PLEP) and average packet lost (APL) per packet loss event,

- We assume that FEC Block errors are uncorrelated and occur with a probability (p)

- Since the efficiency of a TDMA allocation is primarily dependent on the ratio of the transmission overhead to transmission duration of a FEC block, we do our analysis in units of FEC Block transmission duration. For example, at physical layer data rate of 150Mbps, the transmission duration of an FEC block is 27.7msec. Hence the ratio of transmission overhead to FEC block transmission time (represented by H) is 15.16 (i.e., 420/27.7). Since the maximum physical layer data rate of HomePlug AV is 150Mbps, we are interested in $H \in (0, 15.16]$.

The organization of the rest of the section is as follows. Analysis of Fixed Allocation and Average Allocation requirements without transmission overheads is presented in Section 7.2. An approximate analysis of Fixed Allocation and Average Allocation requirements in the presence of transmission overheads is presented in Section 7.3. This section also includes simulation based validation of the analysis. The effect of

transmission overhead on allocation requirements is presented in Section 7.4 and conclusions are presented in Section 7.5.

7.2 Allocation Requirements without Transmission Overheads

In this section we investigate the allocation requirements when no transmission overheads are present. In practice, it is not possible to design systems that do not such overheads. Hence, the results presented are of theoretical importance as they provide optimal bounds with which to compare actual achieved efficiency.

To successfully transmit each Segment, an average of $(1-p)^{-1}$ number of transmission opportunities will be needed. Hence the Average Allocation, T_{avg}, requirement for transmitting N Segments is given by,

$$T_{avg}(N,p)=\frac{N}{(1-p)}$$

The computation of the Fixed Allocation that can enable the required PLEP is more involved and depends upon whether L = 1 or L > 1.

7.2.1 Fixed Allocation, L = 1

Fixed Allocation for L=1 can be computed by nothing that the probability that k out of N Segments remain when an allocation of size A (A>N) is granted on a channel with FEC Block error probability p, is given by

$$\Pr\left(m\,Segments\,remain \middle/ N,p,A\right)=\begin{cases}\binom{A}{m}p^{A-(N-m)}(1-p)^{N-m}\ ;\ 0<m\le N\\ 1-\sum_{k=1}^{N}\binom{A}{k}p^{A-(N-k)}(1-p)^{N-k};\ m=0\end{cases}$$

From this, the packet loss event probability (PLEP) and Average packet loss (APL) per packet loss event can be obtained for an allocation A, as follows,

$$PLEP = \sum_{m=1}^{N} \binom{A}{m} p^{A-(N-m)} (1-p)^{N-m}$$

$$APL = \sum_{m=1}^{N} \binom{A}{m} p^{A-(N-m)} (1-p)^{N-m} m$$

Based on the above equation, the Fixed Allocation $T_{N,p}^{fixed}$ can be obtained by determining the minimum value of A that will achieve the required PLEP.

7.2.2 Fixed Allocation, L > 1

Analytical solution for the Fixed Allocation cannot be obtained for L > 1. Hence we resort to a Markov chain [45] based analysis. This analysis assumes a retransmission strategy in which the oldest segment in the queue will be transmitted before transmitting any other Segments. Since no transmission overhead is incurred, this strategy is optimal in the sense that it provides the retransmission opportunities to the most urgent Segment.

First, consider the buffer backlog of the stream at the end of each beacon period. It can be readily seen that the variation of the buffer backlog is only dependent on the current backlog and the size of the Fixed Allocation for a given FEC block error probability. Furthermore, the maximum buffer backlog is bounded by N(L-1). Note that this upper bound is a manifestation of latency bound associated with the Segments. A discrete-time, finite state Markov chain model can be used to determine the steady state probabilities of buffer backlog from which the PLEP can be computed. Figure 7-3 shows the state transition diagram of buffer backlog when L > 2.

The state transition probabilities, $p_{i,j}$, are given by

$$p_{i,j}^{NP} = \begin{cases} \Pr\left({}^{j}\!/\!_{N+i}, p, A \right) & 0 \le i \le NL - N,\ \max(N+i-A, 0) \le j \le N+i \\ 0 & otherwise \end{cases}$$

Where, $\Pr\left({}^{j}/_{N+i,p,A} \right)$ is given by,

$$\Pr\left({}^{j}/_{N+i,p,A} \right) = \begin{cases} \binom{A}{j} p^{A-(N+i-j)} (1-p)^{N+i-j} \; ; 0 < j \le N \\ 1 - \sum_{k=1}^{N+i} \binom{A}{k} p^{A-(N+i-k)} (1-p)^{N+i-k} ; \; j = 0 \end{cases}$$

The steady state probabilities, P_i^{NP}, can be obtained from the state transition probabilities by solving the equation,

$$\left[p_{i,j}^{NP} \right] \left[P_i^{NP} \right] = \left[P_i^{NP} \right]$$

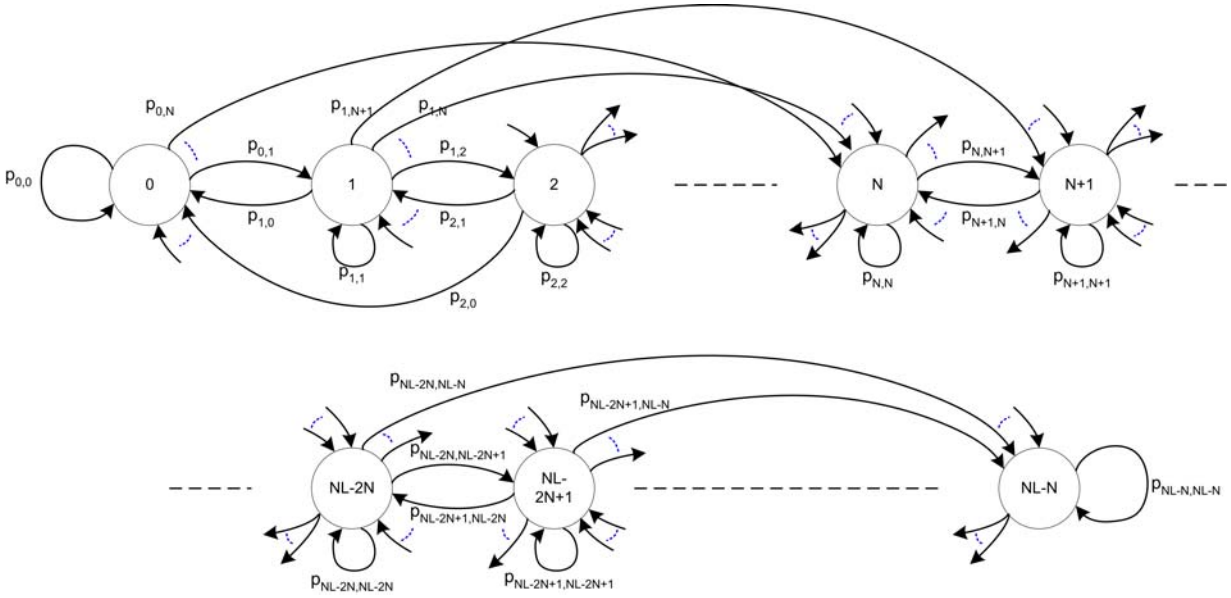

Figure 7-3: State transition diagram for no MPDU overhead case

From the steady state probabilities the packet loss event probability and average packet loss per packet loss event can be computed based on the set of transitions that result in a packet loss. Figure 7-4 shows the excess allocation required to achieve a packet loss event probability of 10^{-5} for N = {50,100, 200} and L = [1, 2, 3]. Note that a PLEP of 10^{-5} will result in one packet loss event in an hour and hence is a reasonable

choice for most multimedia applications. Also, N = 50, 100 and 200 correspond to application data rates of 6Mbps, 12Mbps and 24Mbps, respectively when the beacon period is 33.33msec. The excess allocation is measured as the difference between the actual and the minimum allocations required to ensure stability (i.e., $\frac{N}{1-p}$). These results show that for L = 1, a large amount of over allocation is required to achieve low packet loss event probability. However for L > 1, the amount to over allocation required is negligible. Figure 7-5 shows the average number of packets lost per packet loss event for N = {50,100, 200} and L = [1, 2, 3]. Results also show that the APL tends to be small and show a slight increase as N, L or p increases.

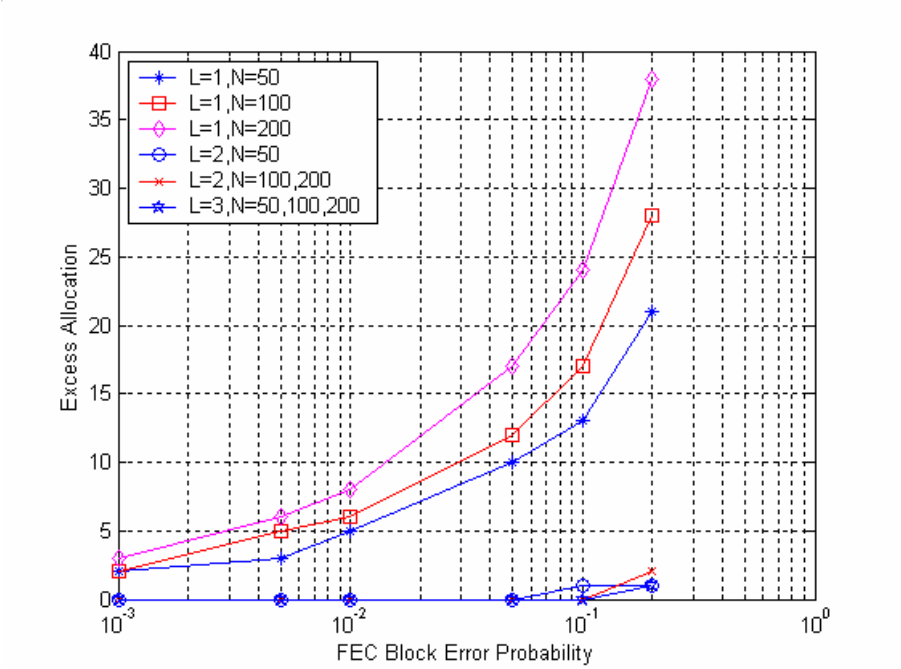

Figure 7-4: Excess allocation as a function of FEC block error probability when no transmission overhead present

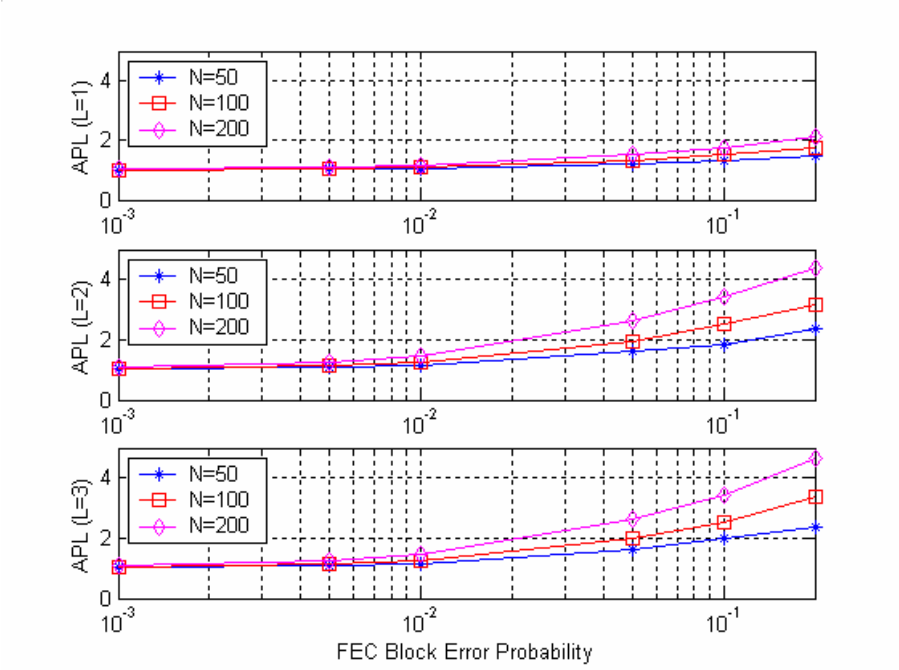

Figure 7-5: Average packet loss per packet loss event when no transmission overheads are present

7.3 Allocation Requirements with Transmission Overheads

Results from previous section show that when no MPDU overhead is incurred, for latencies greater than one, the allocation requirement are very close to the optimal allocation i.e., $\frac{N}{1-p}$. In the presence of transmission overheads, the retransmission strategy used in the previous will result in a Fixed Allocation and Average Allocation of $\frac{N}{(1-p)}(1+H)$. It can be readily seen that for the range of values of H we are interested in, this can result in gross inefficiencies and hence is not viable.

A better approach is to use a hybrid of immediate and delayed retransmission strategies where in at each transmission opportunity, as many Segments as possible are transmitted starting from the oldest pending Segment based on the time available in the TDMA allocation. We are interested in determining the duration of Fixed Allocation and

the Average Allocation for this retransmission strategy. Unfortunately, due to the intricate interaction between the allocation size, FEC errors, and transmission overheads this retransmission strategy is not amicable to direct analysis. In theory, it is possible to conduct a Markov chain analysis by defining the Markov chain state as a L-tuple of backlogs, $(b_0,b_1,\ldots,b_{L-1})$, where b_i indicates the backlog of Segments that expire at the end of i^{th} beacon period following the current beacon period. Thus, b_0 will indicate the backlog of Segments that expire at the end of the current beacon period and so on. The number of state for such a Markov chain will be (N+1)L. Due to the computational requirement for obtaining steady state probabilities of the Markov chain, this method will only be useful for small values of N and L. To overcome these problems, we use a combination of simplified analysis and simulations to provide approximate estimates of the Fixed Allocation and Average Allocation.

7.3.1 Fixed Allocation

Consider a multimedia stream with a data rate of N Segments per beacon period being transmitted over a channel with FEC Block Error probability of p. If each of the Segments is provided with T_{total}, transmit opportunities, the probability that a given Segment gets successfully delivered is $\left(1-p^{T_{total}}\right)$. Since FEC Block errors are uncorrelated, the probability that all N Segments will get successfully delivered is $\left(1-p^{T_{total}}\right)^N$. Hence the packet loss event probability, PLEP, is given by

$$PLEP = 1-\left(1-p^{T_{total}}\right)^N$$

The above equation can be used to determine the number of transmission attempts required to achieve a given PLEP as shown below. Note that $\lceil \bullet \rceil$ represents the ceil operation.

$$T_{total} = \left\lceil \frac{\log_{10}\left(1-(1-PLEP)^{1/N}\right)}{\log_{10}(p)} \right\rceil$$

Figure 7-6 shows the number of transmission opportunities required to achieve a PLEP of 10^{-5} for N = [50, 100, 200] and various values of p. These results shows that the number of T_{total} increases with N and p. These results also show that T_{total} is not highly sensitive to N.

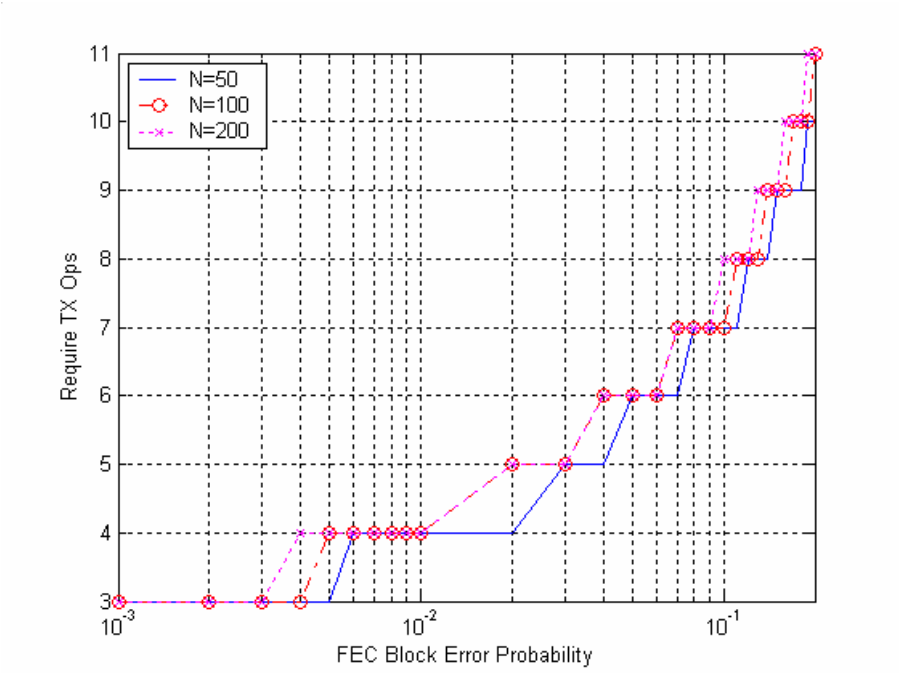

Figure 7-6: Transmission opportunities required to achieve PLEP = 10^{-5} at various FEC block error probabilities

Since a minimum of T transmit opportunities needs to be provided in L TDMA allocations, the number of transmit opportunities per TDMA allocation is,

$$T_{alloc} = \left\lceil \frac{T_{total}}{L} \right\rceil$$

Based on this, an approximate estimate of Fixed Allocation (FA_Theory) can be obtained as,

$$FA\_Theory = \left\lceil \frac{T}{L} \right\rceil H + \left\lceil \frac{N}{1-p} \right\rceil$$

The first term in this equation reflects the contribution of transmission overheads to the Fixed Allocation. The second term shows the contribution due to multiple retransmissions of Segments. We basically use the minimum Segment allocation required for stability as a first order approximation. In reality, due to the statistical nature of the FEC block errors there will be a complex interaction between the FEC Block errors and number of retransmissions. For example, in some TDMA allocations the FEC block errors can be small resulting in lager number of retransmission opportunities and vice versa. Simulations were used to validate how well the theoretical estimate matches the actual allocation requirement.

Simulations were performed for N = [50, 100, 200], L = [1, 2…8] and p = [0.001, 0.005, 0.01, 0.05, 0.10, 0.15, 0.20]. Each simulation was run for 10^7 beacon periods with varying allocations to determine the Fixed Allocation (FA_Sim) that would guarantee PLEP less than 10^{-5}. Figure 7-7 shows the Fixed Allocation estimation error in for N=100. Estimation error is measured relative to the theoretically computed Fixed Allocation. These results show that the estimation error is large for small values of latencies and large values of FEC block error probabilities. This can be attributed to the use of average value of allocation for Segments in the theoretical estimate. Figure 7-8 shows the probability distribution of the estimation error for all the simulation runs. These results show that the theoretical estimates remain within 5% of the actual Fixed Allocation in 90% of the data points. In general, for L > 3, our theoretical estimates accurate showed an error of less than 5% in 99% of the data points and an error of less

than 2% in 97% of the data points. Our simulations also showed that the estimation errors remain similar for PLEP of 10^{-3}, and 10^{-4}.

Figure 7-9 shows that average packets lost per packet loss event as a function of FEC block error probability for all the simulations. Results show that the average number of packets lost per packet loss event tends to remain very close to 1 in all the simulations except for H = 1, L = 1. In the later case, the average packet loss showed slight increase with N or p.

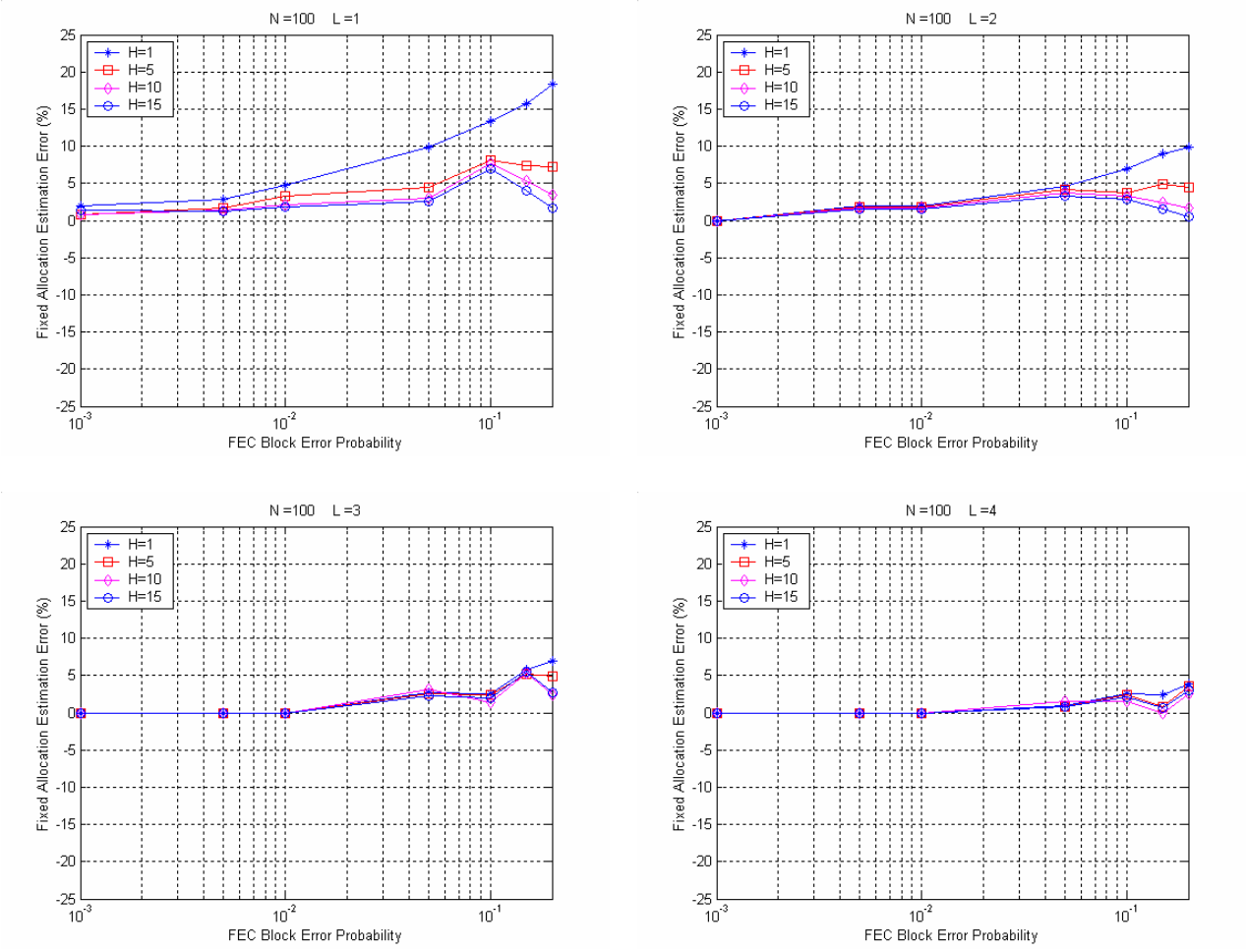

Figure 7-7: Fixed Allocation estimation error for N = 100 and L = 1, 2, 3, 4, 6, and 8

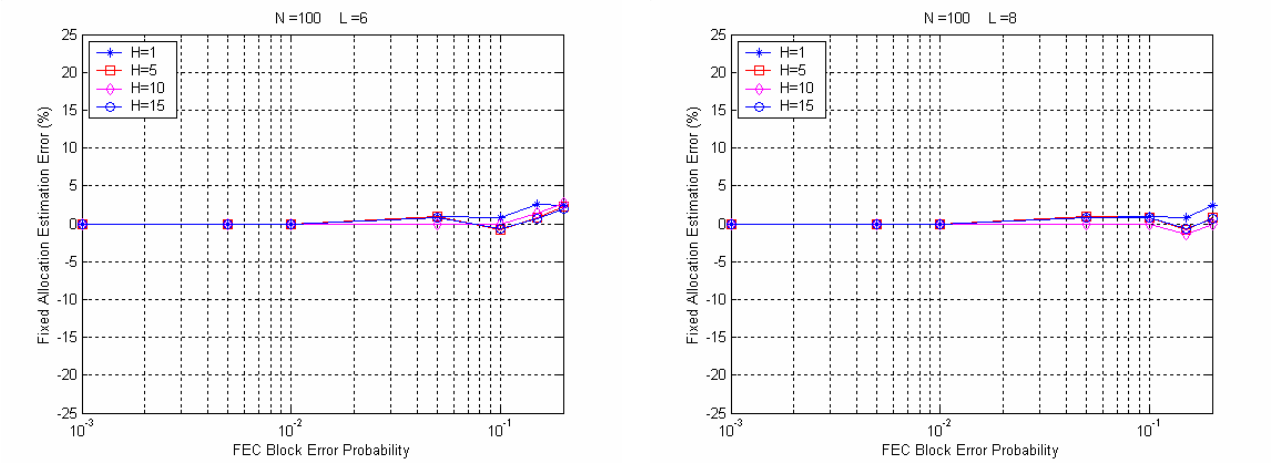

Figure 7-7: Continued

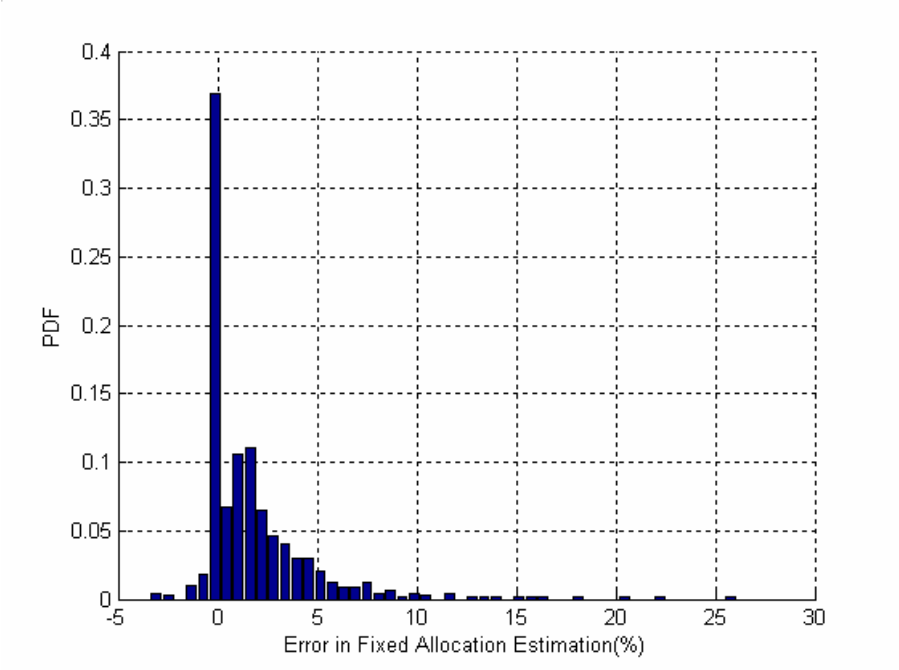

Figure 7-8: Probability distribution function of the Fixed Allocation estimation error

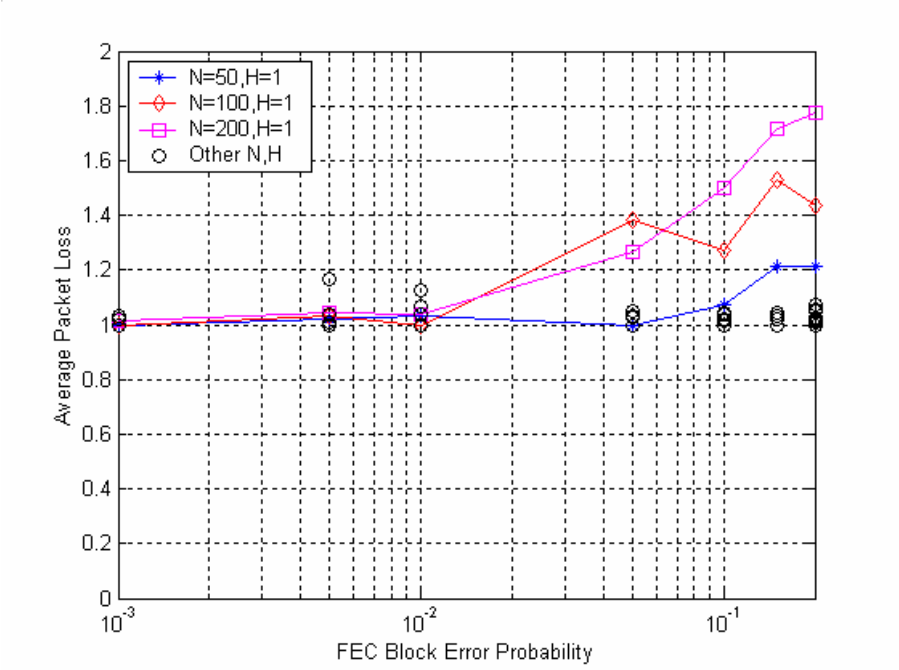

Figure 7-9: Average packet loss per packet loss event when transmission overheads are present

7.3.2 Average Allocation

To successfully transmit each Segment, an average of $(1-p)^{-1}$ number of transmission opportunities will be needed. Hence the contribution of Segment transmit times to the Average Allocation is exactly $\frac{N}{(1-p)}$. The average time used by transmission overheads will depend on the probability distribution of the transmission attempts. To obtain this, we assume that the number of transmission attempts will be upper bounded by T_{alloc} i.e., the minimum number of transmission attempts per TDMA allocation required to achieved the required PLEP. We further assume that all pending Segments will be transmitted at each transmission opportunity (i.e., no truncation effects due to fixed size allocation). Since the probability that a Segment gets delivered

successfully in an allocation is $\left(1-p^{T_{alloc}}\right)$, the average number of Segments pending at the start of each TDMA allocation ($N^{'}$)is given by,

$$N^{'}=\left\lceil \frac{N}{1-p^{T_{alloc}}} \right\rceil$$

To obtain the distribution of transmission attempts, we first note that the probability of delivering $N^{'}$ Segments in exactly i transmission attempts is $\left(1-p^{i}\right)^{N^{'}}-\left(1-p^{(i-1)}\right)^{N^{'}}$, where i $\in$ [1,∞]. Since the maximum number of transmit attempts is upper bounded by T_{alloc}, the condition distribution of transmitted attempts is given by,

$$\Pr\left(transmit\ attempts, t=i\right)=\frac{\left(1-p^{i}\right)^{N^{'}}-\left(1-p^{(i-1)}\right)^{N^{'}}}{\sum_{j=1}^{T_{alloc}}\left(1-p^{j}\right)^{N^{'}}-\left(1-p^{(j-1)}\right)^{N^{'}}}$$

Thus, the average time required for transmission overheads ($\overline{H}$) is given by,

$$\overline{H}=\sum_{i=1}^{T_{alloc}}\Pr\left(t=i\right)\times H$$

From this, the theoretical estimate of Average Allocation (AA_Theory) can be obtained as,

$$AA\_Theory=\overline{H}+\frac{N}{1-p}$$

We again use simulations to determine how well the theoretical estimate matches the actual Average Allocation (AA_Sim). Figure 7-10 shows the error in estimation of Average Allocation (i.e., AA_Sim - AA_Theory) for N=100. These results show that the theoretical estimates for Average Allocation are very accurate. This is further validated in Figure 7-11, where we plot the probability distribution of the estimation error for all the simulations.

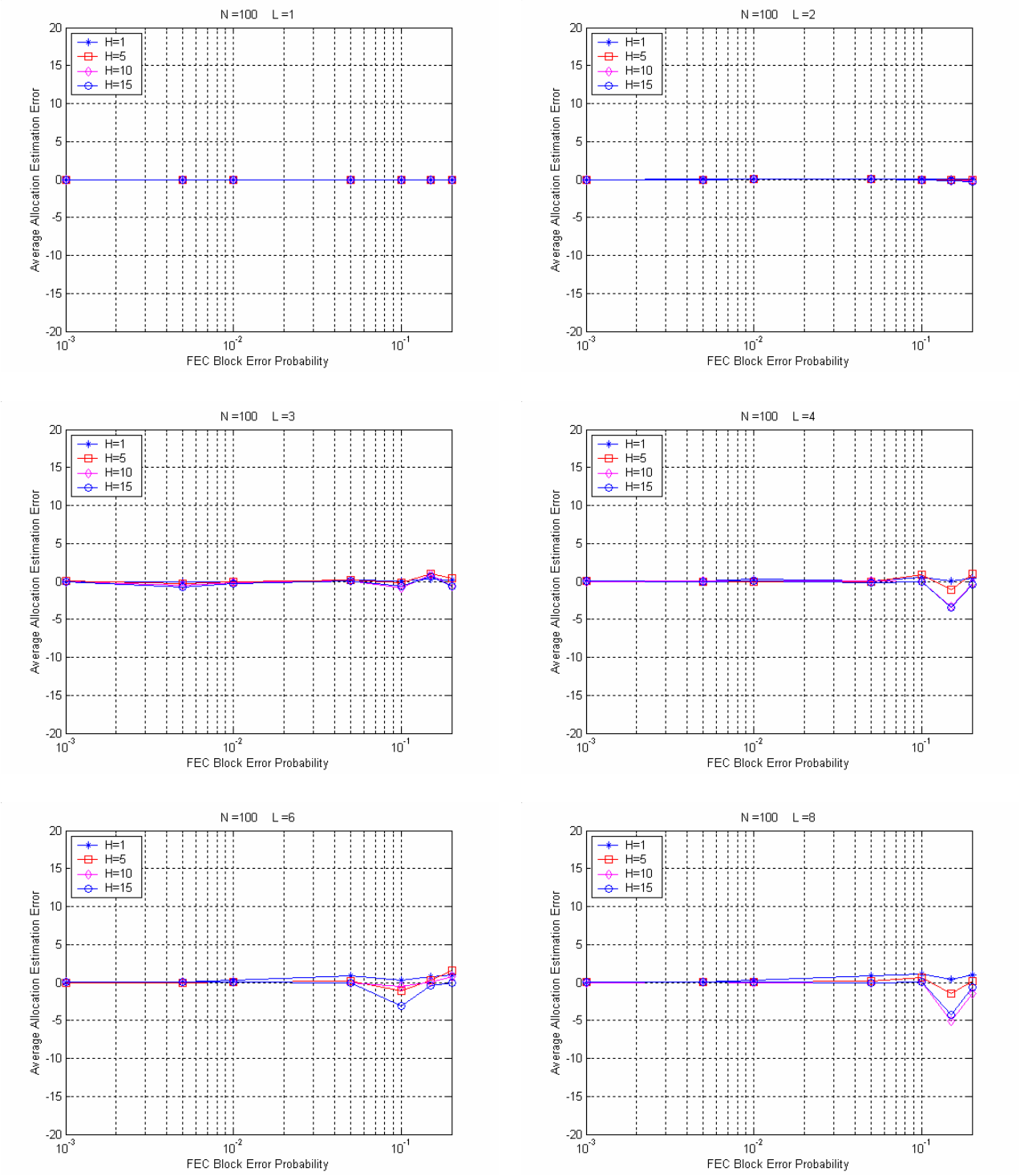

Figure 7-10: Average Allocation estimation error for N = 100 and L = 1, 2, 3, 4, 6 and 8

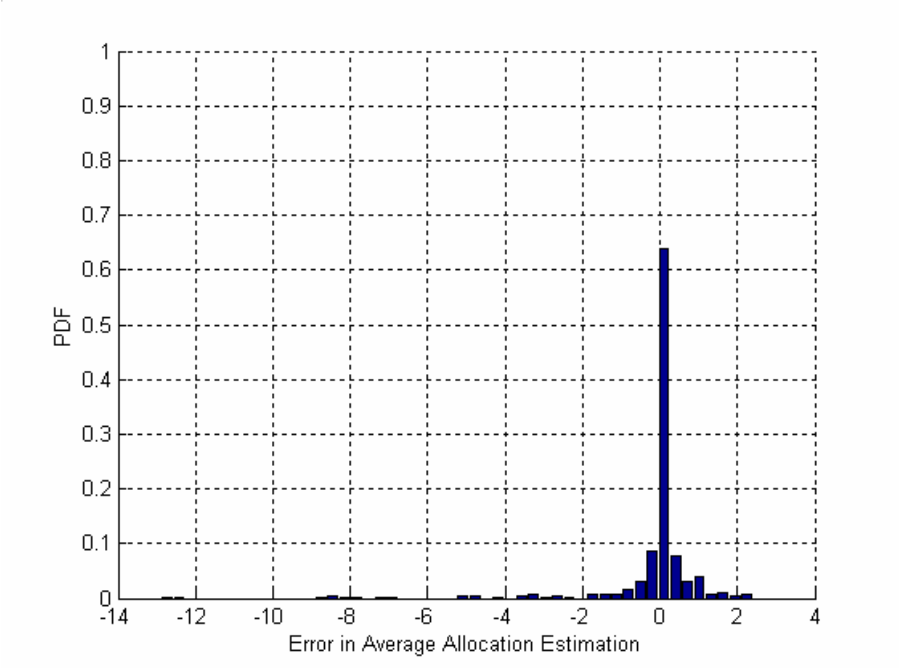

Figure 7-11: Probability distribution function of the Average Allocation estimation error

7.4 Effect of Transmission overheads on Allocation Requirements

In this section we use the simulation results and analytical estimates of the Fixed Allocation and Average allocation to determine the impact of transmission overheads on on the allocation requirements efficiency. We first note that in the presence on transmission overheads multimedia streams whose latency L is much larger than the number of transmission opportunities required to achieve the PLEP, the Fixed Allocation and Average Allocation required are given by,

$$FA\_Min = H + \left\lceil \frac{N}{1-p} \right\rceil$$

$$AA\_Min = H + \frac{N}{1-p}$$

These represent the minimum allocation requirement, as large allocations will be necessary at lower values of latencies due to transmission overheads.

Figure 7-12 shows the percentage difference in the Fixed Allocation (FA_Sim) and minimum Fixed Allocation (FA_Min) for N = [50,200], and p = [0.01, 0.10]. These results show that for low latencies, significantly large TDMA allocations are required to support the stream For example, for H=10, and p=0.01, 16% additional allocation will be needed to support a Latency of 3 beacon periods compared to the Latency of 4. The percentage increase in TDMA allocation requirement reduces as the data rate of the stream increases. This can be expected as the transmission overhead does not change significantly (refer to Figure 7-6) with the data rate of the stream.

Figure 7-13 shows the percentage difference in the Average Allocation (AA_Sim) and minimum Average Allocation (AA_Min) for N = [50,200], and p = [0.01, 0.10]. Comparing these with Figure 7-12, we see that at low latencies, the utilization of the TDMA allocation will remain poor. For latencies larger that four, the differences between the Fixed Allocation and Average Allocation are minor.

The analytical results on Average Allocation can be used to determine the effective transmission overhead (i.e., $\overline{H}$ /H) incurred for multimedia streams. Figure 7-14 shows the effective transmission overhead incurred for various values of latencies and FEC block error probabilities for N=50, 200. These results show that,

- Latencies greater than 10 and 7 will be needed at 20% and 10% FEC Block error rates, respectively, to support streams with N = 200 (or 24Mbps application data rate), and PLEP=10^{-5} with minimal overheads. Providing one additional transmission overhead of allocation will enable support of latencies greater than 5 and 3 at 20% and 10% FEC Block error rate, respectively
- Latencies greater than 10 and 7 will be needed at 20% and 10% FEC Block error rates, respectively, to support streams with N = 200 (or 24Mbps application data rate), and PLEP=10^{-5} with minimal overheads. Providing one additional transmission overhead of allocation will enable support of latencies greater than 5 and 3 at 20% and 10% FEC Block error rate, respectively

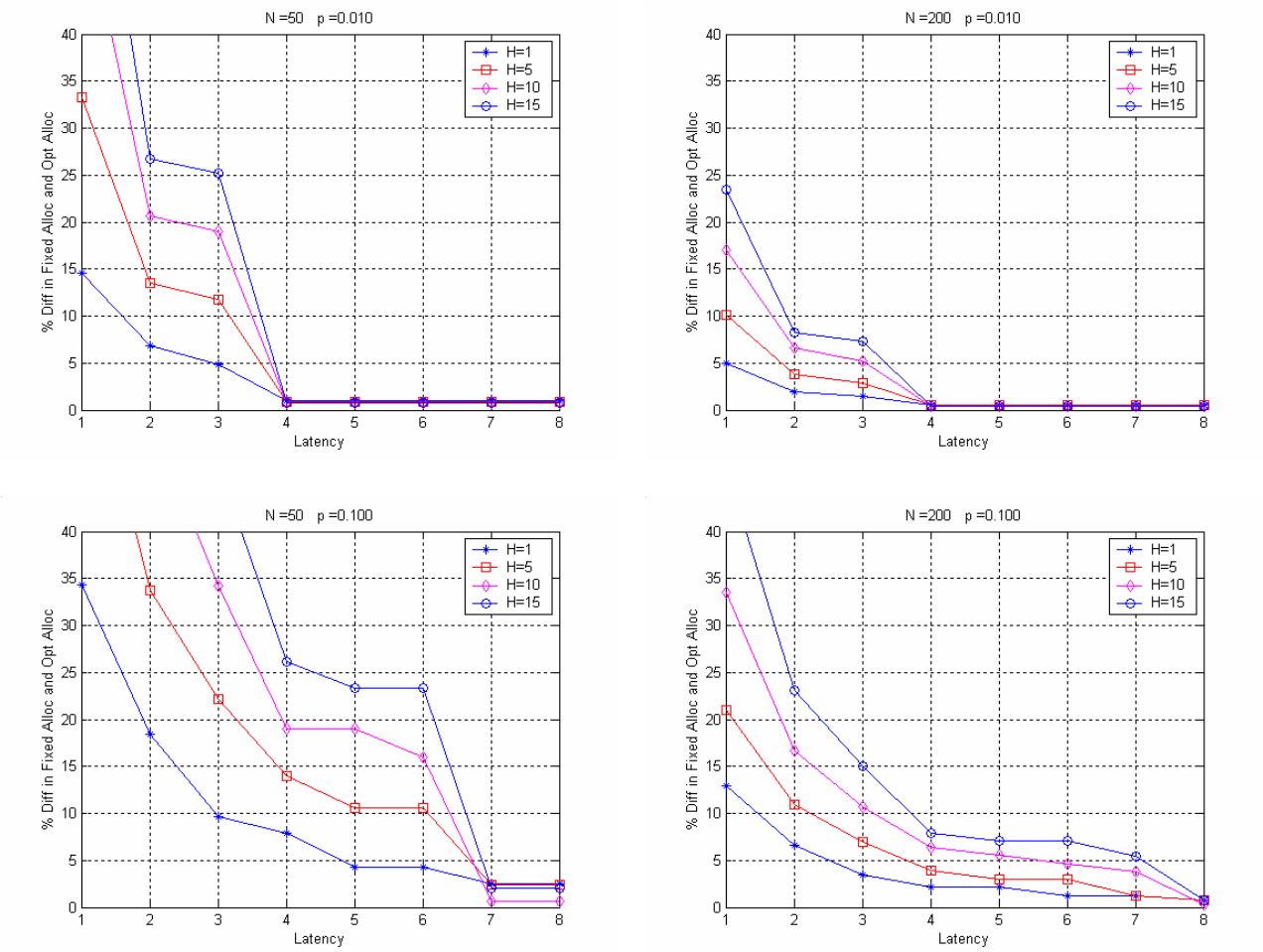

Figure 7-12: Percentage difference in Fixed Allocation and Optimal Allocation for N = [50, 200], p= [0.01, 0.10]

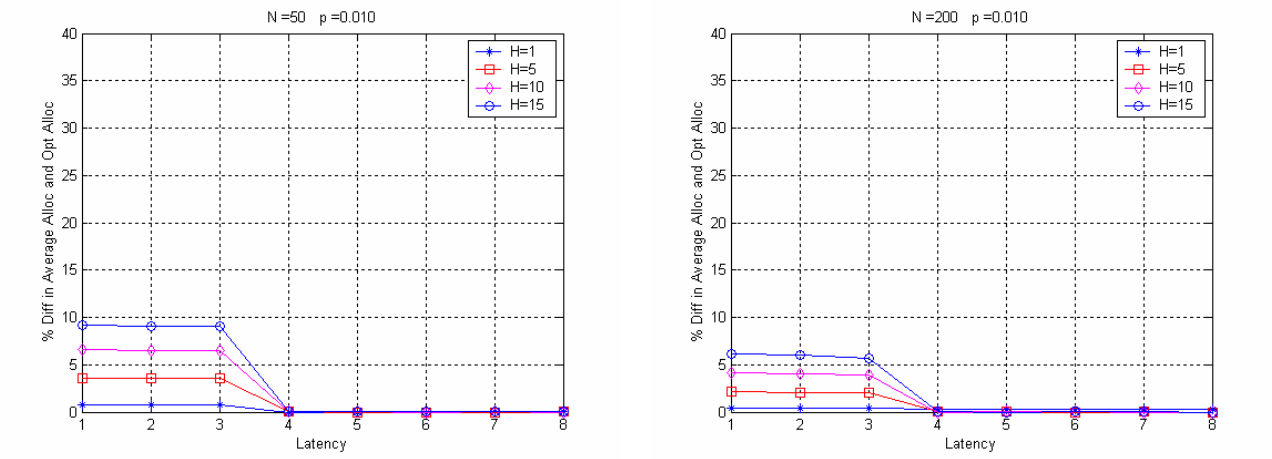

Figure 7-13: Percentage difference in Average Allocation and Optimal Allocation for N = [50, 200], p= [0.01, 0.10]

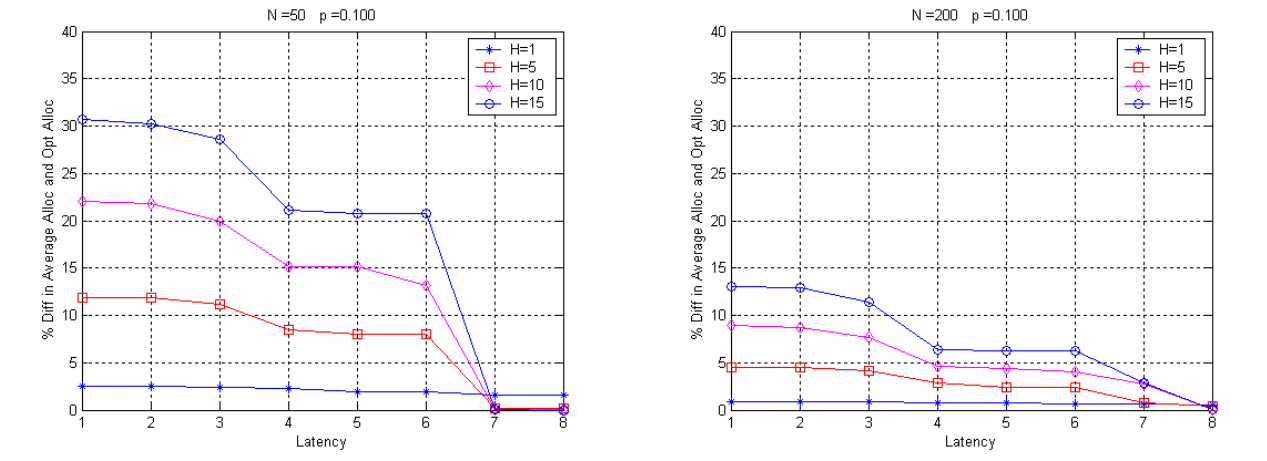

Figure 7-13: Conclusions

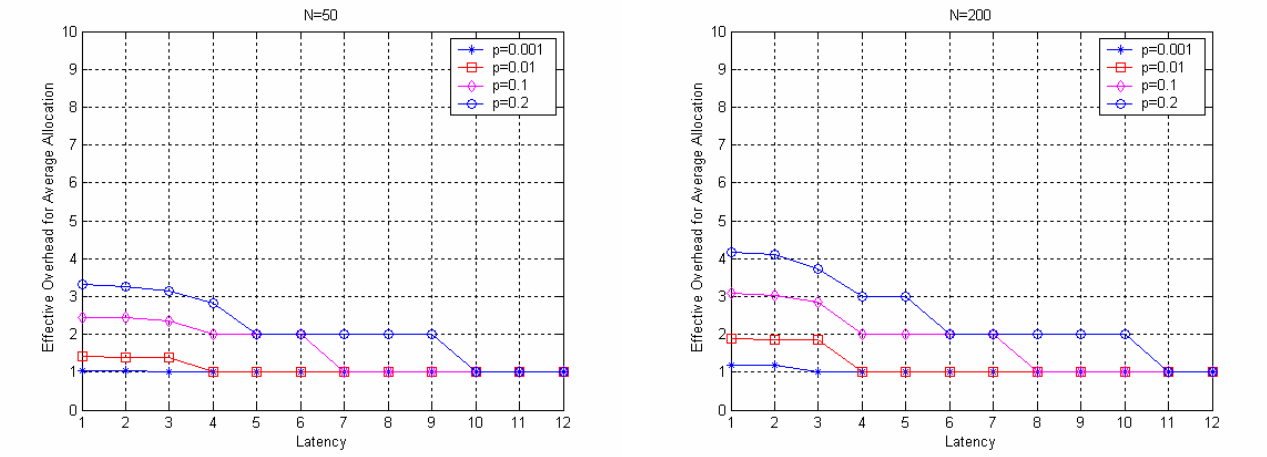

Figure 7-14: Effective transmission overhead for Average Allocations with N = 50 and 200

7.5 Conclusions

In this section we investigated the effect of FEC Block errors on the allocation requirements for multimedia stream. To overcome the complexities incurred in direct analysis and Markov chain based analysis, we presented an approximate analytical estimate of the Fixed Allocation and Average Allocation. Simulations were used to validate the accuracy of the analytical estimates. Our results show that, for supporting low latency applications the average allocation size has to be increased by one or more

transmission overheads. Further, the increase in allocation requirement does not show strong dependency on the application data rate. Thus, low data rate applications can suffer significant loss in efficiency under her FEC block error. Hence, channel adaptation should take into consideration the application data rate and QoS requirement to increase the overall system capacity.

CHAPTER 8
BEACON SCHEDULE PERSISTENCE TO MITIGATE BEACON LOSS

HomePlug AV uses a beacon based Time Division Multiple Access (TDMA) technique for providing guaranteed bandwidth to multimedia streams. Beacons in HomePlug AV carry TDMA allocation (or scheduling) information for various active multimedia streams. Since a station that missed a beacon will not know the schedule for that beacon period, it will not be able to transmit. Due to the large attenuation and impulse noise, beacon detection cannot always be guaranteed. To overcome occasional beacon loss, HPAV uses persistent beacon schedules. Persistent schedules are valid for multiple beacon periods, thus enabling a station to transmit even if it misses one or more beacons.

In this section we use a Markov chain based analysis to investigate the impact of beacon loss on systems with and without persistent beacon schedule. Results show that significant loss in efficiency, and in the level of guarantees on QoS, can occur when no schedule persistence is used. The analysis further shows that the use of persistent current and preview schedule or persistent preview schedules can enable HPAV systems to tolerate up to 10% beacon loss probability with minimum impact of MAC efficiency and QoS guarantees. A subset of the results presented in this chapter are also published in [46]

8.1 Introduction

HomePlug AV Medium Access Control (MAC) layer is based on a hybrid of Time Division Multiple Access (TDMA) and Carrier Sense Multiple Access (CSMA). Each

HPAV network has a designated device, the Central Coordinator (CCo), that coordinates access to medium. The CCo periodically generates a beacon with information about the temporal location of TDMA and CSMA allocations for the stations in the network. TDMA is used by applications requiring QoS, while CSMA is used for transport of regular data. In HPAV, CCo beacon is synchronized to the underlying AC line cycle and is transmitted once every two AC line cycle periods. Thus in North America, CCo beacon has a period of 33.33msec, while in Europe a 40msec beacon period is used. Stations with multimedia traffic continuously communicate with the CCo regarding the required duration of their TDMA allocations. This continuous communication is essential as traffic characteristics and channel characteristics can change with time. Based on this feedback, the CCo updates the schedules. In general, the schedule can change on each beacon Period. Hence, a station that failed to receive beacon cannot transmit in the corresponding beacon Period.

The CCo beacons in HPAV are 136-octets long. To enable robust reception under a variety of channel conditions, they are encoded using ½ rate turbo convolutional codes, spread in frequency and time by using 5-time repetition code, and are modulated use QSPK modulation. Under AWGN conditions, this encoding will enable reliable beacon reception up to -3dB Signal-to-Noise ratio. In typical homes, the beacon loss probability can be expected to be less that 1%. However, due to the large dynamic range of attenuation and (impulse) noise over power line, beacon loss can be large than 1% in some cases. To overcome such scenarios, HPAV provides two mechanisms,

1. Proxy Networking, and
2. Beacon Schedule Persistence

Using the proxy networking procedure, a CCo can appoint one or more stations as Proxy Coordinators. Proxy Coordinators are provided with TDMA allocations to retransmit the CCo's beacon. This repetition of the CCo's beacon enables propagation of schedule information to stations that cannot reliably hear the CCo but can hear the proxy station(s). Proxy Networking in HPAV is primarily suited for handling hidden stations; however this function can also be used for enhancing beacon schedule reliability.

HPAV standard uses beacon schedule persistence to deal with occasional beacon losses. Beacon schedule persistence enables the CCo to publish a schedule that is valid for multiple beacons. This will enable station(s) that misses to beacon to transmit in a beacon period where the schedule information is known based on previously received beacons. In this section, we provide an in depth analysis on the effect of beacon loss in HPAV networks and investigate the performance gain that can be achieved by using persistent schedules.

The organization of the remaining sections is as follows. Section 8.2 provides details on the various Persistent Beacon Schedules allowed in HomePlug AV. We investigate the effect of beacon loss on efficiency in Section 8.3. Section 8.4 provides a frame work for detailed study of the complex interaction between application QoS, MAC Efficiency and beacon loss probability. The effect of beacon loss on the lower bound of packet loss probability for various scheduling strategies is analyzed in section 8.4. Detailed Markov chain based analysis of the effect of beacon loss on QoS and efficiency is presented in Section 8.6. Comparison of the performance of various Persistent Beacon Schedules is presented in Section 8.7 and conclusions are presented in Section 8.8.

8.2 Persistent Beacon Schedules

Beacons in HomePlug AV are 136-octets long and can carry variable length scheduling information. The scheduling information consists of the start and end times of allocations for various multimedia stream, along with the information on the beacon period(s) in which the scheduling information applies. Binding the scheduling information to the beacon period(s) in which it is applicable is achieved by means of a Current Schedule Count Down (CSCD) and a Preview Schedule Count Down (PSCD) fields. These fields allow three different types of persistent schedules,

1. Persistent current schedules,
2. Persistent preview schedules, and
3. Persistent current and preview schedules.

Persistent current schedules are indicated by setting the PSCD field to zero. In this case, the schedule is valid in the current beacon period and the CSCD indicates the number of up coming beacon periods for which the schedule remains valid (i.e., unchanged). Current schedules enable a station that receives a schedule to transmit in all subsequent beacon periods during which it remains valid. Figure 8-1 shows an example of a 2-persistent current schedule. In this example, beacons B1 carries schedule A that is indicated as being valid in beacon period B2 also by setting CSCD to 1. Beacon B2 also carriers schedule A, and indicates that it is valid only in beacon period B2 by setting CSCD to 0. Similarly, beacons B3 and B4 carry schedule B that is valid in beacon periods B3 and B4, and so on. In general, an r-persistent current schedule remains valid for (r-1) beacon periods subsequent to the beacon period in which it is first published. When r-persistent current schedule is used, the maximum latency incurred by the CCo from the time a schedule change is planned to when it becomes effective is (r-1). The

main disadvantage of persistent current schedules is that new schedules are most venerable in the beacon periods where they are first published.

Persistent preview schedules are indicated by setting the PSCD to a non-zero value. In this case, the PSCD field indicates the number of beacon periods (including the current beacon period) in which schedule become active. The CSCD field indicates the number of beacon period for which the preview schedule will remain active minus one. preview schedules enable the CCo to repeat a schedule certain number of times before it becomes active. Figure 8-2 shows an example of a 2-persistent preview schedule. In this example, beacons B1 carriers Schedule B and indicate that it becomes valid in beacon period following beacon B3 (i.e., PSCD = 2) and remains valid for two beacon periods (i.e., CSCD=1).

Beacon B2 also repeats the same scheduling information. Similarly, beacons B3 and B4 carry schedule C that is valid in beacon periods B5 and B6, and so on. In general, an r-persistent preview schedule is repeated in r beacon periods before it becomes active and it also remains active for r beacon periods. The main advantage of this method is that a station is only required to receive any one of the r-beacons to be able to transmit in a beacon period. This increases resilience to beacon loss. The drawback of this approach is the additional latencies incurred for the CCo to change schedules. For r-persistent preview schedules, a latency of up to (2r-1) beacon periods can elapse from the time the CCo decides to change a schedule until the new schedule becomes active.

HPAV allows the CCo to include one preview schedule and one current schedule in the same beacon, if there is sufficient space available. Note that HPAV beacons always carry 136 octets of information and the scheduling information for each TDMA

allocation typically requires 3 octets. So, if is very likely to have sufficient space to include both current and preview schedules into a beacon. Figure 8-3 shows an example of 2-persistent current and preview schedule. In this example, beacon B1 and B2 carry current schedule A that is valid in their respective beacon periods and preview schedule B that is valid in the beacon periods following B3 and B4. Similarly, beacons B3 and B4 carries current schedule B and preview schedule C, and so on. In an r-persistent current and preview schedules, each schedule is transmitted times, thus enhancing its reliability. The maximum latency incurred in changing r-persistent current and preview schedule is the same as the maximum latency of the corresponding r-persistent preview schedule.

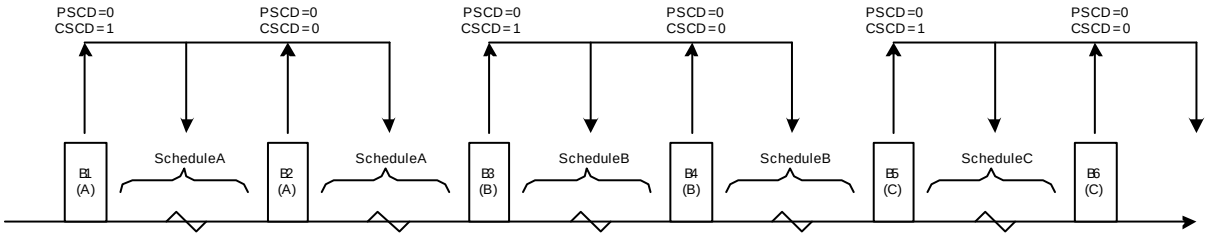

Figure 8-1: Example of 2-persistent current schedules

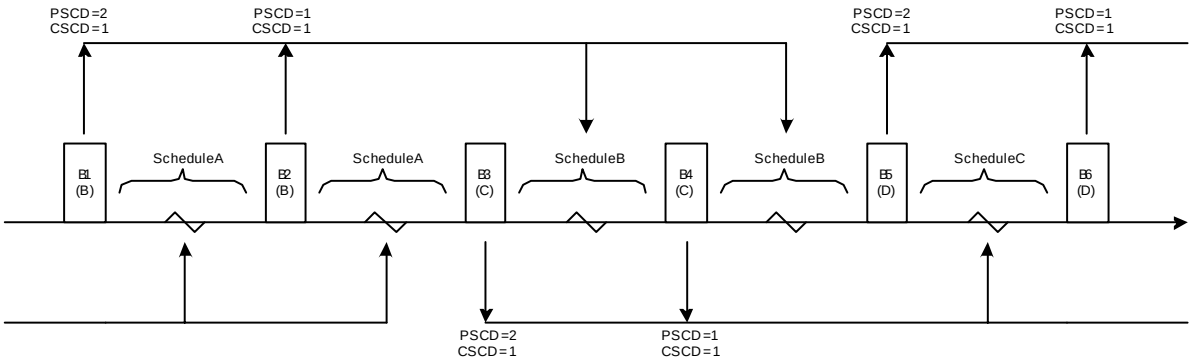

Figure 8-2: Example of 2-persistence preview schedules

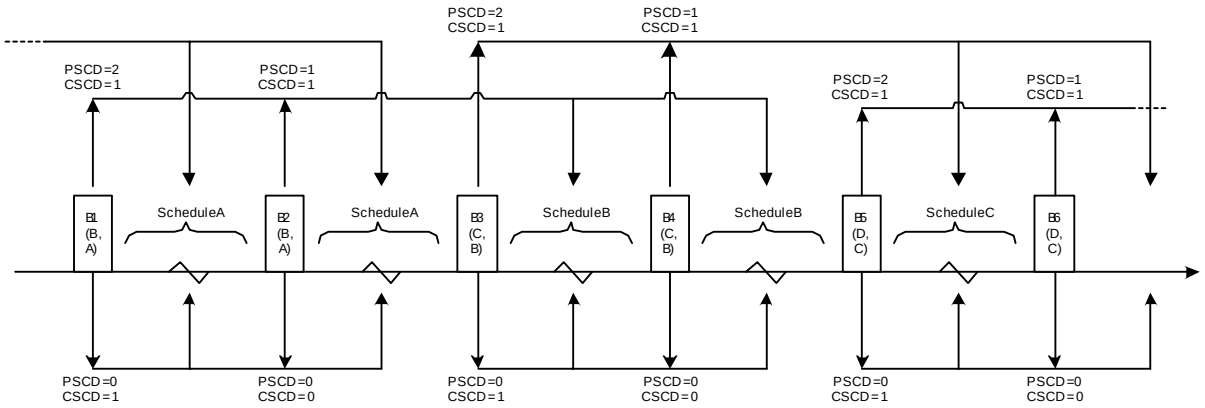

Figure 8-3: Example of 2-persistent current and preview schedules

8.3 Efficiency Analysis

A station that misses a beacon may not be able to transmit in its allocation. This reduces the overall utilization of an allocation, thus reducing the efficiency. In this section we use simple analysis to study the effect of beacon loss on efficiency for various scheduling strategies.

8.3.1 Non-persistent schedule

For non-persistent schedules, every time a beacon loss occurs, the corresponding allocation cannot be used. Hence the efficiency of non-persistent schedules, ρ^{NP}, is

$$\rho^{NP} = 1 - p_b$$

8.3.2 Persistent current schedules

For r-persistent current schedules, effect of a beacon loss will depend on the location of the corresponding beacon period (i.e., beacon period where the beacon loss occurred) relative to the beacon period in which the schedule is first published. To miss an allocation in a beacon period that is t-beacon periods from the first beacon period in which the schedule was published, a total of beacons have to be missed. Hence, the efficiency of the tth beacon period, $\rho_t^{CS,r}$, is given by,

$$\rho_t^{CS,r} = \left(1 - (p_b)^{t+1}\right)$$

Thus, the efficiency of an r-persistent current schedule, $\rho^{CS,r}$, is

$$\rho^{CS,r} = \frac{1}{r}\sum_{t=0}^{r-1}\left(1 - (p_b)^{t+1}\right) = 1 - \frac{p_b\left(1 - (p_b)^r\right)}{r(1 - p_b)}$$

8.3.3 Persistent preview schedules

For r-persistent preview schedules, an allocation can be utilized if any one of the r-beacons in which the schedule was previewed is successfully received. Hence, the average efficiency of a r-persistent preview schedule, $\rho^{PS,r}$, is given by,

$$\rho^{PS,r} = 1 - (p_b)^r$$

8.3.4 Persistent current and preview schedules

For r-persistent current and preview schedules, effect of a beacon loss will again depend on the location of the corresponding beacon period relative to the beacon period in which the schedule is first published. Further it will also depend on the reception station of the beacons carrying the preview schedule. To miss an allocation in a beacon period that is t-beacon periods from the first beacon period in which the schedule was published, a total of beacons have to be missed. Hence, the efficiency of the t^{th} beacon period, $\rho_t^{CS,PS,r}$, is given by,

$$\rho_t^{CS,PS,r} = 1 - (p_b)^{r+t+1}$$

Thus, the efficiency of an r-persistent current and preview schedule, $\rho^{CS,PS,r}$, is

$$\rho^{CS,PS,r} = \frac{1}{r}\sum_{t=0}^{r-1}\left(1 - (p_b)^{r+t+1}\right) = 1 - \frac{(p_b)^{r+1}\left(1 - (p_b)^r\right)}{r(1 - p_b)}$$

8.3.5 Efficiency comparison

A comparison on efficiency loss for various scheduling strategies under different beacon loss probabilities is shown in Figure 8-4. These results can be summarized as follows,

- The efficiency loss for non-persistent schedules in proportional to the beacon reliability. Thus, 10% loss in efficiency will be experienced in environments where the beacon loss probability is 10%.
- Persistent current schedules do not provide significant improvement in efficiency compared to non-persistent schedules. Further, most of the efficiency loss can be attributed to the poor utilization of the beacon period in which the schedule is first published. In environments with 10% beacon loss probability, current schedules with persistence's of 2, 4, and 8 show approximately 5.5%, 2.8% and 1.4% loss in efficiencies, respectively.
- Significant improvement in efficiencies can be obtained by using persistent preview schedules. 2-persistent preview schedules show a 1% loss in efficiency in environments with 10% beacon loss. Preview schedules with persistent greater than 2, will show negligible loss in performance
- Persistent preview and current schedules provide the best performance in terms of efficiency. A 2-persient current and preview schedule shows 0.06% loss in efficiency in environments with 10% beacon loss.

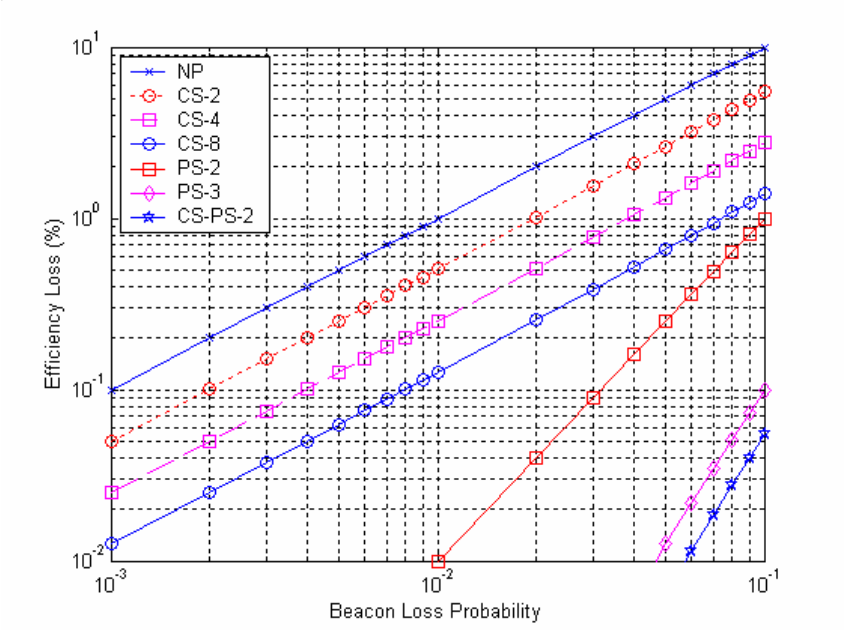

Figure 8-4: Efficiency loss comparison for various scheduling strategies

8.4 QoS Considerations

Apart from reduction in efficiency, beacon loss can also affect the QoS. For example, when non-persistent schedules are used, a burst of beacon errors that span a duration larger than the latency of the multimedia stream will result in a packet loss event. In this section we study the interaction between QoS and beacon loss. In general, the effect of beacon loss on multimedia stream will depend on the following factors,

1. Data rate of the multimedia stream,
2. Latency requirement of the multimedia stream,
3. The maximum packet loss probability tolerated by the multimedia stream,
4. Beacon loss probability observed over the power line channel,
5. The schedule persistent mechanism used by the CCo, and
6. The allocation strategy used by the CCo to clear the backlog created at the station due to beacon loss

In the following sections we derive the relationship between these parameters based on the following assumptions,

- We first assume that the multimedia stream has a constant data rate. Further we assume that the application requires transmission of N Segments (of data) in each beacon period. In HPAV, Segments are 512-octet data units that carry application payload. Hence, N is a function of the data rate of the multimedia stream. In the remainder of the section, we refer to each Segment and packet,

- Since multimedia streams are provided with one allocation each beacon period, we assume that the latency (L) of the application is in terms of a certain number of beacon periods. This does not limit our analysis in any manner, however it simplifies presentation of the results and makes them independent of the beacon Period (with can be either 33.33msec or 40 msec),

- Beacon loss events tend to create burst of packet losses. Hence we measure the QoS in terms of packet loss event probability (PLEP) and the average number of packets lost per packet loss event (APL),

- We assume that the source of the multimedia stream is experiencing uncorrelated beacon loss events with a beacon loss probability of p_b . Beacons in HPAV are synchronized with respect to the AC line cycle, and power line channel characteristics tend to remain static with respect to the AC line cycle [37, 38], justifying the uncorrelated beacon loss assumption. As we are only interested in the effect of beacon loss, to simplify the analysis we further assume that all transmitted

packets will be successfully received (i.e., no packet loss due to errors in the reception of physical layer protocol data units),

- Our analysis studies all Scheduling strategies allowed in HPAV,
- Packets that did not get delivered due to beacon loss should be transmitted in subsequent beacon periods. There are several strategies that can be used by the CCo to enable the station to clear the backlog. These include,

1. Always provide a fixed (X) number of packets of over allocation,
2. Provide a fixed (X) number of packets of over allocation, whenever there is backlog at the station,
3. Provide variable number of packet of over allocation based on backlog, with an upper bound (X) on the maximum over allocation.

Approach (a) is by far the simplest. However, this is also the most inefficient approach as the over allocation will most likely remain unused. Approaches (b) and (c) use dynamic over allocation, and they require the CCo to track the backlog for each stream. In HPAV, all streams provide an indication of their backlog to the CCo, thus making approaches (b) and (c) practical. For our analysis, we use choose approach (b), as it is more efficient than (a) and is simpler to analyze than (c). We also assume that the CCo can always track the backlog at the station. In practice, it is possible for CCo to miss transmissions from the stations (i.e., similar to the station missing beacons). However, since the CCo only needs to determine whether a station transmitted in an allocation (irrespective of whether it properly received or not) this can be very highly reliable, thus justifying our assumption.

8.5 Lower Bound on PLEP

In this section we derive lower bounds on the PLEP that can be achieved for a given Latency requirement (L) and Beacon Loss Probability (p_b). The derivation of the lower bound is motivated by two reasons. Firstly, as we will see in Section 7, the

derivation of the accurate relationship between {N, p_b, L, PLEP and Alloc} is quite involved and requires solving complex Markov chains. In contrast, a closed form expression can be obtained for the upper bound. Secondly, as will be shown in subsequent sections, upper bound does provide a good estimate on the actual performance of two of the more important scheduling schemes i.e., persistent current and preview schedules, and persistent preview schedules.

We derive the lower bound on the PLEP by assuming that the CCo provides sufficient amount of over allocation in each beacon period to completely eliminate any backlog. This assumption essentially makes PLEP a function of the number of consecutive beacons missed by the station, thus simplifying the analysis.

8.5.1 Non-persistent schedules

For non-persistent schedules, a minimum of L consecutive beacons has to be missed to incur a packet loss event. When exactly L consecutive beacons are lost, one packet loss event will occur. When exactly (L+1) beacons are missed, two packet loss events will occur, and so on. For the general case of ℓ consecutive beacons being missed, $(\ell - L + 1)$ packet loss events will occur. Since ℓ consecutive beacons can be lost with probability $(p_b)^{\ell}(1-p_b)^2$, the packet loss event probability for non-persistent schedules, $PLEP^{NP,UB}$, can be obtained as,

$$PLEP^{NP,LB} = \sum_{\ell=L}^{\infty} (p_b)^{\ell}(1-p_b)^2(\ell - L + 1) = (p_b)^L$$

8.5.2 Persistent current schedules

For r-persistent current schedules, the PLEP will not only depend not only on the number of consecutive beacons missed, but also on the location of the first missed beacon relative to the beacon in which the corresponding schedule is first published. For a burst

of beacon losses starting with a beacon in which the schedule was first published, the packet loss event probability can be obtained in a manner similar to that of non-persistent schedule, i.e.,

$$PLEP_{t=0}^{CS,r,LB} = \sum_{\ell=L}^{\infty} (p_b)^{\ell} (1-p_b)^2 (\ell - L + 1) = (p_b)^L$$

For the case of a burst of beacon losses starting with a beacon that is t beacon periods (with t $\in$ [1 r-1]) from the beacon in which the corresponding schedule was first published, (r-t) additional beacons have to be lost to incur the same number of packet loss events as that of t=0. Hence, $PLEP_{t\in[1,r-1]}^{CS,r,LB}$, can be obtained as follows,

$$PLEP_{t\in[1,r-1]}^{CS,r,LB} = \sum_{\ell=L+r-t}^{\infty} (p_b)^{\ell} (1-p_b)^2 (\ell - L - r + t + 1) = (p_b)^{L+r-t}$$

Thus, the average PLEP of r-persistent current schedule, $PLEP^{CS,r,LB}$, is,

$$\begin{aligned} PLEP^{CS,r,LB} &= \frac{1}{r} \sum_{t=0}^{r-1} PLEP_t^{CS,r,UB} \\ &= \frac{1}{r} \left((p_b)^L + \sum_{t=1}^{r-1} (p_b)^{L+r-t} \right) = \frac{(p_b)^L \left(1 - (p_b)^r\right)}{r(1-p_b)} \end{aligned}$$

8.5.3 Persistent preview schedules

As with r-persistent current schedules, the packet loss event probability for r-persistent preview schedules will show dependency on the location of the first beacon lost beacon relative the beacon carrying new schedule. For this analysis, we represent Latency L as,

$$L = k \times r + a; \ \ where, \ 1 \le a \le r$$

Consider the case in which the first beacon missed is the beacon in which a new schedule is first published. The first set of packet loss events will occur when (k+1)r consecutive beacons are missed. Figure 8-5 shows and illustration of the relationship

between latencies and persistent preview schedules. In this example, for a packet loss event to occur all beacons carrying Schedule#0 through Schedule#k have to be missed. It can also be seen that beacon loss bursts of length in the range [(k+1)r, (k+2)r-1], will all result in (r-a+1) packet loss events. Similarly, beacon loss bursts of length [(k+2)r, (k+3)r-1], will result in (2r-a+1) packet loss events, and so on. Hence, the packet loss event probability, $PLEP_{t=0}^{PS,r,UB}$, is given by,

$$\begin{aligned} PLEP_{t=0}^{PS,r,LB} &= \sum_{m=1}^{\infty} \sum_{\ell=(k+m)r}^{(k+m+1)r-1} (p_b)^{\ell} (1-p_b)^2 (mr-a+1) \\ &= \sum_{m=1}^{\infty} (p_b)^{(k+m)r} (1-p_b)\left(1-(p_b)^r\right)(mr-a+1) \\ &= (p_b)^{(k+1)r} (1-p_b)\left(\frac{r}{\left(1-(p_b)^r\right)}-(a-1)\right) \end{aligned}$$

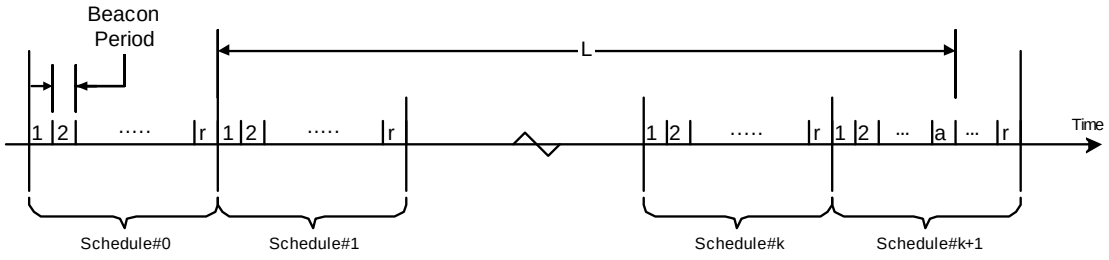

Figure 8-5: Illustration of relationship between latency and persistent preview schedule

Analysis of packet loss event probability for the case a burst of beacon losses starting with a beacon that is t beacon periods (with $t \in [1\ r-1]$) from the beacon in which the corresponding schedule was first published, is similar to the case with t = 0, expect that additions beacons have to be missed before the first PLE occurs. Thus, the packet loss event probability, $PLEP_{t\in[1,r-1]}^{PS,r,LB}$, is given by,

$$PLEP_{t\in[1,r-1]}^{PS,r,LB} = (p_b)^{(k+2)r-t}(1-p_b)\left(\frac{r}{\left(1-(p_b)^r\right)}-(a-1)\right)$$

Hence the average packet loss event probability, $PLEP^{PS,r,LB}$, is given by,

$$\begin{aligned} PLEP^{PS,r,LB} &= \frac{1}{r}\sum_{t=0}^{r-1} PLEP_t^{PS,r,LB} \\ &= \frac{1}{r}\left[PLEP_{t=0}^{PS,r,LB} + \sum_{t=1}^{r-1} PLEP_{t\neq 0}^{PS,r,LB} \right] \\ &= (p_b)^{(k+1)r}\left(1-\frac{\left(1-(p_b)^r\right)(a-1)}{r}\right) \end{aligned}$$

8.5.4 Persistent current and preview schedules

The lower bound for r-persistent current and preview schedules can be determined in a manner similar to that of the r-persistent current schedules. For a burst of beacon losses starting with a beacon in which a new schedule was first published, a minimum of (r+L) beacons has to be missed to cause the first packet loss event. When ℓ consecutive beacons are missed with, $\ell \geq (L+r)$, a total of $(\ell - L - r + 1)$ packet loss events occur. Thus, the packet loss event probability, $PLEP_{t=0}^{CS,PS,r,LB}$, is given by,

$$PLEP_{t=0}^{CS,PS,r,LB} = \sum_{\ell=L+r}^{\infty}(p_b)^{\ell}(1-p_b)^2(\ell - L - r + 1) = (p_b)^{L+r}$$

For a burst of beacon losses starting with a beacon that is t beacon periods from the beacon in which the corresponding persistent schedule was first published, (r-t) additional beacons have to be missed to incur similar number of beacon loss events. Hence, the packet loss event probability, $PLEP_{t\in[1,r-1]}^{CS,PS,r,LB}$, is given by

$$PLEP_{t\in[1,r-1]}^{CS,PS,r,LB} = \sum_{\ell=L+2r-t}^{\infty}(p_b)^{\ell}(1-p_b)^2(\ell - L - 2r + t + 1) = (p_b)^{L+2r-t}$$

Thus, the average PLEP of r-persistent current and preview schedule, $PLEP^{CS,PS,r,LB}$, is,

$$PLEP^{CS,PS,r,LB} = \frac{1}{r}\sum_{t=0}^{r-1} PLEP_t^{CS,PS,r,LB}$$
$$= \frac{1}{r}\left((p_b)^{L+r} + \sum_{t=1}^{r-1} (p_b)^{L+2r-t} \right)$$
$$= \frac{(p_b)^{L+r}\left(1-(p_b)^r\right)}{r\left(1-p_b\right)}$$

8.5.5 Lower Bound comparison

Some interesting properties of the scheduling strategies can be observed by looking at the lower bound.

- For non-persistence schedules, packet loss event probabilities better than $(p_b)^L$ cannot be guarantees. This indicates the degradation in QoS when persistent schedules are not used.

- For persistent current schedules, the packet loss event probability is primarily effected by $((p_b)^L/r)$. This shows that significantly large values of r should be used to reduce PLEP. Thus, at least from an upper bound perceptive, we can expect no significant improvement in the level of guarantees on QoS, compared to the non-persistent schedules.

- Packet loss event for persistent preview schedules shows non-linear behavior with L for a given r. Large improvement in performance can be expected when L = kr + 1. However, when L = kr persistent preview schedules does not provide any improvements in upper bound.

- For persistent current and preview schedules, the packet loss event probability is primarily effected by $((p_b)^{[L+r]}/r)$. Thus from a PLEP point of view, r-persistent current and preview schedules effectively increase the latency of the stream by r, compared to that of the non-persistent schedule.

The goodness of the upper bound will be studies in subsequent sections, by comparing the result obtained in this section to the ones obtained using Markov chain based analysis.

8.6 Markov Chain Analyses

In the following sections we use Markov chain based analysis to investigate the effect of beacon loss on a system using various persistent scheduling strategies. Our goal is to obtain the dependency of the packet loss event probability, PLEP, on {N, L, p_b, and

X}. Note that X is a measure of inefficiency incurred at the MAC layer to overcome beacon loss. Since the minimum value of X needed to overcome any beacon loss is 1, in the subsequent analysis we refer to X=1 as the optimal over allocation.

8.6.1 Non-persistent beacon schedules

In this section we investigate the effect of beacon loss on a system that uses non-persistent schedules. Since non-persistent schedules are valid only in the period in which they are published, a station that misses a beacon cannot transmit in the corresponding beacon period.

First, consider the buffer backlog of the stream at the end of each beacon period. It can be readily seen that the variation of the buffer backlog is only dependent on the reception status of the beacon in the corresponding beacon period. Furthermore, the maximum buffer backlog is bounded by N(L-1). Hence a discrete-time, finite state Markov chain model can be used to determine the steady state probabilities of buffer backlog from which the PLEP can be computed. Figure 8-6 shows the state transition diagram of buffer backlog when non-persistent (NP) beacon schedules are used with L > 2 and X < N.

The state transition probabilities, $p_{i,j}^{NP}$, is given by

$$p_{i,j}^{NP} = \begin{cases} p_b & 0 \le i \le NL - N,\ j = \min(i + N, NL - N) \\ 1 - p_b & 0 \le i \le NL - N,\ j = \max(i - X, 0) \end{cases}$$

The steady state probabilities, P_i^{NP}, can be obtained from the state transition probabilities by solving the equation,

$$\left[p_{i,j}^{NP}\right]\left[P_i^{NP}\right] = \left[P_i^{NP}\right]$$

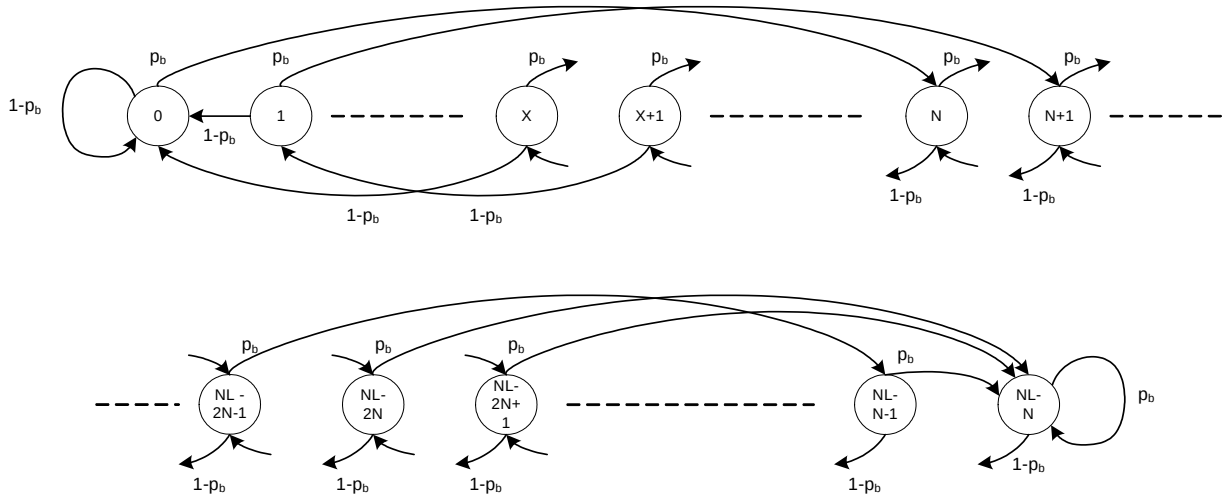

Figure 8-6: State transition diagram for non-persistence beacon schedules

The packet loss event probability ($PLEP^{NP}$) and average packets lost per packet loss event (APL^{NP}) can be obtained from the steady state probabilities (P_i^{NP}) as follows,

$$PLEP^{NP} = \sum_{i=NL-2N+1}^{NL-N} P_i^{NP} \; p_b$$

$$APL^{NP} = \frac{\sum_{i=NL-2N+1}^{NL-N} P_i^{NP} \; p_b \{i - NL + 2N\}}{PLEP^{NP}}$$

One important point to note is that not all buffer backlog states are possible (i.e., the Markov chain is not irreducible). For example, if X and N are even, odd backlog states never occur. Another interesting property that can be observed from the state transition diagram is the effect of scaling N and X by an integer value. This will result in a scaled state transition diagram with the same transition probability between scaled states. This suggests that the ratio X/N primarily determines the $PLEP^{NP}$.

8.6.2 Persistent current schedules

The performance of persistent current schedules can be carried out in a manner similar to that of non-persistent schedules except with one important difference. Instead

of tracking the buffer backlog at the end of each beacon period, we track the buffer backlog at the end of the last beacon period in which a published schedule remains valid. This choice will eliminate the dependency of buffer backlog states on the schedule persistent, thus simplifying the analysis. Note that Markov chain analysis can also be carried out by tracking the buffer backlog at the end of each beacon period. The disadvantage of the later approach is that the number of states will increase by 'r' times. Irrespective of the approach used, the exact relationship between PLEP, N, L, p_b and X can be obtained. Figure 8-7 shows the state transition diagram of buffer backlog when 2-persistent current schedules are used with L > 2 and X < N.

A generalized state transition probability for r-persistent current schedule, $p_{i,j}^{CS,r}$, can be computed by first initializing $p_{i,j}^{CS,r}$ to zeros and following the procedure given in the following equation,

$$p_{i,j}^{CS,r} = \begin{cases} p_{i,j}^{CS,r} + (1-p_b) & 0 \le i \le NL-N,\ j = \max(i - Xr, 0) \\ p_{i,j}^{CS,r} + p_b(1-p_b) & 0 \le i \le NL-N,\ j = \max\{\min(i+N, NL-N) - X(r-1), 0\} \\ \cdots & \\ p_{i,j}^{CS,r} + (p_b)^t(1-p_b) & 0 \le i \le NL-N,\ j = \max\{\min(i+Nt, NL-N) - X(r-t), 0\} \\ \cdots & \\ p_{i,j}^{CS,r} + (p_b)^r & 0 \le i \le NL-N,\ j = \min(i+Nr, NL-N) \end{cases}$$

In the above equation, the first term corresponds to the transition when the first beacon carrying a new schedule is properly received. Subsequent terms correspond to the transition where the first t beacons carrying a new schedule are not properly received. The last term corresponds to the case where all beacons carrying a new schedule are lost. It is important to note that more than one of the above conditions can result in the same

final state. In such cases, the transition probability will be the sum of all events that result in the same final state, as shown in the above equation.

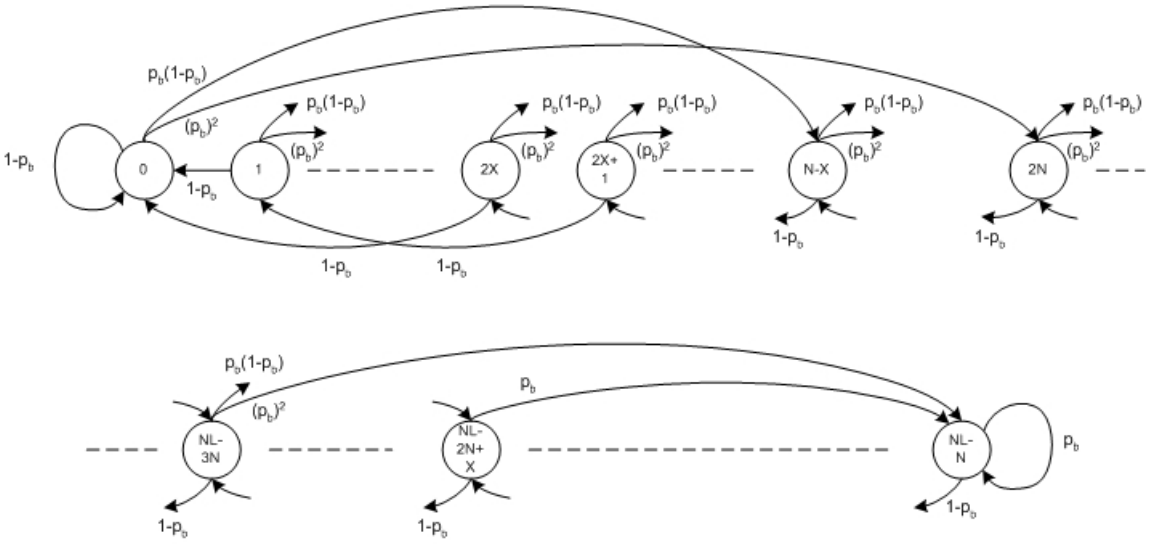

Figure 8-7: State transition diagram for 2-persistence current schedules

The packet loss event probability, $PLEP^{CS,r}$, can be obtained from the steady state probabilities, $P_i^{CS,r}$, as follows,

$$PLEP^{CS,r} = \sum_{i=0}^{NL-N} P_i^{CS,r} PLTP_i^{CS,r}$$

Where, packet loss transition probability from state i, $PLTP_i^{CS,r}$, is given by,

$$PLTP_i^{CS,r} = \left(\sum_{t=1}^{r-1} (p_b)^t (1-p_b) \frac{ceil\left\{ \frac{\max(i+Nt-NL+N,0)}{N} \right\}}{r} \right) + \left((p_b)^r \frac{ceil\left\{ \frac{\max(i+Nr-NL+N,0)}{N} \right\}}{r} \right)$$

The average PBs lost per packet loss event, $APL^{CS,r}$, is given by,

$$APL^{CS,r} = \frac{\sum_{i=0}^{NL-N} P_i^{CS,r} \; APL_i^{CS,r}}{r \times PLEP^{CS,r}}$$

Where, average number of packets lost during transitions from state i, $APL_i^{CS,r}$, is given by,

$$APL_i^{CS,r} = \left(\sum_{t=0}^{r-1} (p_b)^t (1 - p_b) \max(i + Nt - NL + N, 0) \right) + (p_b)^r \max(i + Nr - NL + N, 0)$$

8.6.3 Persistent preview schedules

The performance of persistent preview schedule can be carried out in a manner similar to that of persistent current schedule, by tracking the buffer backlog at the end of the last beacon period in which a published schedule remains valid. However, since there is latency incurred from the time a new schedule is published to the time it becomes effect, each state in the Markov chain should incorporate three state variables,

1. Buffer backlog,
2. The presence or absence of over allocation in the current schedule (represented by "C" and "NC" respectively), and
3. The present or absence of over allocation in the schedule following the current schedule i.e., the immediate future schedule (represented by "F" and "NF" respectively).

Figure 8-8 illustrates the changes in Markov chain states for the case of 2-persistent preview schedule with an over allocation of N packets (i.e., X = N). In this example, it is assumed that beacons carrying schedule A2 are lost. At the end of beacon periods in which schedule A2 becomes effective, the backlog increases to 2N. At this time CCo publishes schedule A4 with N packets of over allocation (since inferred backlog is greater than zero). Due to the latency incurred for a published schedule to become effective, the backlog at the end of beacon periods in which schedule A3 becomes effective remains at

2N. This in turn causes the CCo to publish a schedule A5 with N packets of over allocation. The backlog becomes zero at the end of beacon periods in which schedule A4 becomes effective, however over allocation is provided until the end of schedule A5. Note that over allocation can be chosen to not provide over allocation in Schedule A4. For simplicity, we do not consider such a scheme in our study.

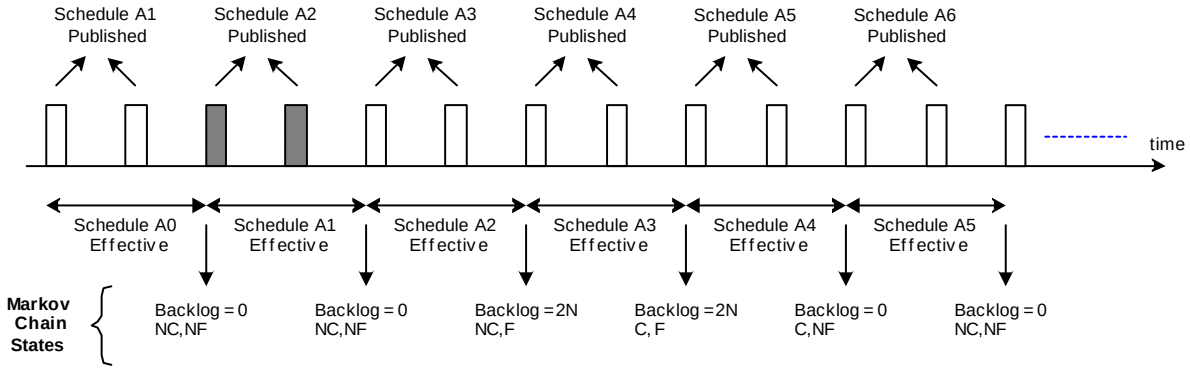

Figure 8-8: Illustration of state changes in Markov chain for 2-persistent preview schedule

The number of states in the Markov chain can be reduced by noting that,

1. Backlog is always going to be zero in a state where there is no over allocation in the current and immediate future schedules (i.e., [NC, NF]),

2. Backlog is always going to be zero in a state where there is over allocation in the current schedule and no over allocation in the immediate future schedule (i.e., [C, NF]),

3. Backlog is always going to be min(Nr, N(L-1)), in a state where there is no over allocation in the current schedule, but there is over allocation in the future schedule (i.e., [NC, F])

Figure 8-9 shows the state transition diagram of buffer backlog when 2-persistent preview schedules are used with $L > 2$ and $X < N$.

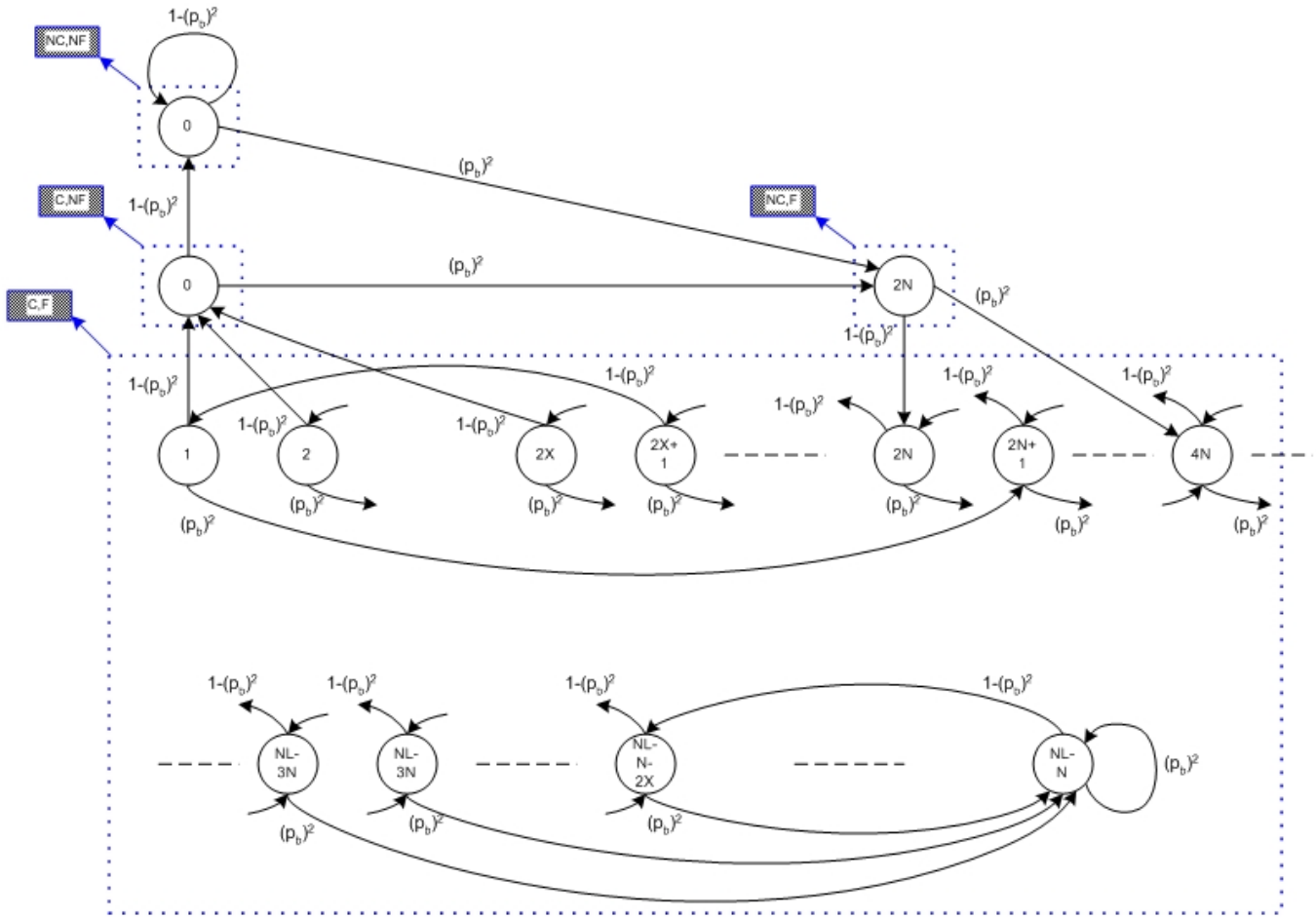

Figure 8-9: State transition diagram for 2-persistence preview schedules

A generalized state transition probability for r-persistent preview schedules, can be computed using the follow equations,

- Transition form state with no current and no future over allocation,

$$\Pr([0, NC, NF], [0, NC, NF]) = 1 - (p_b)^r$$
$$\Pr([0, NC, NF], [N \times r', NC, F]) = (p_b)^r$$

Where, $r' = \min(r, L-1)$

- Transition form state with no current over allocation, but over allocation is provided in the future schedule

$$\Pr([N \times r', NC, F], [N \times r', C, F]) = 1 - (p_b)^r$$
$$\Pr([N \times r', NC, F], [N \times r'', NC, F]) = (p_b)^r, where\ r' = \min(r, L-1)$$

Where, $r' = \min(r, L-1)$, and $r'' = \min(2 * r, L-1)$

- Transition from state with current over allocation, but no future over allocation

$$\Pr([0, C, NF], [0, NC, NF]) = 1 - (p_b)^r$$
$$\Pr([0, C, NF], [N \times r', NC, F]) = (p_b)^r$$

where, $r' = \min(r, L-1)$

- Transition from states with current and future over allocations

$$\Pr([i, C, F], [0, C, NF]) = 1 - (p_b)^r;\ 1 \le i \le \min(rX, N(L-1))$$
$$\Pr([i, C, F], [\max(i - rX, 0), NC, F]) = 1 - (p_b)^r;\ \min(rX, N(L-1)) < i \le N(L-1)$$
$$\Pr([i, C, F], [\min(i + N\,r, N(L-1)), NC, F]) = (p_b)^r;\ 1 \le i \le N(L-1)$$

The packet loss event probability, $PLEP^{PS,r}$, can be obtained from the steady state probabilities, $P^{PS,r}_{[i,x,y]}$ as follows,

$$PLEP^{PS,r} = \sum_{i=1}^{NL-N} \left[P^{PS,r}_{[i,C,F]} \frac{ceil\left\{\frac{\max(i + Nr - NL + N, 0)}{N}\right\}}{r} (p_b)^r \right] +$$

$$\left[P^{PS,r}_{[0,NC,NF]} \frac{ceil\left\{\frac{\max(Nr-NL+N,0)}{N}\right\}}{r}(p_b)^r \right] +$$
$$\left[P^{PS,r}_{[0,C,NF]} \frac{ceil\left\{\frac{\max(Nr-NL+N,0)}{N}\right\}}{r}(p_b)^r \right] +$$
$$\left[P^{PS,r}_{[\min(Nr,N(L-1)),NC,F]} \frac{ceil\left\{\frac{\max(\min(Nr,N(L-1))+Nr-NL+N,0)}{N}\right\}}{r}(p_b)^r \right]$$

The average PBs lost per packet loss event is given by,

$$APL^{PS,r} = \frac{TPL^{PS,r}}{r \times PLEP^{PS,r}}$$

Where $TPL^{PS,r}$ is given by,

$$TPL^{PS,r} = \sum_{i=1}^{NL-N} \left[P^{PS,r}_{[i,C,F]} \max(i+Nr-NL+N,0)(p_b)^r \right] +$$
$$\left[P^{PS,r}_{[0,NC,NF]} \max(Nr-NL+N,0)(p_b)^r \right] +$$
$$\left[P^{PS,r}_{[0,C,NF]} \max(Nr-NL+N,0)(p_b)^r \right] +$$
$$\left[P^{PS,r}_{[\min(Nr,N(L-1)),NC,F]} \max(\min(Nr,N(L-1))+Nr-NL+N,0)(p_b)^r \right]$$

8.6.4 Persistent current and preview schedules

The performance of persistent current and preview schedules can be carried out in a manner similar to that of the persistent preview schedules, with the addition of one additional state variable to the Markov chain. This variable tracks whether at least one beacon was successfully received in the beacon periods where the previous schedule was published. Note that if at least one of the beacons is properly received (represented by "1G"), then the schedule is known and all allocations can be successfully utilized. If none

of the beacons were properly received (represented by "AB") the utilization will depend on when the current schedule will be received (based on current schedule). Thus, eight different states are possible for the same value of backlog,

1. No Current, No Future, At least one good (NC, NF, 1G)
2. No Current, No Future, All Bad (NC, NF, AB)
3. Current, No Future, At least one good (C, NF, 1G)
4. Current, No Future, All bad (C, NF, AB)
5. No Current, Future, At least one good (C, NF, 1G)
6. No Current, Future, All Bad (C, NF, AB)
7. Current, Future, At least one good (C, F, 1G)
8. Current, Future, All Bad (C, F, AB)

Reduction in the number of states in the Markov can be done by noting that,

1. Backlog will always be zero in (NC, NF)
2. Backlog will always be zero in (C, NF)
3. Backlog will be limited to $\{N, 2N, ..., \min(Nr, N(L-1))\}$ when in (NC, F, 1G)
4. Backlog will always be $\min(Nr, N(L-1))$ when (NC, F, AB)

Figure 8-10 shows the state transition diagram of buffer backlog when 2-persistent current and preview schedules are used with L > 2 and X < N.

A generalized state transition probability for r-persistent preview schedules, can be computed by first initializing all transition probabilities to zero and following the procedure,

- Transition probabilities from (NC, NF, 1G)

$$\Pr([0, NC, NF, 1G], [0, NC, NF, 1G]) = 1 - (p_b)^r$$
$$\Pr([0, NC, NF, 1G], [0, NC, NF, AB]) = (p_b)^r$$

- Transition probabilities from (NC, NF, AB)

$$\Pr([0, NC, NF, AB], [0, NC, NF, 1G]) = 1 - p_b$$
$$\Pr([0, NC, NF, AB], [j_k, NC, NF, 1G]) += p_b{}^k (1 - p_b); \; for \; 1 \le k \le r-1$$
$$\Pr([0, NC, NF, AB], [j_r, NC, NF, AB]) = p_b{}^r$$

Where, $j_m = \min(m \times N, N(L-1))$

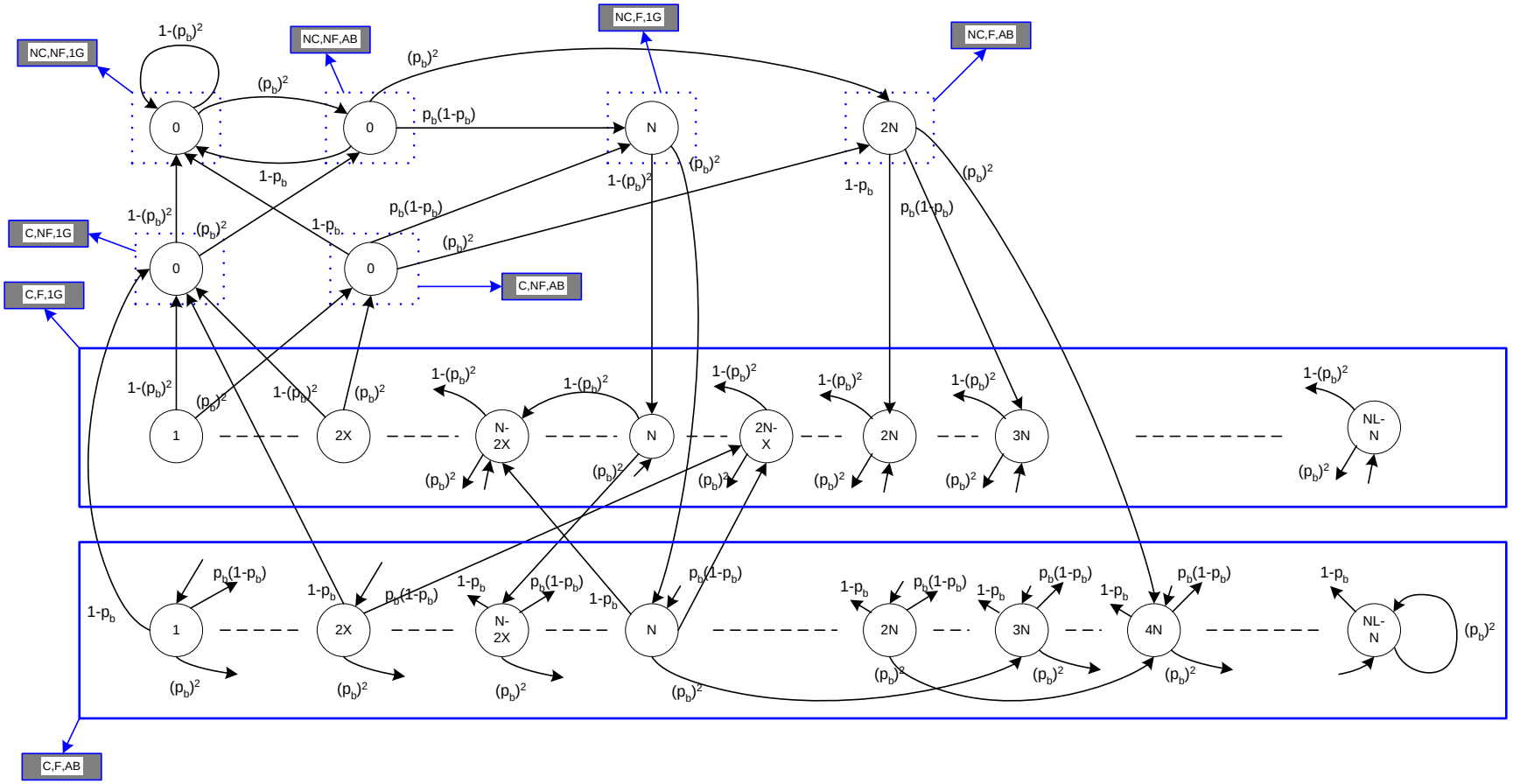

Figure 8-10: State transition diagram for 2-persistence current and preview schedules

- Transition probabilities from (NC, F, 1G)

$$\Pr([j_k, NC, F, 1G], [j_k, C, F, 1G]) = 1 - (p_b)^r;\ for\ 1 \le k \le \min(r, L-1)$$
$$\Pr([j_k, NC, F, 1G], [j_k, C, F, AB]) = (p_b)^r;\ for\ 1 \le k \le \min(r, L-1)$$

- Transition probabilities from (NC, F, AB)

$$\Pr([\min(Nr, N(L-1)), NC, F, AB], [\min(Nr, N(L-1)), C, F, 1G]) = 1 - p_b$$
$$\Pr([\min(Nr, N(L-1)), NC, F, AB], [j_k, C, F, 1G]) + = p_b{}^k (1 - p_b);\ for\ 1 \le k \le r-1$$
$$\Pr([\min(Nr, N(L-1)), NC, F, AB], [j_r, C, F, AB]) = p_b{}^r$$

Where, $j_m = \min(\min(Nr, N(L-1)) + (m \times N), N(L-1))$

- Transition probabilities from (C, NF, 1G)

$$\Pr([0, C, NF, 1G], [0, NC, NF, 1G]) = 1 - (p_b)^r$$
$$\Pr([0, C, NF, 1G], [0, NC, NF, AB]) = (p_b)^r$$

- Transition probabilities from (C, NF, AB)

$$\Pr([0, C, NF, AB], [0, NC, NF, 1G]) = 1 - p_b$$
$$\Pr([0, C, NF, AB], [j_k, NC, NF, 1G]) + = p_b{}^k (1 - p_b);\ for\ 1 \le k \le r-1$$
$$\Pr([0, C, NF, AB], [j_r, NC, NF, AB]) = p_b{}^r$$

Where, $j_m = \min(m \times N, N(L-1))$

- Transition probabilities from (C, F, 1G)

$$\Pr([i, C, F, 1G], [0, C, NF, 1G]) = 1 - (p_b)^r;\ 1 \le i \le \min(rX, N(L-1))$$
$$\Pr([i, C, F, 1G], [0, C, NF, AB]) = (p_b)^r;\ 1 \le i \le \min(rX, N(L-1))$$
$$\Pr([i, C, F, 1G], [\max(i - rX, 0), C, F, 1G]) = 1 - (p_b)^r;\ \min(rX, N(L-1)) < i \le N(L-1)$$
$$\Pr([i, C, F, 1G], [\max(i - rX, 0), C, F, AB]) = (p_b)^r;\ \min(rX, N(L-1)) < i \le N(L-1)$$

- Transition probabilities from (C, F, AB)

$$\Pr([i, C, F, AB], [0, C, NF, 1G]) = 1 - p_b;\ 1 \le i \le \min(rX, N(L-1))$$
$$\Pr([i, C, F, AB], [\min(i - rX, 0), C, F, 1G]) = 1 - p_b;\ 1 \le i \le \min(rX, N(L-1))$$
$$\Pr([i, C, F, AB], [j_{k,i}, C, F, 1G]) + = p_b{}^k (1 - p_b);\ for\ (1 \le k \le r-1)\ and\ (1 \le i \le N(L-1))$$
$$\Pr([0, C, F, AB], [j_{r,i}, C, F, AB]) = p_b{}^r;\ for\ (1 \le i \le N(L-1))$$

Where, $j_{k,i} = \max(\min(i + kN, N(L-1)) - (r-k)X, 0)$

The packet loss event probability, $PLEP^{CS,PS,r}$, can be obtained from the steady state probabilities, $P_{[i,x,y,z]}^{CS,PS,r}$, as follows,

$$PLEP^{CS,PS,r} = \sum_{i=1}^{NL-N} \left[P_{[i,C,F,AB]}^{PS,r} \left\{ \begin{array}{l} \sum_{k=1}^{r-1} \left(\frac{ceil\left\{\frac{\max(i+Nk-NL+N,0)}{N}\right\}}{r} (p_b)^k (1-p_b) \right) \\ + \left(\frac{ceil\left\{\frac{\max(i+Nr-NL+N,0)}{N}\right\}}{r} (p_b)^r \right) \end{array} \right\} \right] +$$

$$\left[P_{[0,NC,NF,AB]}^{PS,r} \left\{ \begin{array}{l} \sum_{k=1}^{r-1} \left(\frac{\max(k-L+1,0)}{r} (p_b)^k (1-p_b) \right) \\ + \left(\frac{\max(r-L+1,0)}{r} (p_b)^r \right) \end{array} \right\} \right] +$$

$$\left[P_{[0,C,NF,AB]}^{PS,r} \left\{ \begin{array}{l} \sum_{k=1}^{r-1} \left(\frac{\max(k-L+1,0)}{r} (p_b)^k (1-p_b) \right) \\ + \left(\frac{\max(r-L+1,0)}{r} (p_b)^r \right) \end{array} \right\} \right] +$$

$$\left[P_{[r'N,NC,F]}^{PS,r} \left\{ \begin{array}{l} \sum_{k=1}^{r-1} \left(\frac{\max(r'+k-L+1,0)}{r} (p_b)^k (1-p_b) \right) \\ + \left(\frac{\max(r'+r-L+1,0)}{r} (p_b)^r \right) \end{array} \right\} \right]$$

Where, $r' = \min(r, L-1)$. The average PBs lost per packet loss event is given by,

$$APL^{CS,PS,r} = \frac{TPL^{CS,PS,r}}{r \times PLEP^{CS,PS,r}}$$

Where $TPL^{CS,PS,r}$ (total PBs lost) is given by,

$$TPL^{CS,PS,r} = \sum_{i=1}^{NL-N} \left[P_{[i,C,F,AB]}^{PS,r} \left\{ \begin{array}{l} \sum_{k=1}^{r-1} \left(\max(i+Nk-NL+N,0)(p_b)^k (1-p_b) \right) \\ + \left(\max(i+Nr-NL+N,0)(p_b)^r \right) \end{array} \right\} \right] +$$

$$\left[P^{PS,r}_{[0,NC,NF,AB]}\left\{\sum_{k=1}^{r-1}\left(\max(kN-LN+N,0)(p_b)^k(1-p_b)\right)+\left(\max(rN-LN+N,0)(p_b)^r\right)\right\}\right]+$$
$$\left[P^{PS,r}_{[0,C,NF,AB]}\left\{\sum_{k=1}^{r-1}\left(\max(kN-LN+N,0)(p_b)^k(1-p_b)\right)+\left(\max(rN-LN+N,0)(p_b)^r\right)\right\}\right]+$$
$$\left[P^{PS,r}_{[r'N,NC,F]}\left\{\sum_{k=1}^{r-1}\left(\max(r'N+kN-LN+N,0)(p_b)^k(1-p_b)\right)+\left(\max(r'N+rN-LN+N,0)(p_b)^r\right)\right\}\right]$$

8.7 Comparison of Persistent Scheduling Mechanism

In this section we compare the performance of various scheduling strategies under different traffic conditions (i.e., N, L, PLEP) and channel conditions (i.e., p_b). The first results of interest is to compare the results from the lower bound analysis in Section 6, with the corresponding results obtained from the Markov chain analysis. We do this by comparing the lower bound on the latency that can be supported for given PLEP and p_b. It is important to note that for Markov chain analysis with over allocation set to N(L-1), the state transition diagram does not depend on the choice of N. Hence these results are independent of the application data rates (N).

Figure 8-11 to Figure 8-14 show the minimum latency that can be supported by various scheduling strategies for p_b in the range [0.001, 0.1], and for PLEP of 10^{-5} and 10^{-7}. Note that PLEP of 10^{-5} and 10^{-7} correspond to packet loss events that occur approximately once an hour and once in 100 hours. It is reasonable to assume that most applications will require packet loss event probability in this range. Figure 8-15 and Figure 8-16 compare the minimum latency that can be supported by scheduling strategies for p_b in the range [0.001, 0.1], and for PLEP of 10^{-5} and 10^{-7} respectively. Figure 8-17 and Figure 8-18 show the schedule persistence required to support Latency of 2, for p_b in

the range [0.001, 0.1], and for PLEP of 10^{-5} and 10^{-7} respectively. These results can be summarized as follows,

- The results for lower bound obtained from analysis match very closely with those obtained based on the Markov chain analysis. The minor differences observed in case of persistent preview schedules can be attributed to the latency effects of our over-allocation strategy.

- As expected, the results show that non-persistent schedules limit the levels of QoS (in terms of L, PLEP) than can be guaranteed to applications. As can be see from Figure 8-15, latencies less than 4 cannot be supported when p_b>1% at PLEP = 10^{-5}. Furthermore, latencies less than 6 cannot be supported when p_b>1% at PLEP = 10^{-7}. These results justify the need for schedule persistence over power line channels.

- Current schedules does not show any significant improvement in the minimum latency supported even at large values of persistence. This is clearly evident in Figure 12, which shows that an 8-persistent current schedule will only reduces the minimum latency supported by at most 1, when the persistence is changed for 2 to 8. Further, as can be seen in Figure 8-15 and Figure 8-16, 8-persistent current schedule does not provide any significant improvement in minimum latency compared to that of non-persistent schedules. While in theory, improvements in performance can be achieved by using large values of persistence for the current schedule; large persistence's are not practical as they limit dynamic adjustment of schedules with channel and traffic changes. So, it is safe to conclude that in practice current schedules does not enable significant improvements in QoS compared to non-persistent schedules.

- In contrast to current schedules, preview schedules enable significant improvements in QoS with modest values of persistence. For example, a persistence of 4 should be sufficient to enable L=2 for up to 6% beacon loss probability at PLEP = 10^{-5} (Figure 8-15). A persistence of 6 should be sufficient to enable L=2 for up to 7% beacon loss probability at PLEP = 10^{-7} (Figure 8-16).

- Current and preview schedules provide the highest performance. From Figure 8-15 it can be see that a persistence of 2 is sufficient to handle up to 6% beacon loss probability at PLEP = 10^{-5}. A persistence of 4 should be sufficient to handle up to 8% beacon loss probability at PLEP = 10^{-5} (Figure 8-16).

For practical systems, apart from the QoS that can be supported the amount of over allocation that is needed is also important. The over allocation represents the amount of bandwidth the needs to be set aside for enabling speedy reduction of backlog. Hence over allocation will effectively reduce the maximum amount of time that can be allocated for

multimedia streams. Figure 8-19 to Figure 8-22 shows variation of over allocation with latency for various scheduling strategies for p_b values of [0.001, 0.005, 0.01, 0.05, 0.1], N=100 and PLEP = 10^{-7}. These results show that,

- Non-Persistence schedules require large amounts of over allocation the support their minimum latencies. Furthermore, the reduction in the over allocation with latency is slow. Hence, it can be concluded that non-persistent schedules can result in large inefficiencies especially at beacon loss probabilities greater than 1%,
- Current schedules enable significantly faster reduction in over allocation compared to non-persistent schedules. So, although current schedules do not enable significant improvements in QoS, they do enable significant improvements in efficiencies at the QoS levels that they can support,
- Both preview schedules and current and preview schedules require minimum amount of over allocations at and near the minimum latencies that can be supported.

Our analysis has also shown that the average number of packets lost per packet loss event is large. For non-persistent schedules and persistent current schedules, they are typically 30%-50% of the number of packet to be delivered in a beacon period (N). For persistent schedules, average packet loss tends to be 50% to100% of N. Since an over allocation of X=1 is the minimum required to deal with any beacon loss, we consider latency that can be supported with X=1 as the optimal latencies. In contrast to minimum latencies, optimal latencies depend on application data rates (i.e., N). Figure 8-23 to Figure 8-26 show the optimal latency that can be supported by scheduling strategies for p_b in the range [0.001, 0.1], N = [50, 75, 100] and for PLEP of 10^{-5} and 10^{-7}. Figure 8-27 and Figure 8-28 compare the optimal latency that can be supported by scheduling strategies for p_b in the range [0.001, 0.1], N=100, and for PLEP of 10^{-5} and 10^{-7} respectively. Figure 8-29 and Figure 8-30 show the schedule persistence required to optimally support Latency of 2, for p_b in the range [0.001, 0.1], N=100, and for PLEP of 10^{-5} and 10^{-7} respectively. These results can be summarized as follows,

- The optimal latency than can be supported decreases as that application data rate (N) increases. This can be expected, as the backlog resulting from a packet loss event is larger.
- The optimal latencies for non-persistent schedules are very large. For pb loss greater than 1%, latencies below 14 cannot be supported.
- Persistent current schedules provide significant improvement in the minimum latency compared to non-persistent schedules.
- For persistent preview schedules and persistent current and preview schedules, the optimal latency and minimum latency are the same for the data points we have tested.

These results show that whenever there is sufficient space available in the beacon, persistent preview and current schedules should be used. In scenarios where there is no space available, implementations should use persistent preview schedules. The choice of persistence should be based on the QoS requirement of the application and the beacon loss probabilities experience by the stream. Implementations can use the analytical lower bound to determine the values of minimum value of persistence that needs to be used.

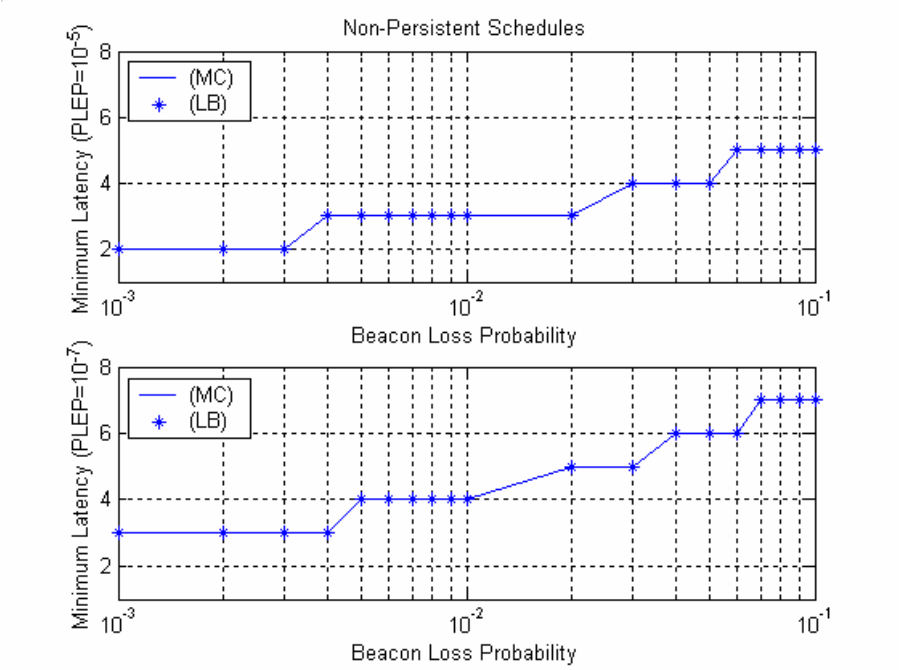

Figure 8-11: Minimum latency required to achieve PLEP of $\{10^{-5}, 10^{-7}\}$ at various beacon loss probabilities in a system with non-persistent schedules

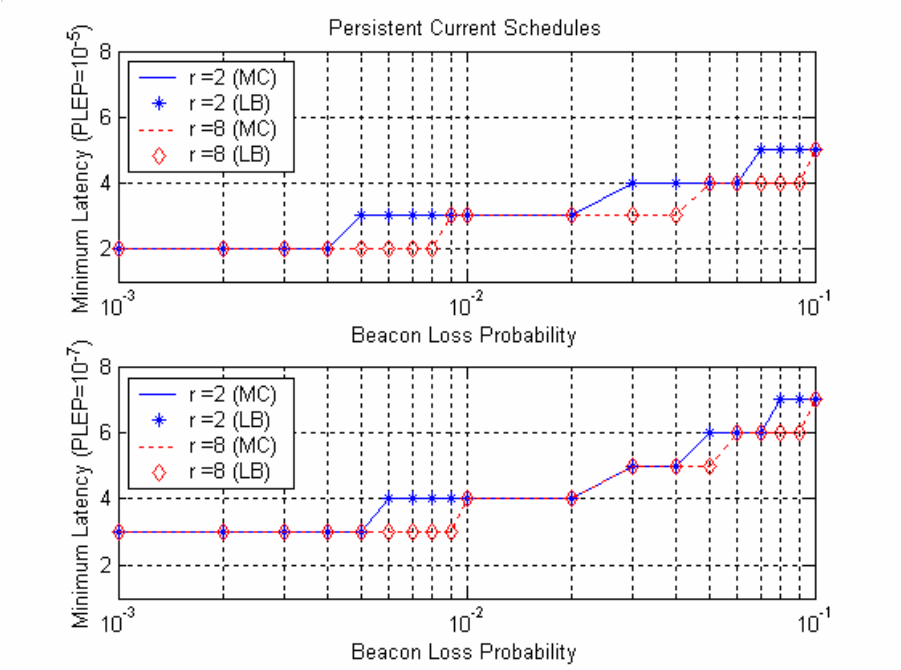

Figure 8-12: Minimum latency required to achieve PLEP of $\{10^{-5}, 10^{-7}\}$ at various beacon loss probabilities in a system with r-persistent current schedules

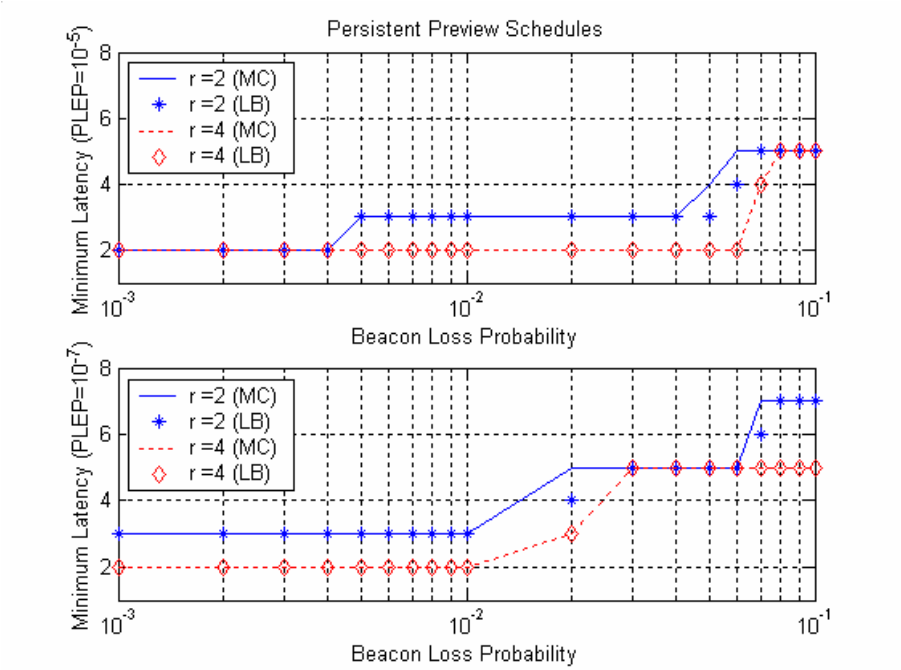

Figure 8-13: Minimum latency required to achieve PLEP of $\{10^{-5}, 10^{-7}\}$ at various beacon loss probabilities in a system with r-persistent preview schedules

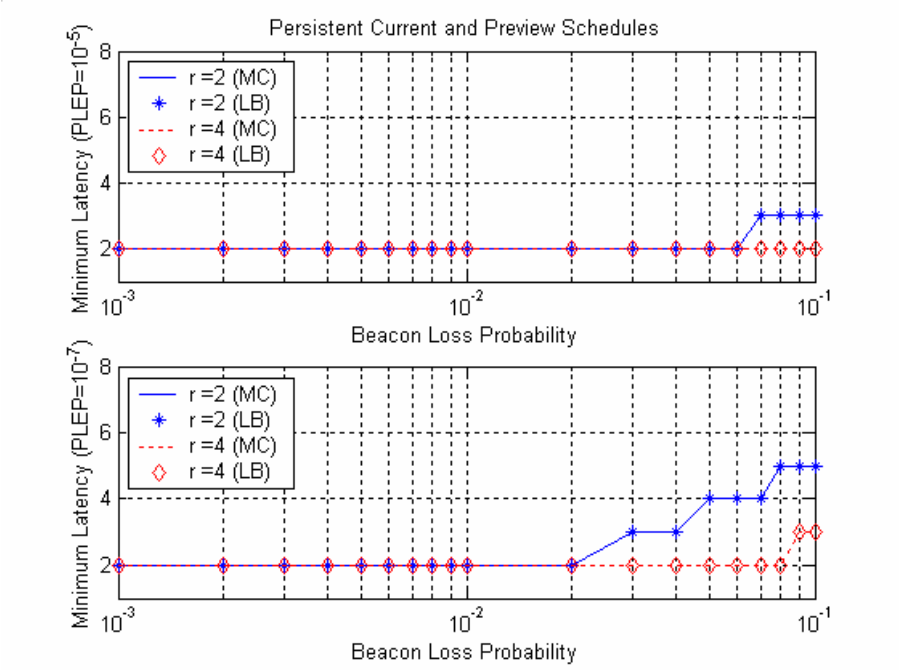

Figure 8-14: Minimum latency required to achieve PLEP of $\{10^{-5}, 10^{-7}\}$ at various beacon loss probabilities in a system with r-persistent current and preview schedules

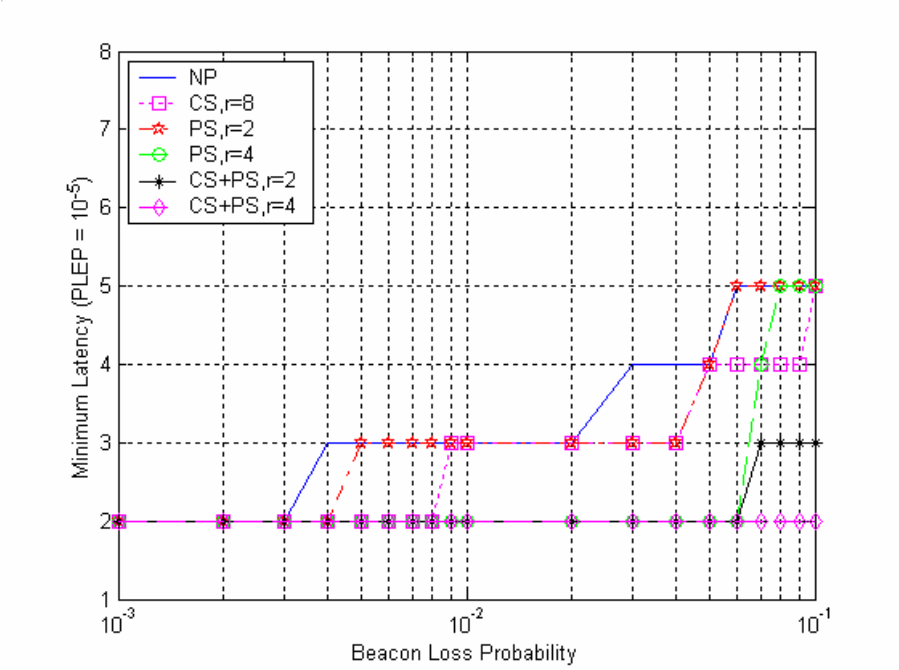

Figure 8-15: Comparison of minimum latency supported by various scheduling strategies at various beacon loss probabilities for PLEP = 10^{-5}

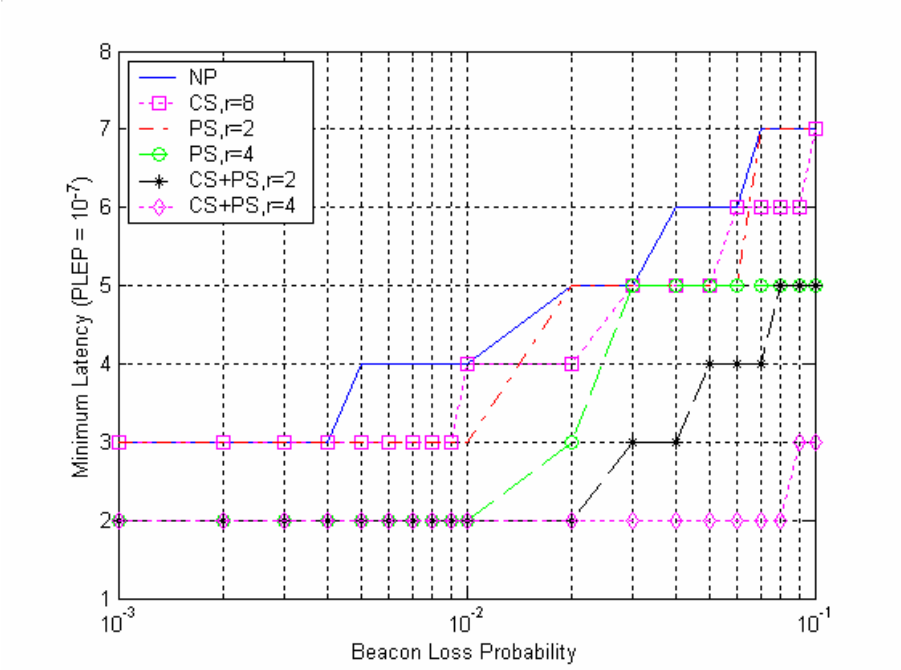

Figure 8-16: Comparison of minimum latency supported by various scheduling strategies at various beacon loss probabilities for PLEP = 10^{-7}

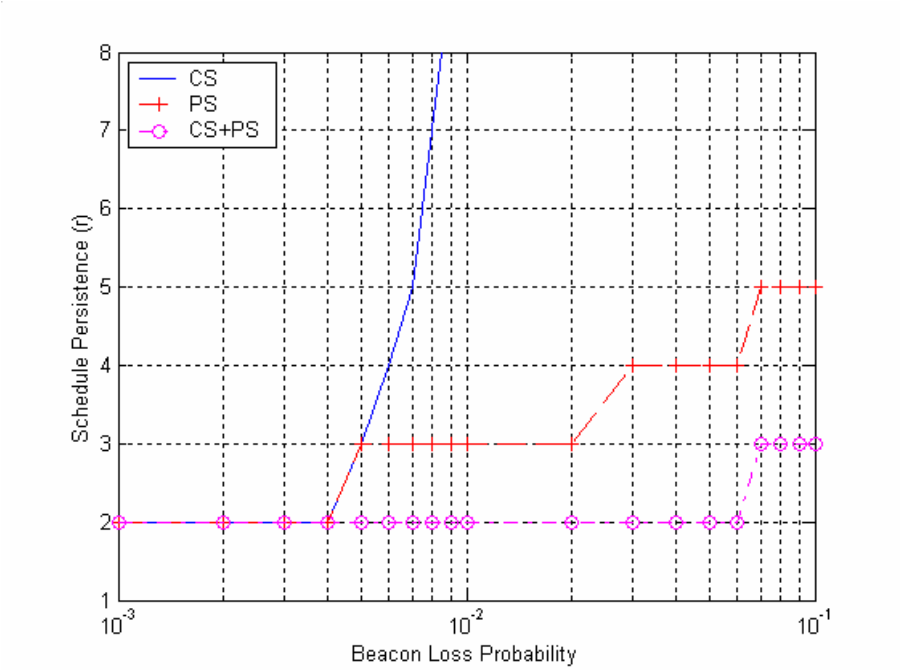

Figure 8-17: Minimum schedule persistence required to support L = 2 for various scheduling strategies at PLEP = 10^{-5}

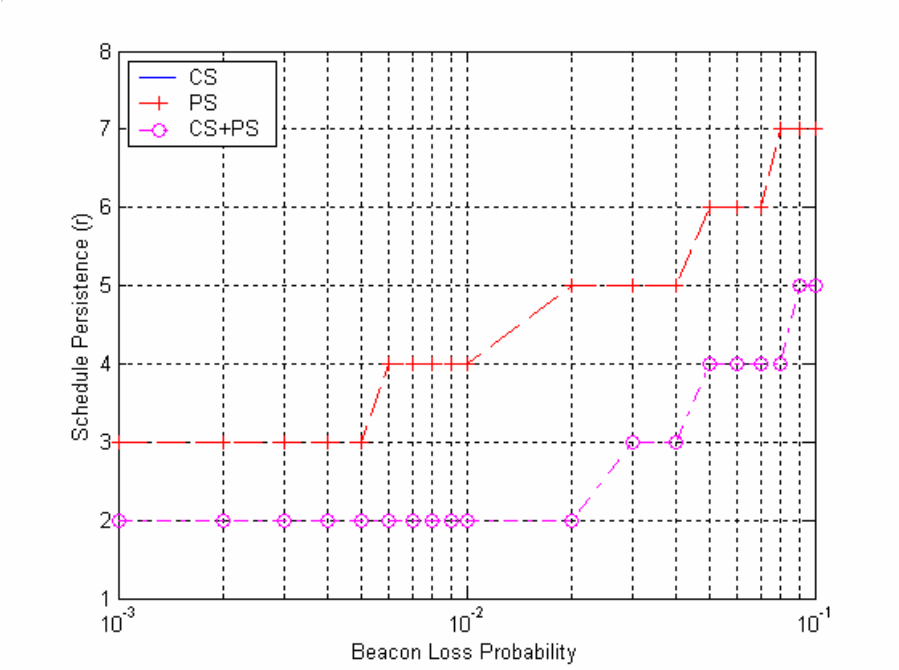

Figure 8-18: Minimum schedule persistence required to support L = 2 for various scheduling strategies at PLEP = 10^{-7}

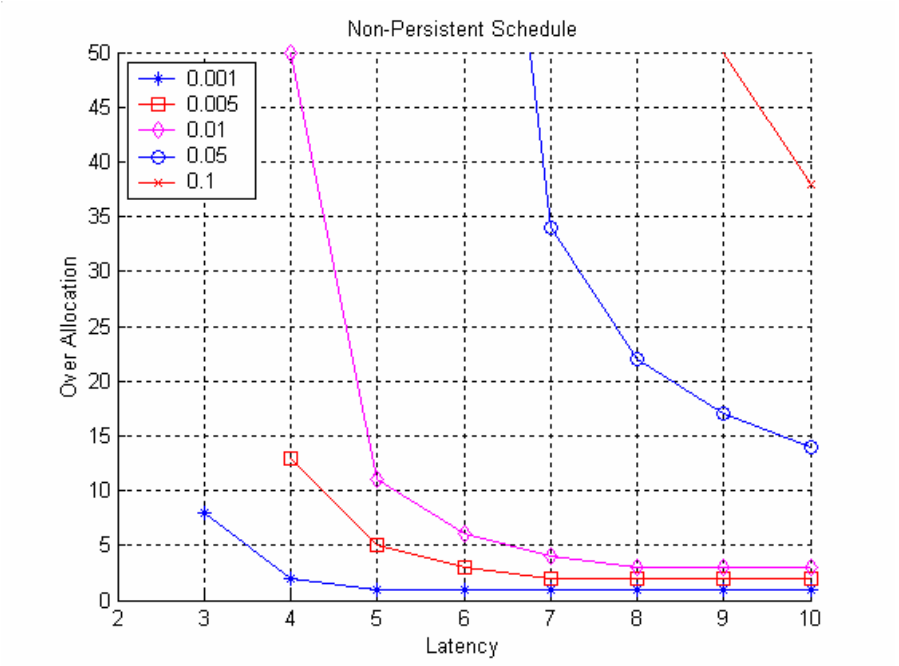

Figure 8-19: Over allocation required to support various latencies in a system with non-persistent beacon schedules, N = 100, PLEP = 10^{-7}

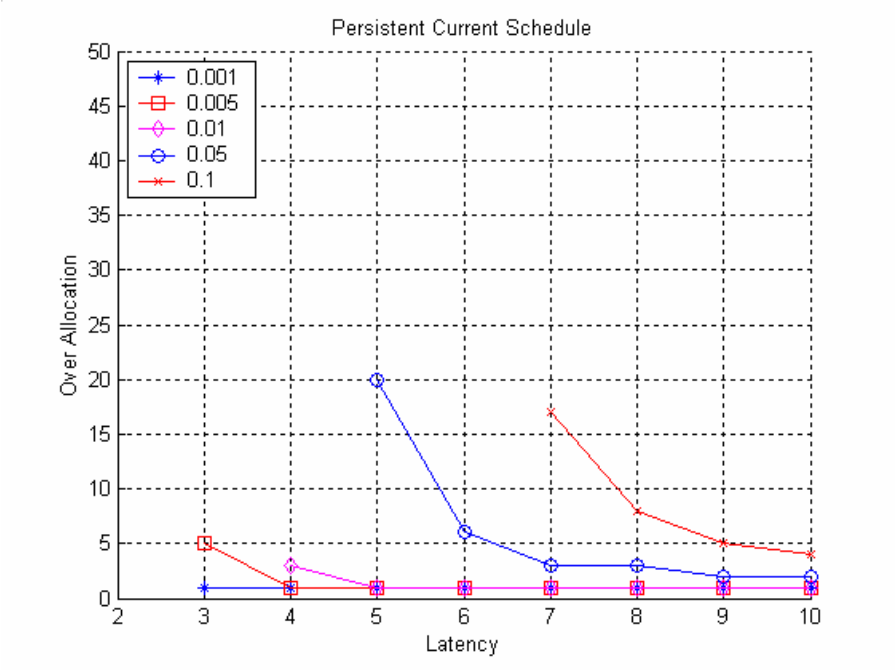

Figure 8-20: Over allocation required to support various latencies in a system with 2-persistent current schedules, N = 100, r = 8,PLEP = 10^{-7}

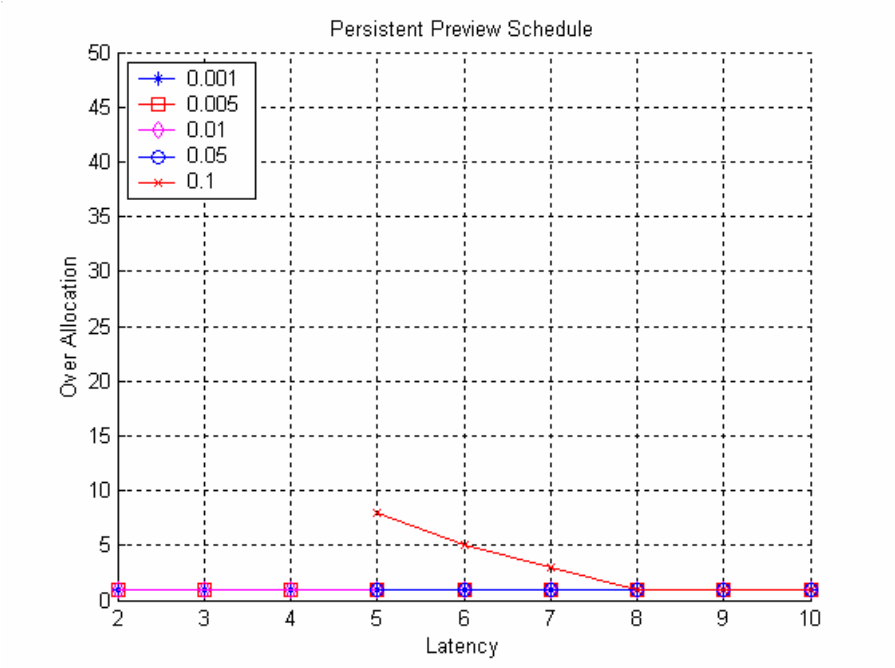

Figure 8-21: Over allocation required to support various latencies in a system with 2-persistent preview schedules, N = 100, r = 4,PLEP = 10^{-7}

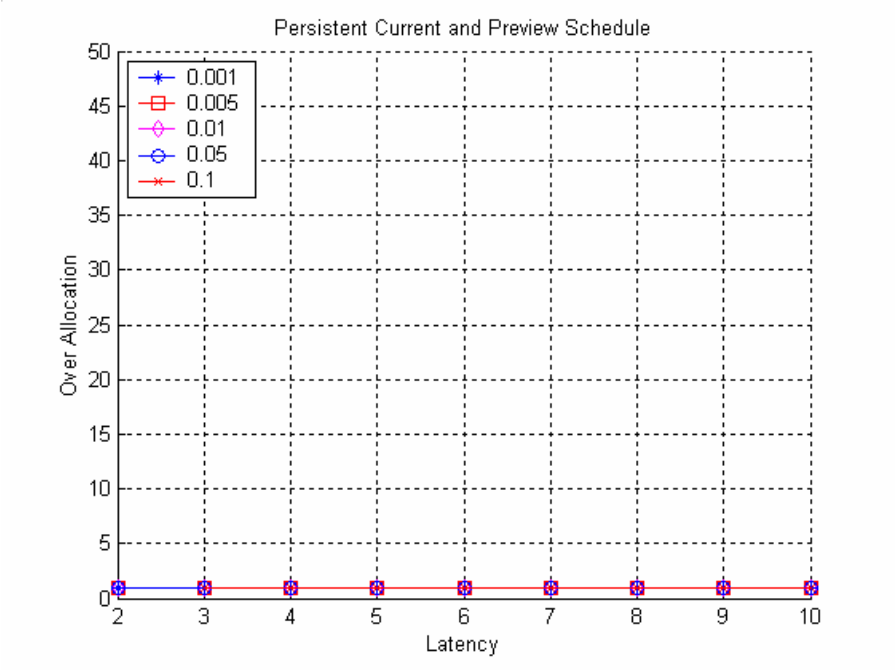

Figure 8-22: Over allocation required to support various latencies in a system with 2-persistent current and preview schedules, N = 100, r = 4,PLEP = 10^{-7}

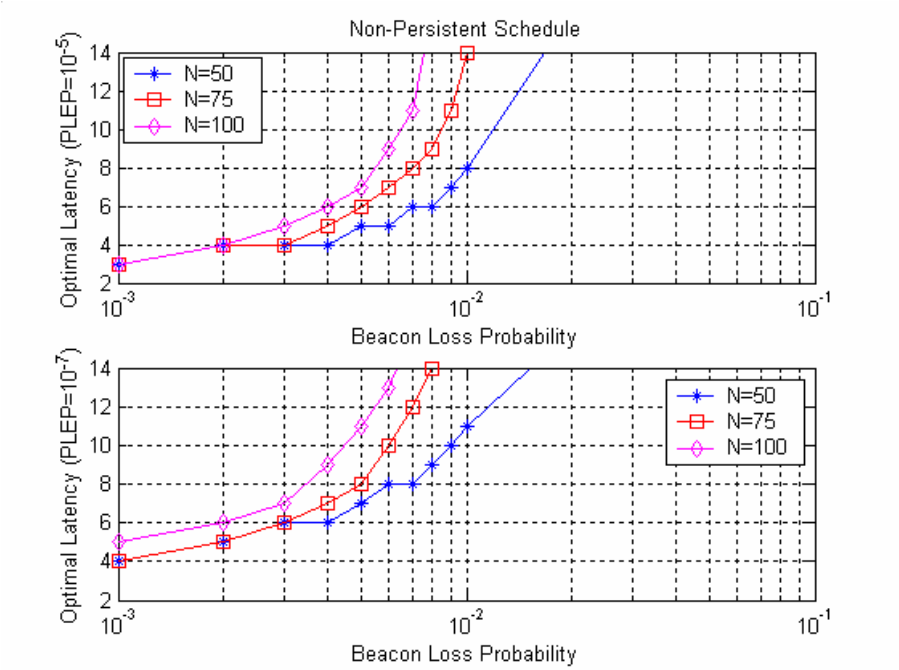

Figure 8-23: Latencies required to support a stream with optimal over allocation for a system with non-persistent schedules for PLEP = {10^{-5}, 10^{-7}}

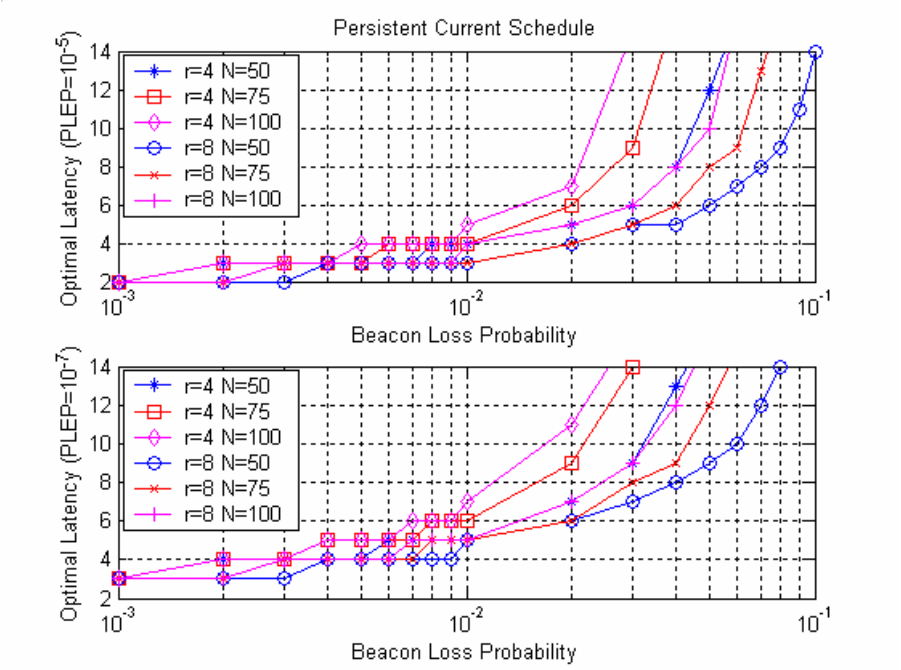

Figure 8-24: Latencies required to support a stream with optimal over allocation for a system with r-persistent current Schedules for PLEP = $\{10^{-5}, 10^{-7}\}$

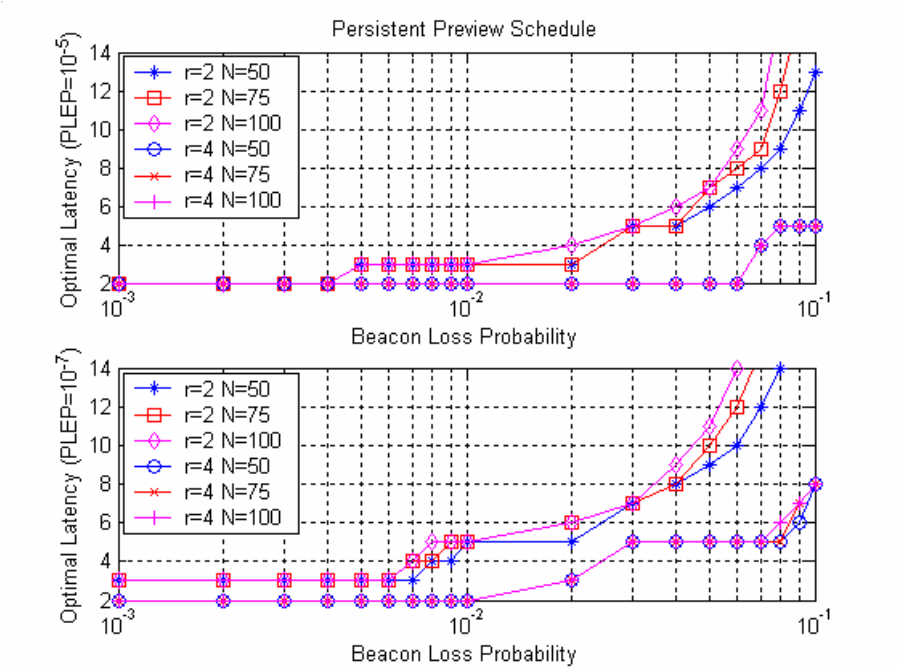

Figure 8-25: Latencies required to support a stream with optimal over allocation for a system with r-persistent preview schedules for PLEP = $\{10^{-5}, 10^{-7}\}$

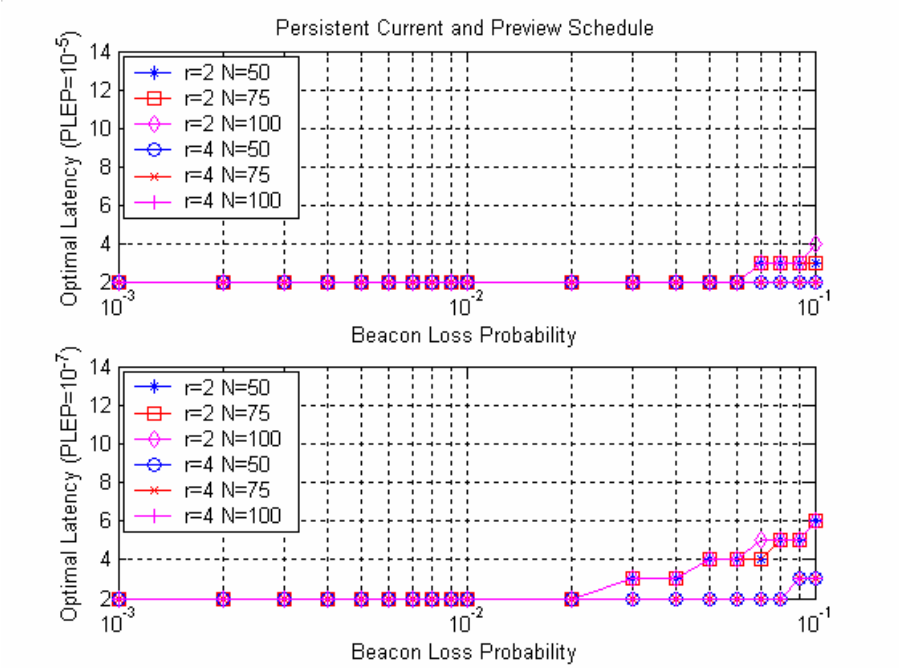

Figure 8-26: Latencies required to support a stream with optimal over allocation for a system with r-persistent preview schedules for PLEP = $\{10^{-5}, 10^{-7}\}$

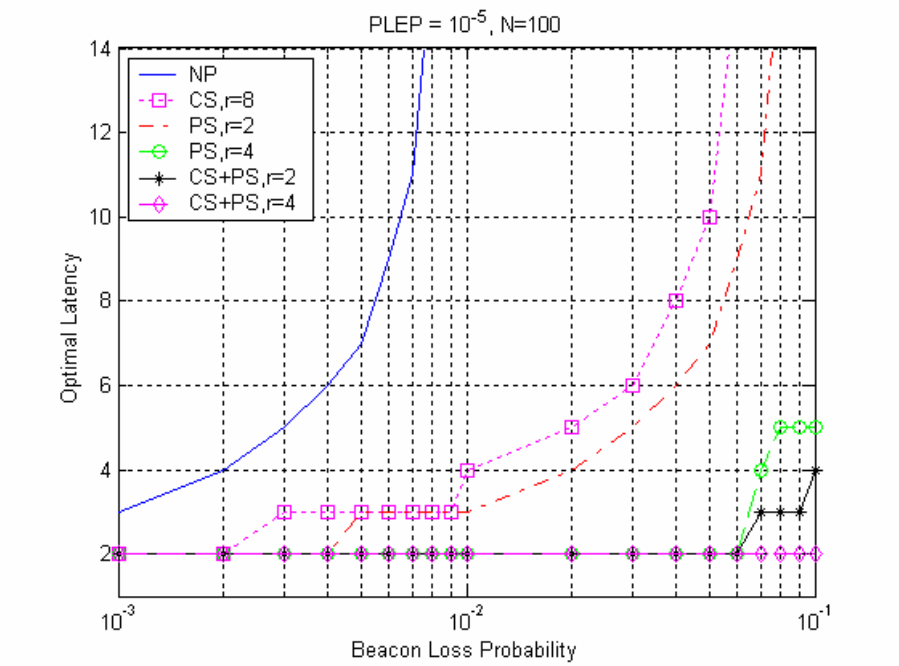

Figure 8-27: Comparison of optimal latency supported by various scheduling strategies at various beacon loss probabilities for N = 100, PLEP = 10^{-5}

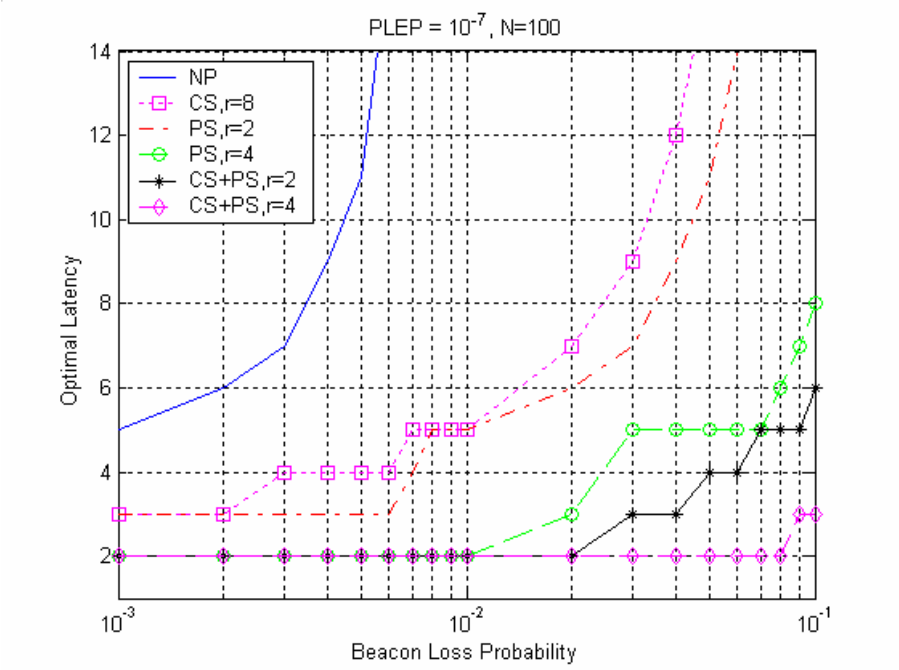

Figure 8-28: Comparison of optimal latency supported by various scheduling strategies at various beacon loss probabilities for N = 100, PLEP = 10^{-7}

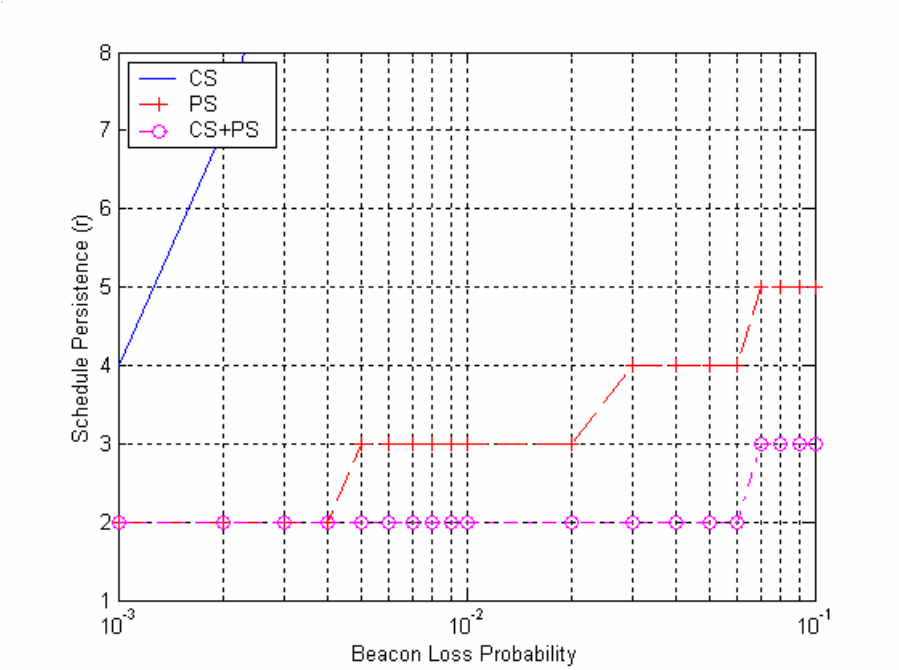

Figure 8-29: Minimum schedule persistence required to support L = 2 with X = 1 for various scheduling strategies at PLEP = 10^{-5}

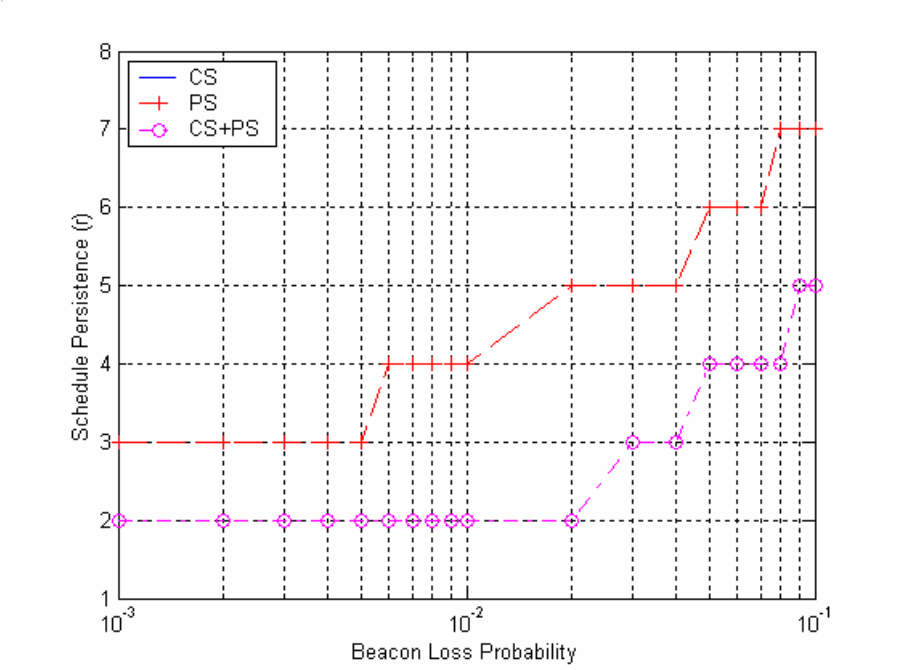

Figure 8-30: Minimum schedule persistence required to support L = 2 with X = 1 for various scheduling strategies at PLEP = 10^{-7}

8.8 Conclusions

The new generation of home networking applications requires guaranteed QoS. The recently released HomePlug AV standard is designed to overcome the harsh PLC channel conditions and to provide guaranteed QoS. The harsh channel conditions on power line can result in beacon loss. In this section we investigated the effect of beacon loss on QoS and the enhancement that can be achieved by using persistent current schedules, persistent preview schedules, and persistent current and preview schedules.

Our average efficiency study showed that all persistent schedules can significantly improve the efficiency due to missed transmission opportunities. A details study of the QoS enhancements using analytical lower bound and Markov chain analysis have shown that persistent current and preview schedules are highly effective in dealing with beacon

loss. Results showed that a persistent of 4 should enable current and preview schedules to provide PLEP of 10^{-7} while tolerating up to 8% beacon loss.

Persistent preview schedules also provided significant performance improvements at slightly higher values of persistence compared to persistent current and preview schedules. Results also show that current schedules do not provide any significant improvements in QoS support. However, they do enable better efficiency at the latencies that can be supported.

For both persistent preview schedules and persistent current and preview schedules, the analytical lower bound can be used to determine the optimal latencies with very low margin of error. We recommend implementation to use either persistent preview schedules or persistent current and preview schedules.

Our analysis assumes constant bit rate traffic and no PB errors. Since allocation strategies to deal with such conditions will include over allocation, and since persistent preview schedules and persistent current and preview schedules are not much sensitive to the size of over allocation, if the over allocations are designed to be slightly more conservation, they should also enable them to deal with beacon loss.

CHAPTER 9
CONCLUSIONS AND FUTURE WORK

Most houses are not equipped with specialized wiring for networking purpose, and retrofitting them with new wiring is prohibitively expensive. Hence, the use of existing power line infrastructure for networking purpose can come a long way in solving the in-home connectivity problem. The challenges to enabling high-speed power line communications (PLC) are many. Power line channels are characterized by large attenuations, frequency selective fading and impulse noise. Often the channel also exhibits a temporal dependence with the underlying AC line cycle frequency. The regulatory environments, while still maturing, also place several restrictions on transmit power levels and frequency bands.

One of the major contributions of this work is the evaluation of the viability of PLC based home networking. Extensive simulations and field testing has shown that HomePlug 1.0 based PLC systems can not only provide ubiquitous connectivity, but they also out performs IEEE 802.11b/a based wireless home networking solutions. One of the limitations of this study is the use of proto-type equipment for PLC and off the shelf equipment for wireless. Neither of these captures the true capabilities of these technologies due to implementation choices and limitations. Nonetheless, our evaluation definitively concludes that PLC is a viable option for home networking. At present more that 5 million HomePlug 1.0 devices have been deployed through out the world. This fact re-enforces our conclusions.

Another major contribution of this work is the study of QoS design issues involved in enabling multimedia communications over power line channels. This study is motivated in part by the work we did in the development of HomePlug AV standard. As part of this, we investigate three issues that the new generation PLC systems need to overcome to enable multimedia communications: (a) AC line cycle variation in noise, (b) Impulse noise, and (c) Beacon Loss.

One of the peculiarities of PLC channels is the cyclic variation of their characteristics with the AC line cycle phase. Exploiting this cyclic variation is crucial for not only obtaining the data rates required to support the multimedia applications, but also for enabling guarantees on QoS. Our channel characterization measurements and analysis have show that a 30% improvement in physical layer (PHY) data rates can be obtained by continuously adapting to, and synchronizing communications with, the AC line cycle. Since continuous adaptation with respect to time is unduly complex for practical systems, we propose dividing the AC line cycle into multiple regions and adapting independently in each region. Results show that using a region size of 1-2 milliseconds provides up to 10% improvements in MAC throughput. Significant work still remains in understanding the AC line cycle based variation of PLC channel characteristics and the mechanisms that can be used by practical systems to optimize the performance gains. This includes,

- A limitation of our study is the use on only one full AC line cycle duration of noise captures. Larger captures that can span multiple AC line cycles will enable more accurate measurements of channel capacities variations.
- Our study only takes into consideration the variation of noise with the phase of the AC line cycle. While changes in channel attenuation characteristics are relatively rare, they are definitely possible. Future studies should take this into account to accurately measure the channel capacity variations.
- In our study we propose dividing AC line cycle into fixed size macro slots for simplifying practical implementations. In general, an optimal channel adaptation

scheme should be able to divide AC line cycle into variable number of regions based on the underlying channel characteristics. Algorithm for doing this is still an open research item.

Proper handling of impulse noise events is another design aspect that is crucial for enabling multimedia communications over PLC channels. Impulse noise will produce temporal effects in channel capacity. Between two impulse noise events, the channel capacity can be very high, while during the impulse noise the capacity is very low. To obtain low FEC block error rates, the channel has to be adapted close to the lower end of its capacity (i.e., capacity near impulse noise event) and hence is undesirable. Physical layer adapting to the higher end of the channel capacity hinges on the ability to efficiently retransmit corrupted portions of the data at the MAC layer. One of the major contributions of this work is a novel 2-level MAC framing mechanism that enables efficiency retransmissions even under higher FEC block error rates. 2-level MAC framing enables retransmission of only the corrupt FEC block, thus providing optimal performance. Simulation and analysis based comparison with other viable approaches confirmed the superior performance of 2-level MAC framing.

Apart from framing overheads, transmission overhead can also negatively impact the MAC efficiency on channels with high FEC Block Error rate due the need for a large number of retransmissions to successfully deliver packets. One of the contributions of this work is the study of the complex interaction between FEC block errors, transmission overhead, Quality of Service (QoS) requirements of a multimedia stream and its TDMA allocation requirements. We provide an approximate analytical estimate of the Fixed Allocation and Average Allocation requirements for multimedia streams. Our results show that, to support low latency applications at high FEC Block errors, the average allocation size has to be increased by one or more transmission overheads. Further, the

increase in average allocation is not a strong function of application data rate. Hence, low data rate applications can suffer significant loss in efficiency at high FEC Block error rates. Our results also show that using a fixed size TDMA allocation can lead to poor utilization when the latency requirements of the application are less than four beacon periods. These results can be used by the channel adaptation algorithm to optimize the overall system capacity. Derivation of more accurate estimates of Fixed Allocation and Average Allocations is an area of future work in this topic.

Ability to handle beacon loss is another design issue that needs to be properly handled to enable QoS over PLC channels. HomePlug AV uses robust physical layer parameters for transmission of beacons. However, due to the large dynamic range of attenuation and (impulse) noise over power line, beacon loss cannot be completely avoided. To overcome occasional beacon loss, HomePlug AV uses persistent beacon schedules. One of the major contributions of this dissertation is the evaluation of performance enhancements that can be achieved by using persistent beacon schedules. Detailed Markov Chain based analysis was used to show that using persistent current and preview schedule or persistent preview schedules, HomePlug AV systems can handle up to 10% beacon loss, with minimal impact on MAC efficiency and QoS guarantees. Schedule persistent limits the frequency with which schedules can be changed. Hence the minimum value of the persistence that enables the required QoS should be used by the Central Coordinator. To simplify practical implementations, we propose a lower bound based schedule persistence estimation mechanism that provides highly accurate estimates of the required schedule persistence under any beacon loss rate and application QoS requirements.

Apart from the three design issues that we investigated in this dissertation, there are several other issues that need to be properly addressed by PLC based multimedia networks. These include,

- Hidden stations – Due to the large attenuation and noise over power line channels, it is possible to have stations that are hidden with respect to each other. Hidden stations are relatively rare in PLC based home networks, but are definitely possible. Channel access mechanism that enable proper coordination of hidden stations and repeating/routing mechanism that enable communications between hidden devices are areas of future work.

- Neighbor Networks – Power line transmissions from one house can interfere with transmissions from neighboring houses. Ability to handle such neighbor networks is one of the major hurdles for PLC. This problem is aggravated due to the absence of multiple frequency bands. Mechanisms for coordination between neighbor networks while achieving maximum spatial reuse is still an open research topic.

- Encryption and Privacy – Since power line transmissions in one house can leak into neighboring houses; there is a need for mechanism that can be used for ensuring privacy of the data.

- Coexistence with Legacy device – New generation PLC systems should be able to peacefully coexist with the widely deployed HomePlug 1.0 systems. Mechanisms that enable such coexistence is another area for future work.

LIST OF REFERENCES

1. Philipps Holger: Performance Measurements of Power line Channels at High Frequencies, Proceedings of International Symposium on Power Line Communications and its Applications, Tokyo, Japan, 1998, pp. 229-237

2. Brown A. Paul: Some Key Factors Influencing Data Transmission Rates in the Power Line Environment when Utilizing Carrier Frequencies above 1MHz, Proceedings of International Symposium on Power Line Communications and its Applications, Tokyo, Japan, 1998, pp. 67-75

3. Halid Hrasnica, Abdelfatteh Haidine, Ralf Lehnert: Broadband Powerline Communications Networks, John Wiley & Sons, Chichester, England, 2004

4. Dosterr Klaus: Telecommunications Over the Power Distribution Grid: Possibilities and Limitations, Proceedings of the International Symposium on Power Line Communications and its Applications, Essen, Germany, 1997, pp. 1-9

5. Brown A. Paul: Power Line Communications – Past Present and Future, Proceedings of International Symposium on Power-line Communications and its Applications, Lancaster, U.K., 1999, pp. 1-5

6. Brackmann Ludwig: Power line Applications with European Home Systems, Proceedings of International Symposium on Power Line Communications and its Applications, Essen, Germany, 1997, pp. 24-31

7. Kaizawa Yasuhito and Gen Marubayashi: Needs for the Power Line Communications, Proceedings of International Symposium on Power-line Communications and its Applications, Tokyo, Japan, 1998, pp. 153-157

8. John Newbury: Technical Developments in Power Line Communications, Proceedings of International Symposium on Power Line Communications and its Applications, Lancaster, U.K, 1999, pp. 66-78

9. John S. Barnes: A Physical Multi-Path Model for Power Distribution Network Propagation, Proceedings of International Symposium on Power Line Communications and its Applications, Tokyo, Japan, 1998, pp. 76-89

10. Yu-Ju Lin, Haniph A. Latchman, Minkyu Lee, Srinivas Katar: A Power Line Communication Network Infrastructure for The Smart Home, IEEE Wireless Communications, December 2002, Volume 9, Issue 6, pp. 104-111

11. Minkyu Lee, Richard E. Newman, Haniph. A. Latchman, Srinivas Katar, Larry Yonge: HomePlug 1.0 Powerline Communication LANs – Protocol Description and Performance Results, Special Issue of the International Journal on Communication Systems on Powerline Communications, April 2003, Volume 16, Issue 5, pp. 447-473

12. Yu-Ju Lin, Haniph A. Latchman, Richard E. Newman, Srinivas Katar: A Comparative Performance Study of Wireless and Power Line Networks, IEEE Communications Magazine, April 2003, Volume 41, Issue 4, pp. 54-63

13. IEEE 1394B-2002: IEEE Standard for a Higher Performance Serial Bus-Amendment 2, http://www.ieee.org/, April 2006

14. IEEE 1394-1995: IEEE Standard for a High Performance Serial Bus, http://www.ieee.org/, April 2006

15. IEEE 802.11, 1999: IEEE Standards for Information Technology - Telecommunications and Information Exchange between Systems - Local and Metropolitan Area Network - Specific Requirements - Part 11: Wireless LAN Medium Access Control (MAC) and Physical Layer (PHY) Specifications, http://www.ieee.org/, April 2006

16. IEEE 802.11b, 1999: Supplement to 802.11-1999,Wireless LAN MAC and PHY Specifications: Higher Speed Physical Layer (PHY) Extension in the 2.4 GHz band, http://www.ieee.org/, April 2006

17. IEEE 802.11a, 1999: IEEE Standard for Information Technology - Telecommunications and Information Exchange between Systems - Local and Metropolitan Area Networks - Specific Requirements - Part 11: Wireless LAN Medium Access Control (MAC) and Physical Layer (PHY) Specifications—Amendment 1: High Speed Physical Layer in the 5 GHz Band, http://www.ieee.org/, April 2006

18. IEEE 802.11g, 2003: IEEE Standard for Information technology - Telecommunications and Information Exchange between Systems - Local and Metropolitan Area Networks - Specific Requirements - Part 11: Wireless LAN Medium Access Control (MAC) and Physical Layer (PHY) Specifications - Amendment 4: Further Higher-Speed Physical Layer Extension in the 2.4 GHz Band, http://www.ieee.org/, April 2006

19. IEEE 802.15.1: IEEE Standard for Information Technology - Telecommunications and Information Exchange between Systems - Local and Metropolitan Area Networks - Specific Requirements. Part 15.1: Wireless Medium Access Control (MAC) and Physical Layer (PHY) Specifications for Wireless Personal Area Networks (WPANs(tm)) , http://www.ieee.org/, April 2006

20. IEEE 802.15.3: IEEE Standard for Information Technology - Telecommunications and Information Exchange between Systems - Local and Metropolitan Area Networks - Specific Requirements Part 15.3: Wireless Medium Access Control (MAC) and Physical Layer (PHY) Specifications for High Rate Wireless Personal Area Networks (WPAN) , http://www.ieee.org/, April 2006

21. WiMedia Alliance: http://wimedia.org/, April 2006

22. UWB Forum: http://www.uwbforum.org/, April 2006

23. HomePNA Alliance: http://www.homepna.org/, April 2006

24. Multimedia over Coax Alliance: http://www.mocalliance.org/, April 2006

25. HomePlug Powerline Alliance: http://www.homeplug.org, April 2006

26. Intellon Corporation: http://www.intellon.com, April 2006

27. Shu Lin and Daniel J. Costello: Error Control Coding and Fundamentals and Applications, Prentice-Hall, New Jersey, 2004

28. Shannon C. E.: A Mathematical Theory of Communication, Bell System Technical Journal, 1948, Volume 27, pp. 379-423

29. Andrew S. Tanenbaum: Computer Networks, Prentice Hall, Fourth Edition, 2003

30. Prasad Ramjee and Richard Van New: OFDM wireless Multimedia Communications, Artech House, Boston, 2000

31. Thomas Starr, John M. Cioffi, and Peter J. Silverman: Understanding Digital Subscriber Line Technology, Prentice Hall, 1999

32. Baowei Ji, Archana Rao, Minkyu Lee, Haniph A. Latchman, Srinivas Katar: Multimedia in Home Networking, Proceedings of CITSA 2004 / ISAS 2004, Volume 1, pp. 397-404

33. Kaywan H. Afkhamie, Srinivas Katar, Larry Yonge, and Richard E. Newman: An Overview of the upcoming HomePlug AV Standard, Proceedings of the International Symposium on Power Line Communications and its Applications, Vancouver, British Columbia, 2005, pp. 400-404

34. HomePlug AV White Paper: http://www.homeplug.com/en/products/whitepapers.asp, April 2006

35. Srinivas Katar, Brent Mashburn, Kaywan Afkhamie, Haniph Latchman, Richard Newman: Channel Adaptation based on Cyclo-Stationary Noise Characteristics in PLC Systems, Proceedings of International Symposium on Power-line Communications and its Applications, Orlando, USA, 2006, pp. 17-21

36. Osamu Ohno, Masaaki Katayama, Takaya Yamazato and Akira Ogawa: A Simple Model of Cyclo-Stationary Power-Line Noise for Communication Systems, Proceedings of International Symposium on Power-line Communications and its Applications, Tokyo, Japan, 1998, pp. 115-122

37. Masaaki Katayama, Saori Itou, Takaya Yamazato and Akira Ogawa: Modeling of Cyclo-Stationary and Frequency Dependent Power-Line Channels for Communications, Proceedings of International Symposium on Power-line Communications and its Applications, Limerick, Ireland, 2000, pp.123–127

38. Yuichi Hirayama, Hiraku Okada, Takaya Yamazato, Masaaki Katayama: Noise Analysis on Wide-Band PLC with High Sampling Rate and Long Observation Time, Proceedings of International Symposium on Power-line Communications and its Applications, Kyoto, Japan, 2003, pp. 142-147

39. Canete F. J., Cortes J. A., Diez L., Entrambassaguas J. T. and Carmona J. L.: Fundamentals of the Cyclic Short-Time Variation of Indoor Power-line Channels, Proceedings of International Symposium on Power-line Communications and its Applications, Vancouver, Canada, 2005, pp. 157-161

40. Cortes J. A., Canete F. J., and Entrambassaguas J.T.: Characterization of the Cyclic Short-Time Variation of Indoor Power-line Channels Response, Proceedings of International Symposium on Power-line Communications and its Applications, Vancouver , Canada, 2005, pp. 326-330

41. John G. Proakis: Digital Communications, McGraw-Hill International, Third Edition, 1995

42. Srinivas Katar, Larry Yonge, Richard Newman and Haniph Latchman, “Efficient Framing and ARQ for High-Speed PLC Systems”, Proceedings of the IEEE International Symposium on Powerline Communication and Its Applications, Vancouver, Canada, 2005, pp. 27-31

43. Chan M. H. L., Donaldson R.W.: Amplitude, Width, and Interarrival Distributions for Noise Impulses on Intra-Building Power Line Communication Networks, IEEE Transactions on Electromagnetic Compatibility, 1989, Volume 31, Issue 3, pp. 320-323

44. Zimmermann Manfred, Dostert Klaus, "An Analaysis of the Broadband Noise Scenario in Powerline Network", Proceedings of the IEEE International Symposium on Powerline Communication and Its Applications, Limerick, Ireland, 2000, pp. 131-138

45. Leonard Kleinrock: Queueing Theory - Volume 1:Theory, Wiley – Interscience, First Edition, 1975

46. Srinivas Katar, Manjunath Krishnam, Brent Mashburn, Kaywan Afkhamie, Richard Newman, Haniph Latchman: Beacon Schedule Persistence to Mitigate Beacon Loss in HomePlug AV Networks, Proceedings of International Symposium on Power-line Communications and its Applications, Orlando, USA, 2006, pp. 184-188

BIOGRAPHICAL SKETCH

Srinivas Katar was born on May 19, 1975, in Vadluru, Andhra Pradesh, India. He obtained his Bachelor of Technology degree from the Department of Electrical Engineering from the Indian Institute of Technology, Kanpur, India, in 1998. In May 2000, he received his master's degree from University of Florida. He is currently a Principal Research and Development Engineer at Intellon Corporation. During his tenure at Intellon, Srinivas Katar was instrumental in the development and standardization of HomePlug AV medium access control layer.